University of Southampton
Faculty of Engineering and Physical Sciences
Southampton High Energy Physics (SHEP)

Right-handed Dark Matter from Higgs Portal Induced Mixing

by
Adam Murphy

Thesis for the degree of Doctor of Philosophy

January 2025

Acknowledgements

Before we start with the physics, let me first and perhaps most importantly show my gratitude to all who have helped me over the last few years. The first person I would like to thank is my supervisor, Pasquale Di Bari, who has shown nothing but support and compassion, through both my ups and downs over this period of study. His guidance, insight and instruction have been truly appreciated; without his help, this thesis would not have been possible. Secondly, I would like to thank the University of Southampton, in particular the Southampton High Energy Physics group (SHEP) and the Next Generation Computational Modelling group (NGCM). Within SHEP and the NGCM, I would like to thank the tutors, fellow students, and all other staff affiliated with the groups. Again, thanks for accepting me onto such a fantastic PhD programme.

On a more personal level, I would like to thank my long-term partner Rebecca Doughty for putting her life on hold for me over the last few years; she has been there for me through the various highs and many lows over this time. She has never stopped believing in me, even when perhaps I had. I would also like to thank my parents Alison and Peter Murphy, who have done nothing but help and assist me in times of need. As is fair, I would also like to thank my two brothers, John and Liam; I am extremely proud of the men you have become. I would also like to thank my family members who are no longer here; I wish you were here and I wish we could have spent more time together towards the end. On a lighter note, I also would like to thank my friends old and new. Last but not least, I would like to thank my cat Seren, without whom this journey would have been a lot darker and much more lonely.

Abstract

Right-handed (RH) Higgs-induced neutrino mixing (RHINO) is an extremely exciting model that is capable of accounting for not only dark matter (DM), but also neutrino masses through the type-1 seesaw model along with the matter-antimatter asymmetry of the universe with leptogenesis. Within this model, the standard model is extended by not only introducing Majorana RH neutrino fields but also a five-dimensional Higgs portal-like effective operator, which is capable of producing and converting a source RH neutrino into a dark RH neutrino, which can play the role of DM. This operator harbours the potential to also induce decays of the dark RH neutrino, which could, in theory, be detected. This is extremely interesting as recently a neutrino flux excess at $\mathcal{O}(100\text{TeV})$ energies has been confirmed by the IceCube collaboration when analysing the 7.5yr HESE data, wherein the DM neutrino decays could contribute to this excess. The novel aspect of this work is the realisation that the five-dimensional operator could be expanded to allow production of the source RH neutrino, which in turn allows the particle to thermalise without requiring some external physics, thus allowing one to successfully account for the relic abundance whilst allowing a much higher seesaw scale. This higher scale can be above the sphaleron freeze-out temperature and can be as high as $\sim$100TeV, therefore allowing the incorporation of strong resonant leptogenesis within the model; thus, one can resolve the matter-antimatter asymmetry of the universe. Within our results, we obtain a $\sim$1TeV-1PeV allowed neutrino mass range for the dark RH neutrino. Additionally, our results indicate an effective scale for the Higgs portal interactions, which appears to be that of the hypothetical grand-unified scale $\sim 10^{16}$GeV, which is many orders of magnitude below the effective mixing scale $\sim 10^{23}$GeV. Within this work, we also explain how this apparent hierarchy can arise from two UV-complete theories, where the first theory features a SM extension involving a heavy scalar as the mediator, whilst the second and more interesting extension involves a heavy fermion as the mediator, where we see that the first scale corresponds to the scale of new physics, whilst the second much smaller scale is related to very small couplings that can be identified with a symmetry breaking parameter. To summarise, the RHINO model allows us to simply unify neutrino masses, the matter-antimatter asymmetry of the universe, and DM in a testable manner, due to potential decays of the dark RH neutrino, which can be successfully embedded within a grand unified model.

Contents

List of Figures

1 Introduction

In this section we start by briefly outlining dark matter, whilst introducing our solution to this problem based on right-handed dark matter from Higgs portal induced mixing. Finally, an overview of the thesis is divulged. The novel work in this thesis is based on the work published in Ref. [1] - "Completing RHINO", and is discussed in Sections 10, 11, and 12.

1.1 Introduction to Dark Matter and RHINO

> "If this would be confirmed, we would get the surprising result that dark matter is present in much greater amount than luminous matter." - Fritz Zwicky [2]

At the start of the last century, multiple obstacles were reached in our goal of a complete rule book for the universe. One of these obstacles is a supposed novel form of matter, which according to evidence interacts only gravitationally. This novel form of matter has been named *dark matter* (DM) due to its apparent lack of electromagnetic interactions. The initial evidence for DM is often accredited to Swiss astronomer Fritz Zwicky [3], and in the years since, a wealth of evidence has been acquired, resulting in many others arriving at this same conclusion. DM is currently one of the greatest cosmological and phenomenological mysteries in physics, with evidence suggesting that DM plays an extremely important role in the formation of the large-scale structure of the universe, where the structure of the universe is such that it also implies that should DM exist, it is expected to be kinetically cold. DM accounts for approximately 26% of the energy density of the universe, with a density parameter determined by *Planck satellite* given by [4]

$$\Omega_{\rm DM}h^2 = 0.11933 \pm 0.00091. \tag{1.1}$$

There are many different proposed cosmological models, the most favourable is the $\Lambda_{\rm CDM}$, in which the universe contains three components, the first being the cosmological constant denoted by Λ and is symbolic for *dark energy*, the

second is cold DM denoted by CDM, whilst the third and final component is ordinary matter. The Λ_{CDM} model is favoured as it can successfully account for the existence and structure of the *cosmic microwave background* (CMB), the large-scale structure, and thus the distribution of galaxies, the observed abundance of hydrogen and helium within the universe, and the accelerating expansion of the universe. Results within the Λ_{CDM} model can successfully account for DM contributing around 26% of the energy density of the universe, with ordinary baryonic matter accounting for around 4%, and the final 70% being accredited to the other mysterious dark phenomena, dark energy. Extensive research and models are being produced in many particle physics institutes across the globe in the hope of solving this fundamental cosmological and particle problem. Unfortunately, DM has not yet been observed directly and not much is known about its nature other than its gravitational effects. It is theorised that DM will be comprised of one (or more) currently undiscovered particle species, and even though there is no direct evidence of DM, there is plenty of indirect evidence that some form of DM does exist. Proposed DM candidates are produced through different mechanisms that can be subdivided into two categories; thermal or non-thermal production. Currently, large volumes of work are being partaken in an effort to constrain the properties of DM [5, 6, 7]. An estimate of the DM abundance as a function of the proposed mass of the DM candidate can be obtained by

$$\Omega_X h^2 = \frac{\rho_X}{\rho_c} h^2 = \frac{m_X n_X h^2}{\rho_c}, \tag{1.2}$$

where Ω_X is the density parameter of DM and h is a dimensionless quantity that is related to the Hubble constant by $H_0 = 100h$ kms^{-1} Mpc^{-1}. The DM density parameter can be expressed in terms of the density of the DM particle ρ_X, and the critical density of the universe $\rho_c = 1.054 \times 10^{-5} h^2$ GeV cm^{-3}, which is given by $\rho_c = 3H^2/8\pi G$, where H is the Hubble constant and G is the gravitational constant. The density of DM ρ_X can also be expressed in terms of the mass of the DM particle m_X, and the number density of the DM particle n_X, by $\rho_X = m_X n_X$[1]. One particle species with the potential to play a role in DM is the neutrino, which is a rather devious little particle. Although predicted to be massless in the pure *standard model* (SM), they are

[1]There is no reason to assume that only one particle species accounts for the relic abundance.

known to mix, a phenomenon that can only occur if the neutrinos possess mass. Thus, neutrino masses and mixing along with other mysteries, such as DM, quantum gravity, and the *matter-antimatter asymmetry* of the universe require us to extend the SM. In an ideal situation, proposed extensions would be minimal and testable; unfortunately, many extensions are based on new physics at inaccessible energy scales. In the case specifically of neutrinos, it is hopeful that extensions are able to unify neutrino masses and mixing, along with the potential to resolve DM, and the matter-antimatter asymmetry through a process called *leptogenesis* if they are related. One possibility is DM from Higgs-induced right-handed neutrino mixing (RHINO DM) [8, 9]. RHINO DM is based on a traditional extension using a *type-I seesaw* Lagrangian, but with the addition of a non-renormalisable operator.

The minimal type-I seesaw mechanism [10] introduces *right-handed* (RH) neutrino fields to the SM and provides a rather minimal way to explain neutrino masses and mixing, whereby ordinary neutrinos are extremely light compared to the other SM particles, yet for some unexpected reason also feature large mixing angles [11] in the leptonic mixing matrix. Another advantage of the seesaw model is its compatibility with other beyond SM extensions [12], whilst also easily incorporating leptogenesis, which is a scenario of *baryogenesis* [13] that is capable of explaining the matter-antimatter asymmetry that we see in the universe. Within the RHINO model, a RH neutrino plays the role of kinetically cold DM rather than the typical warm DM that is obtained by introducing lighter keV RH neutrinos [14]. The key extension this model proposes is the introduction of a dimension 5 nonrenormalisable operator, which is capable of producing a dark RH neutrino $N_{\rm D}$ which features an almost non-existent *Yukawa coupling* to the SM. This dark RH neutrino is then produced through Higgs-induced mixing with another RH neutrino that we call the source RH neutrino $N_{\rm S}$. This new operator is an effective dim-5 non-renormalisable *Higgs portal*-like operator known as *Anisimov operator* and, in older work, it is only concerned with the mixing it induces between $N_{\rm D}$ and $N_{\rm S}$, and as such takes the form [15, 8]

$$\mathcal{L}^{A}_{\rm DS} = \frac{\lambda_{\rm DS}}{\Lambda}\Phi^{\dagger}\Phi\overline{N^{c}_{\rm D}}N_{\rm S}, \tag{1.3}$$

where Λ is the effective scale above which full theory is required. These dark RH neutrinos, which are produced through the mixing induced by the Anisimov operator, can then in certain instances account for the DM we see

in the universe. Interestingly, this operator also predicts the possibility that these particles decay [8, 9]. These decays are even induced at zero temperature by the effective small Yukawa couplings which are generated by the mixing this operator induces [16]. Naturally, if this RH neutrino is capable of being the DM, it must be produced with the abundance one expects and long-lived enough to evade detection and constraints at neutrino telescopes [17]. These conditions are then imposed on the effective neutrino mixing scale $\tilde{\Lambda}_{\rm DS} \equiv \Lambda_{\rm DS}/\lambda$ along with the particle mass, resulting in a highly predictive DM model. The origin of the mixing between the source and the dark RH neutrino is a misalignment between the Majorana mass eigenbasis and the new basis where the Higgs-induced interactions are diagonal. This interaction features a strong temperature dependence that is encoded within a thermal self-energy, whereby the neutrino mixing can be expressed by an effective potential or a thermal mass. The strong temperature dependence allows the interaction to efficiently produce DM in the early universe when the interaction is stronger than today, whilst also allowing the particle to be generally long-lived and stable at present time with a chance to decay due to the mixing induced at zero temperature. Originally, the dark RH neutrinos' abundance was calculated using the *Landau-Zener* (LZ) approximation[2] [8, 9], while more recently the abundance was calculated using the *density matrix* formalism. Upon comparison, it was found that the LZ approximation overestimated the dark RH neutrino abundance [16].

In this previous work, two scenarios were explored, these being an initial vanishing source RH neutrino abundance and a thermal source RH neutrino abundance. In the case of a vanishing source RH neutrino abundance, a stringent bound was obtained where the source mass has to be below the W gauge boson mass, $m_W \sim 80$GeV, with the four-body decay rate getting suppressed, whilst the dark RH neutrino must fulfil $M_{\rm D} \gtrsim 10^7$GeV. Unfortunately, within this scenario, strong thermal leptogenesis[3] from non-relativistic decays is not possible, as the matter-antimatter asymmetry should arise from resonant production due to the decaying seesaw neutrinos with masses roughly double that of the sphaleron freeze-out temperature, $T_{\rm SF} \sim 132$GeV [18]. However, within this scenario the matter-antimatter asymmetry could still be generated by other methods [19, 20]. If one compares this to νMSM one can

[2]The LZ approximation requires extremely quasi-degenerate DM-source neutrino masses.

[3]When the matter-antimatter asymmetry is independent of the initial conditions and produced through thermal interactions.

still obtain relatively low-scale leptogenesis with $\mathcal{O}$(GeV) seesaw neutrinos; however, the DM would be extremely heavy. Within low scale leptogenesis featuring $\mathcal{O}$(GeV) neutrinos the matter-antimatter asymmetry is produced within the relativistic regime and is therefore dependent on the initial conditions as well as precise descriptions of the many different processes involving the particles. For successful dark RH neutrino production it is required that $T_{\rm RH} \gtrsim 10^9$GeV, and as such a large pre-existing asymmetry is potentially natural. Having the requirement to circumnavigate this potentially large pre-existing asymmetry is certainly an unattractive proposition; however, there is a rather simple solution, and that is what is proposed in this work. The key idea is that the Anisimov operator is actually one side of a multi-faceted operator, where the whole effective Lagrangian can be given by [8] ($I, J = {\rm D}, {\rm S}$)

$$\mathcal{L}_A = \sum_{I,J} \frac{\lambda'_{IJ}}{\Lambda} \Phi^\dagger \Phi \overline{N_I^c} N_J, \tag{1.4}$$

which can be expanded into three terms which include the mixed Anisimov term and two pure Anisimov terms given by

$$\mathcal{L}_A = \frac{\lambda_{\rm DS}}{\Lambda} \Phi^\dagger \Phi \overline{N_{\rm D}^c} N_{\rm S} + \frac{\lambda_{\rm SS}}{\Lambda} \Phi^\dagger \Phi \overline{N_{\rm S}^c} N_{\rm S} + \frac{\lambda_{\rm DD}}{\Lambda} \Phi^\dagger \Phi \overline{N_{\rm D}^c} N_{\rm D}, \tag{1.5}$$

where the coupling strength between the dark and source RH neutrino, $N_{\rm D}$ and $N_{\rm S}$ respectively, is given by $\lambda_{\rm DS} = \lambda'_{\rm DS} + \lambda'_{\rm SD}$, where $\lambda'_{\rm DS}$ is the interaction strength of $N_{\rm D}$ coupling to $N_{\rm S}$, whilst $\lambda'_{\rm SD}$ is the interaction strength of $N_{\rm S}$ coupling to $N_{\rm D}$, through the Higgs-Higgs interaction[4].

In previous models [8, 9, 21], it was assumed that Higgs portal interactions did not play any role in DM production. However, we show that

[4]This is as $\overline{N_{\rm D}^c} N_{\rm S} = \overline{N_{\rm S}} N_{\rm D}^c = \overline{N_{\rm S}^c} N_{\rm D}$. This equality follows from the properties of charge conjugation (discussed in Section 3.4) and the symmetry of the bilinear forms, where the antisymmetric nature of the charge conjugation matrix C, and also for Majorana particles one has $N = N^c$. Importantly it is possible to express the coupling as

$$\frac{\lambda'_{\rm DS}}{\Lambda} \Phi^\dagger \Phi \overline{N_{\rm D}^c} N_{\rm S} + \frac{\lambda'_{\rm SD}}{\Lambda} \Phi^\dagger \Phi \overline{N_{\rm S}^c} N_{\rm D} = \frac{\lambda'_{\rm DS} + \lambda'_{\rm SD}}{\Lambda} \Phi^\dagger \Phi \overline{N_{\rm D}^c} N_{\rm S} = \frac{\lambda_{\rm DS}}{\Lambda} \Phi^\dagger \Phi \overline{N_{\rm D}^c} N_{\rm S}. \tag{1.6}$$

these interactions are capable of allowing one to still incorporate strong leptogenesis within the RHINO DM model, along with allowing $M_{\rm D} \sim 100$TeV decaying DM, which is currently favoured at neutrino telescopes. From Eq. 1.5 one can see that there is an avenue for direct N_D production from two of the terms[5], however, we assume that these terms do not contribute to the DM abundance themselves and are neglected and later will justify this decision. We are not assuming that these terms do not contribute at all, as these interactions may as an example play a role in thermalisation of the dark sector before a phase transition [22].

In this work we show that by including the source-source Higgs portal[6] interactions the allowed parameter space for strong leptogenesis enlarges at higher seesaw scales for the non-relativistic regime. The reason for this is that they can fully or partly thermalise the source RH neutrinos before mixing occurs, for example, at temperatures higher than the Yukawa interactions. Therefore, one can reproduce the observed relic density for values higher than the previous of the effective RHINO scale $\tilde{\Lambda}_{\rm DS} \equiv \Lambda/\lambda_{\rm DS}$, and thus it is possible to satisfy the four-body decay constraint for values of the seesaw scale beyond the W gauge boson mass. In our work, we show that the seesaw scale can actually be as high as ~ 100TeV, which is well below the leptogenesis scales lower bound for the RHINO model of $\sim 10^9$GeV which holds for hierarchical seesaw neutrinos [23] so that production is either resonant [24, 25] and/or some form of combined *fine-tuning* in the seesaw formula [26, 27, 28] is required for enhancement of the CP asymmetries. Seesaw scales that are as high as those present in our work are regarded attractive because they can be more easily incorporated into realistic flavour models [12]. Finally, for such a high seesaw scale, the DM mass range is in the $\sim$1TeV-1PeV range and is thus compatible with the excess found at neutrino telescopes, which is roughly $\sim$100TeV.

1.2 Thesis Outline

This thesis is structured as follows. In Section 2 the historical evidence for DM is first explored, before moving on to give a brief overview on advancements in physics that helped formulate the SM. Next, popular DM candidates

[5] One is pure dark neutrino production $\phi + \phi^\dagger \to N_{\rm D} + N_{\rm D}$, one is mixed source and dark from the mixed term $\phi + \phi^\dagger \to N_{\rm D} + N_{\rm S}$.

[6] $\phi + \phi^\dagger \to N_{\rm S} + N_{\rm S}$.

are divulged before finally moving on to neutrinos as DM candidates. In Section 3 important facts of the SM are explored with a particular emphasis on neutrinos, which are predicted to be massless by the SM. In Section 4 we move away from the standard model and discuss neutrino mixing and oscillations, whilst also introducing the density matrix formalism. In Section 5 neutrino masses are discussed, along with the type-I seesaw which is of great importance to the RHINO model, which is produced from a Dirac mass for neutrinos along with a Majorana mass for RH neutrinos. Section 6 discusses the early universe; this is a rather lengthy section involving topics such as degrees of freedom of the early universe, the Boltzmann equations, the famous WIMP miracle, and leptogenesis. Section 7 introduces the Higgs portal operators along with a discussion of operators in the SM. In Section 8 the three avenues of DM detection are discussed with these being; collider searches, direct searches, and indirect searches. Section 9 then discusses neutrino experiments specifically. Section 10 then introduces RHINO DM in detail, before Section 11 modifies RHINO by introducing source-source terms to thermalise the source RH neutrinos. In Section 12 the results from including the novel source-source terms are included and discussed, along with introducing two UV-complete theories from which RHINO DM can arise, before finally concluding in Section 13.

2 Dark Matter and Particle Physics

In this section, the observational evidence for dark matter is introduced mostly in chronological order. Then major milestones of particle physics are introduced that led to the production of the SM. After this popular dark matter candidates are introduced, before finally discussing neutrinos as DM.

2.1 The History of Observational Evidence of Dark Matter

Let us now dive a little deeper into the history of observational evidence for DM. Historically, the DM problem was first theorised by Lord Kelvin in a talk in 1884, after estimating the number of dark bodies in the Milky Way from the velocity dispersion of stars near the galactic core [29]. The velocity dispersion of a group of astronomical objects is the statistical dispersion of velocities of the group around the mean velocity, where the group could be stars within a galaxy or a group of galaxies, and the velocities are often measured with some form of astronomical spectroscopy. From his results, Lord Kelvin stipulated that most of the 'stars' could in fact be dark bodies. Shortly after, the term DM was coined by Henri Poincare in a discussion of Lord Kelvins work. It was in 1933 that the Swiss astrophysicist Fritz Zwicky was accredited with the discovery of DM [3]. Zwicky took this earlier work further by applying the virial theorem to the Corma Cluster, and in doing so he calculated the mass of the cluster which was greater than expected. The virial theorem is given by

$$\langle T \rangle = -\frac{1}{2} \sum_{k=1}^{N} \langle \mathbf{F}_k \cdot \mathbf{r}_k \rangle, \tag{2.1}$$

with T being the kinetic energy, F_k the force on the particle k^{th} and r_k the position of the k^{th} particle or object, with the angled brackets indicating that it is a time averaged quantity. Zwicky made a comparison of his results to estimations from apparent luminosity, and upon doing so, Zwicky deduced that there must be far more mass present than the apparent visible mass. With more accurate measurements in recent times, it turns out that Zwicky overestimated the amount of DM present by more than an order of magnitude.

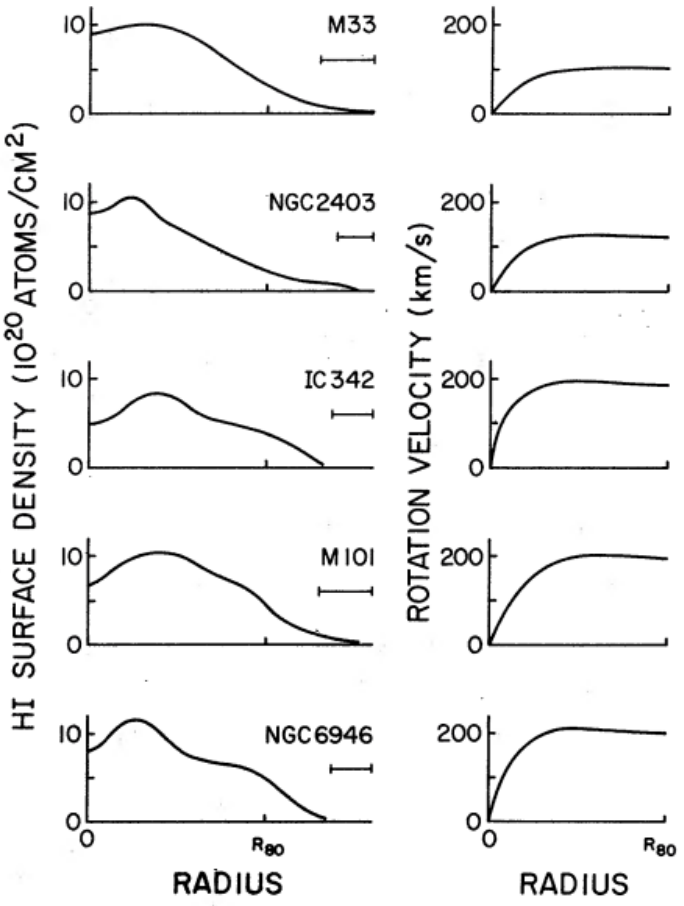

Figure 1: Flat rotation curves of five galaxies from 21cm observations obtained by D. H. Rogstad and G. S. Shostak in 1972 from Ref. [30]. The hydrogen surface density is shown in the left panels, whilst the rotation curves are shown in the right panels, where R_{80} on the x-axis is the point at which 80% of the hydrogen is contained within the galaxy. The bars underneath the galaxies name indicate their effective spatial resolution.

In the years following Zwicky's discovery, others made similar discoveries, such as that from Horace W. Babcock's PhD in 1939 where he found very high rotational velocities at large radii [31], which he wrongly accredited to some form of modified dynamics in the outer portions of the galaxy arising from flat galaxy rotation curves. It was expected from the visible mass that the rotational speed of stars and dust within the galaxy would slow down

past some distance, but what they found was that the velocities would only increase with distance away from the galactic core, which was not expected when one considers Kepler's third law. As awful as World War Two was, it did create some advancements in science, especially in the field of astronomy. Ex-military radars were recognised as extremely useful for astronomical observations, which was driven by famous Dutch scientist Jan Oort, with a particular emphasis on the 21cm hydrogen line, which was then found in 1958, and thus offered a massive boost to the novel field of radio astronomy. In the 1960s radio astronomy was still in its infancy; however, evidence was acquired by Seth Shostak showing that multiple galaxies certainly did rotate too fast in the outer portion of the galaxy [32]. Also, in the 1960s and 1970s Vera Rubin, Kent Ford, and Ken Freeman implemented galaxy rotation curves using new technology which allowed more accurate measurements of the velocity curve of spiral galaxies which were aligned side-on providing yet more evidence for the existence of DM [33, 34], in the form of a flat optical rotation curve when inspecting the M31 galaxy.

In the 1970s we benefited from improved radio telescopes, this allowed the mapping of the 21cm line of atomic hydrogen (H-I) in nearby galaxies. This enabled the measurements of distributions within galaxies at much larger radii than was previously possible optically. This extended the sampling of the total mass distribution to a novel dynamical regime. Early examinations of Andromeda showed that the velocity of H-I did not decrease radially as expected when Kepler's laws of planetary motion were considered. Morton Roberts and Robert Whitehurst traced the rotational velocity of Andromeda to about 30kpc, which was much further than what optical telescopes allowed; these novel H-I results from approximately 30kpc were then combined with optical data below 30kpc from the galactic core, which ultimately showed that the cumulative mass was still increasing linearly at the outermost data points, which was not at all in alignment with the optical results which peaked in the centre of the galaxy [35]. At the same time as these advancements in the H-I mapping of galaxies, the development of interferometric arrays for extragalactic H-I was being developed. In 1972 David Rogstad and Seth Shostak provided results for H-I rotation curves of five spiral galaxies and found that the rotation curves of all five were flat, which suggested large values of the mass-to-light ratio in the outer region of their H-I disks [30], these results are displayed in Fig. 1.

The 1980s and onwards involved many novel observations that provided a whole wealth of evidence for the existence of DM, these include gravitational

lensing, the cosmic microwave background, and structure formation within the universe. Gravitational lensing [36, 37] arises from general relativity, we know from general relativity that massive objects bend space-time, therefore if a massive object lies between an observer and another massive object which acts as a source, the massive object in between the source and the observer should act in a similar manner to a lens, with a more massive object producing a more significant lensing effect.

Figure 2: The appearance of the "Molten Ring" Galaxy due to gravitational lensing obtained by the Hubble Space Telescope. Credits: Author - Anastasio Díaz-Sánchez (Universidad Politécnica de Cartagena), Image - Saurabh Jha (Rutgers, The State University of New Jersey), Acknowledgement - Leo Shatz.

Strong gravitational lensing distorts background galaxies into arcs as seen in Fig. 2, the distortion of the object between the source and the observer can be measured and from this distortion the mass of this middle object can be determined; a classic example of gravitational lensing is that of Abell 1689 [38]. When this calculation is performed, the mass-to-light ratios obtained can act as a measurement of the DM within the astronomical object. Using this method, it is also possible to produce a map of the DM distribution around an astronomical object, as is the case with the MACS J0416.1-2043 [39]. Unfortunately, gravitational lensing rarely produces the large arcs seen from strong gravitational lensing, and most lines of sight in the universe are in fact affected by weak gravitational lensing. Weak gravitational lensing seeks to investigate minuscule distortions of galaxies and is more statistical in

nature; however, in doing so one can characterise the mean DM distribution [40] and other properties of the lensing object.

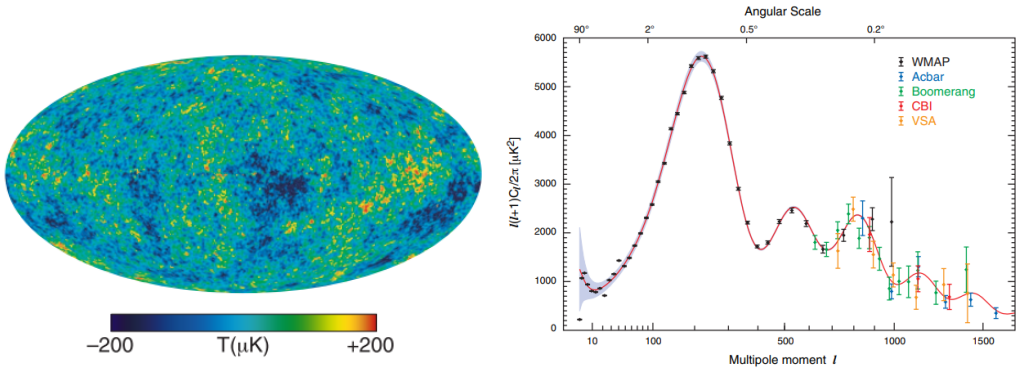

(a) The CMB map.

(b) The CMB acoustic peaks.

Figure 3: The left figure is the CMB map from the nine-year Wilkinson Microwave Anisotropy Probe from Ref. [41]. The right figure shows the WMAP three-year power spectrum in black compared to other measurements produced at a similar time, these other measurements are as indicated, extracted from Ref. [42].

The CMB shown in Fig. 3a exhibits characteristics of a nearly perfect black body spectrum, but exhibits small variations in temperature, known as temperature anisotropies. During the early stages of the universe, regular baryonic matter was ionised and interacted significantly with radiation through processes such as Thomson scattering. DM on the other hand, does not participate in these interactions. Nevertheless, the presence of DM does leave an imprint on the CMB due to its gravitational potential on large scales that influences the distribution and velocities of regular matter. Perturbations caused by DM and regular baryonic matter during the early universe evolved differently, thereby leaving distinct signatures on the CMB. The CMB's temperature variations across the sky can be analysed through an angular power spectrum, which exhibits acoustic peaks with approximately uniform spacing. These peaks can be fitted using computational models and cosmological parameters to align theoretical predictions with observed data, enabling one to constrain the cosmological parameters.

The results obtained from such a fitting process displays several peaks, as shown in Fig. 3b. The first peak corresponds primarily to the curva-

ture of the universe and the overall density of matter (both dark matter and baryonic matter). Baryonic matter has a major influence on the second peak, where the second peak is inversely proportional to the density of the baryonic matter, such that a larger density of baryonic matter reduces the second peak. This second peak essentially represents the rarefaction phase of the acoustic oscillations that are present in the early universe. The third peak is important for DM, the reason DM affects the third peak is that DM contributes to a deepening of the gravitational potential wells of the early universe. DM is unlike baryonic matter, which undergoes electromagnetic interactions and thus experiences radiation pressure. Therefore, DM interacting only gravitationally results in a more intense compressional phase in the acoustic oscillations, where more DM results in deeper wells and a more prominent third peak compared to the second peak. The presence of these observed acoustic peaks in the angular power spectrum of the CMB provides compelling evidence in favour of DM, specifically supporting the Λ_{CDM} model [43, 4].

These CMB acoustic peaks are difficult to replicate through alternatives such as kinetically hot DM or modifications to Newtonian dynamics. Similarly to the CMB is the proposed cosmic neutrino background (CνB) [44], which has not yet been detected although it is hopeful that at some point in the future it will be. The CνB is of interest as neutrinos are weakly interacting, and thus are expected to have decoupled from the universe earlier than the relic photons and as such these relic neutrinos are expected to allow one to peer further back into the universe's history than ever before. This sounds extremely promising, however, considering the difficulty in detecting high-energy neutrinos, the possibility of detecting neutrinos with an expected energy of $\sim 10^{-4} - 10^{-6}$eV is still far off [7].

Another vital piece of evidence we have for DM is structure formation of the universe after the dark ages when density perturbations in the universe collapsed and formed stars, galaxies, and clusters of galaxies [45]. Before structure formation, the universe was thought to be almost homogeneous, but over time small anisotropies gradually grew from their gravitational effect; however, if DM were not present, these anisotropies would not have the necessary gravitational influence to grow into the structures we see in the universe today due to the expansion of the universe. In this sense, DM acts almost as a fundamental framework or seed for the formation of cosmic

[7] One has that the cross section is proportional to the energy of the particle, $\sigma \propto E$

structures [46]. DM also solves problems in relation to where the centre of mass resides within colliding galaxies, as without DM general relativity must be wrong, but with DM present, the centre of mass is where it is expected to be, with an example of this being the Bullet Cluster [47].

2.2 A Brief History of Particle Physics

Parallel to us obtaining so much evidence for DM, our fundamental knowledge of the underlying physical processes too was increasing rapidly. Currently, particles and their interactions underlie much of what we know of the universe, with many of these interactions described by a *quantum field theory* (QFT). QFT is a mathematical framework for calculating these interactions, and currently we have a QFT for three of the four fundamental forces of nature. The forces we currently have a QFT framework for is the electromagnetic force, the weak nuclear force, and the strong nuclear force, whilst we do not have a QFT for the gravitational force, which is also a major open question currently in physics. Anyway, QFT was born from combining three fundamental pillars of physical sciences and was developed in the late 19th century and the very early 20th century. The first of these three pillars was classical field theory, which essentially takes point-like problems to the continuum and assigns every point in space a value; this value is the strength of the field at that point in space. Our first real application of fields was reached with the development of the classical theory of electromagnetism [48].

The second pillar was special relativity proposed by Einstein in 1905 to remedy the misalignment of Newtonian mechanics with Maxwell's equations of electromagnetism. Special relativity essentially corrects the mechanics of an object when moving at speeds close to that of causality, and from it many exotic and interesting physical consequences arose, things such as relativity of simultaneity, length contraction, time dilation, a universal speed limit, the famous mass-energy equivalence, amongst others [49]. One extremely important consequence of special relativity is the Lorentz transformations that allow us to switch between inertial reference frames that are moving at constant velocity relative to each other. The third and final pillar combined to form a QFT was in fact quantum mechanics (QM). The birth of quantum physics is often accredited to Max Planck [50] and his black-body radiation results, in which he treated atoms as tiny harmonic oscillators. Quantisation is the process of restricting energies to discrete values, which Niels Bohr managed to achieve with the atomic structure in the Bohr model of an atom,

which remedied the discrete nature of atomic spectral lines. Louis de Broglie then proposed the hypothesis of wave-particle duality in 1924. Through the uniting of these ideas a QM framework was developed by Max Planck, Louis de Broglie, Werner Heisenberg, Max Born, Erwin Schrodinger, Paul Dirac, and Wolfgang Pauli, and others. Although much success arose from QM there were still glaring problems, such as the lack of explanation for spontaneous emission, a lack of ability to explain the photon, and QM was not consistent with special relativity due to treating time as an ordinary number but treating spatial coordinates as quantum operators (or more accurately linear operators).

It was British physicist Paul Dirac who arrived at the first relativistic formulation of quantum mechanics in 1927 in which he managed to successfully describe some light- and matter interactions, with the photon featuring as the force-carrying particle. This theory was named quantum electrodynamics (QED), and with this formulation Dirac correctly explained spontaneous emission. A year later Dirac produced a wave equation, known as the Dirac equation, which described relativistic electrons [51]. QED was our first QFT and our basis going forward for quantising the other fundamental forces; however, QED was not without its problems, as results could only be obtained in first-order perturbation theory as at higher-orders infinities arose. This problem was eventually overcome in the 1940s by physicists such as Freeman Dyson [52, 53], Julian Schwinger [54, 55], Richard Feynman [56, 57, 58], and others. Another great computational tool, the Feynman diagram was also developed by Richard Feynman; an example diagram is displayed in Fig. 4. Finally, with this new achievement matter and light interactions could be explained accurately on the quantum scale, and almost 100 years later QED is still one of our most accurate physical theories.

Going forward, QED served as the template for other QFTs and their attempts to quantise the other fundamental forces. Over the next few decades, a QFT was developed to explain the weak force, which is fundamental to beta decay that occurs in radioactive isotopes; the QFT for this fundamental force is known as quantum flavour dynamics (QFD). Key contributions to QFD were made by Steven Weinberg, Sheldon Glashow, and Abdus Salam [59]. It was also found that QED could be combined with QFD at some arbitrary energy level to form the electroweak force. The third of the four fundamental forces that has been quantised is the strong nuclear force, and the theory describing it is called quantum chromodynamics (QCD), with major contributions from Harald Fritzsch, Murry Gell-Mann, and Heinrich Leutwyler

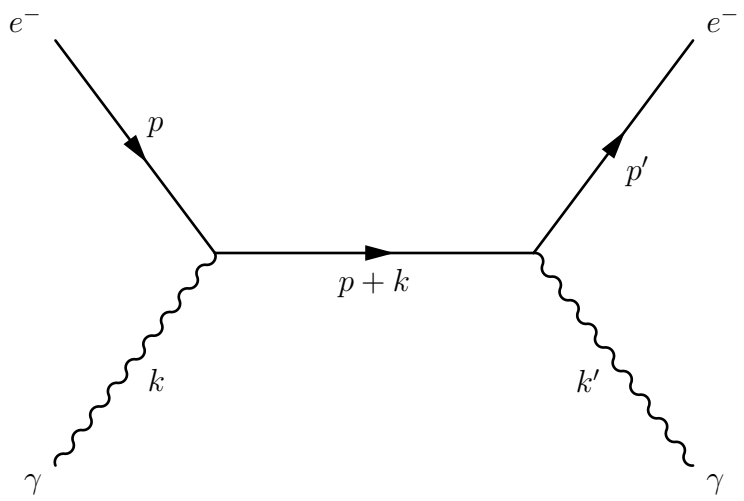

Figure 4: An example tree-level Feynman diagram of the s-channel contribution to Compton scattering. The arrows on the fermion lines indicate not momentum but the flow of charge in typical diagrams.

[60]. Both the weak and the strong interaction are based on Yang-Mills theory [61], a gauge theory for nonabelian groups. From the development and combination of these quantum field theories we obtained the pure SM of particle physics. Within the SM exist all the subatomic particles known today, these particles can be split into two types of particles these being; fermions (matter particles) and bosons (force carrying particles). Fermions and bosons are two different but fundamental particle types, with differences based on their intrinsic and statistical properties. Bosons have integer spin values, whilst fermions have half-integer spin values. Additionally, fermions obey the Pauli Exclusion Principle, which states that no two fermions can occupy the same quantum state simultaneously (this leads to the structure of atoms and thus to the periodic table). Bosons do not obey this principle and thus can occupy the same quantum state; this results in phenomena such as Bose-Einstein condensation. This leads to differing statistical models being used to describe bosons and fermions, with fermions described by Fermi-Dirac statistics and bosons described by Bose-Einstein statistics. In QED both quarks and charged leptons are involved in interactions, with the photon acting as the force-carrying boson and is based on a $U(1)_{EM}$ gauge symmetry. Whilst QFD interactions involve left-handed helicity quarks and leptons (both neutrino-like and electron-like leptons) and right-handed he-

licity antiquarks and antileptons. QDF features three large bosons as the force carrying particles, two of which are charged bosons called the W^+ and W^- bosons and one neutral boson, the Z boson. Electroweak interactions are based on $SU(2)_L \times U(1)_Y$ symmetry. QCD interactions involve only quarks, with gluons as the force-carrying particles and is based on a $SU(3)_c$ gauge symmetry. Overall, the SM is based on a gauge field theory with a $SU(3)_c \times SU(2)_L \times U(1)_Y$ symmetry.

Within the SM there are 18 free input parameters which are not predicted by theory and, as such, have been measured. In no particular order, these parameters are [62]:

- The fine structure constant, α, which determines the electromagnetic coupling strength between charged leptons and photons.
- The Weinberg or weak mixing angle θ_W, which determines the mixing of the electroweak gauge bosons after symmetry breaking.
- The strong coupling constant, g_3, which couples the quarks to the gluons in QCD.
- The Higgs potential vacuum expectation value, v, the scale of electroweak symmetry breaking.
- The coupling constant of the Higgs potential, λ, from which the Higgs mass is determined.
- The three mixing angles ($\theta_{12}, \theta_{23},$ and θ_{13}) found in the Cabibbo-Kobayashi-Maskawa (CKM) matrix, which parameterise the mixing of the down-type quarks' weak interaction states.
- One physical CP-violating phase, which arises from the complex nature of the CKM matrix and contributes to CP violation in weak interactions.
- The nine Yukawa couplings, which couple the SM fermions to the Higgs, and after symmetry breaking, result in the fermions' masses. There are no Yukawa couplings for neutrinos in the pure SM.

Many extensions of the SM increase the number of these parameters; however, it is hopeful that a complete theory of everything has no free parameters.

No particle in the pure SM has the right properties or characteristics to account for DM and as such we are expected to look to new physics for these answers. Dark matter must possess specific properties: it must be massive, stable, dark, weakly interacting, and must not participate in the electromagnetic or strong nuclear forces. Additionally, it must fit cosmological observations, such as gravitational effects and the structure of galaxies, which no known Standard Model particle can fully account for.

Other problems also arise in the SM; there is no quantum theory of gravitation, confusion around neutrino mass generation, CP violation and many other problems on closer inspection. The fact that the SM is incomplete drives research for physics beyond the SM, however, with QFT's being so successful so far at explaining so many fundamental phenomena, it is both hopeful and expected that some extension of the SM featuring novel particles and interactions could remedy the current problems in particle physics.

2.3 Popular Dark Matter Candidates

There are many proposed DM candidates; some are microscopic particle candidates while others are macroscopic. Two examples of macroscopic DM candidates include primordial black holes [63, 64], and massive compact halo objects (MACHOs) [65, 66]. Modified gravity [67] is perhaps another explanation of DM, which include modifications such as; modified Newtonian dynamics (MoND) [68], tensor vector-scalar gravity (TeVeS) [69], and entropic gravity [70]. Particle candidates include novel light particles, particles arising from the weak scale, and other proposed weakly interacting particles, such as *sterile neutrinos*[8]. Some of these candidates are shown in Fig. 5.

[8]Sterile in the sense of SM interactions, they may partake in dark sector/hidden interactions.

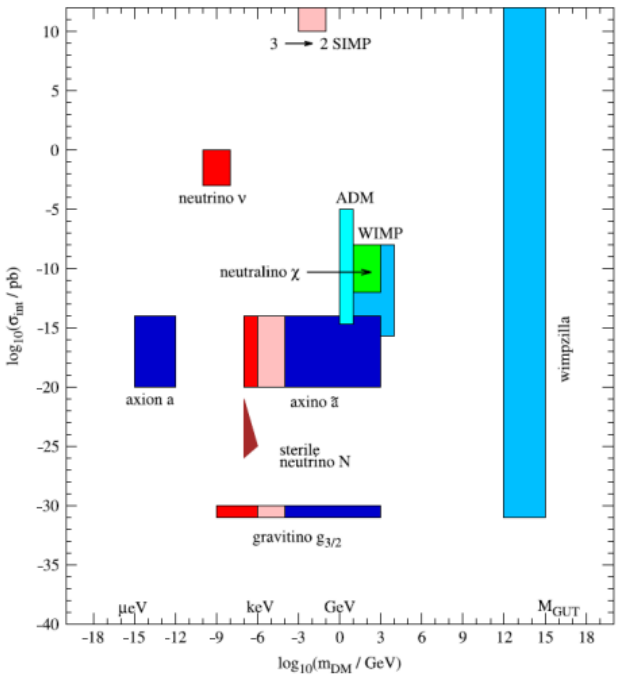

Figure 5: Some popular DM candidates shown in the interactions strength-mass plane. The colours red, pink, and blue represent whether the particle is expected to be hot, warm, or cold DM respectively, from Ref. [71].

Light DM candidates include QCD axions that were initially introduced to resolve the strong CP problem that arises in QCD [72, 73], and are expected to have a low mass in the range of 10^{-5} to 10^{-3}eV. Weakly interacting slender particles (WISPs) [74, 75], such as axion-like particles (ALPs) and hidden photons, are also potential candidates for DM which are thought to behave similarly to active SM neutrinos. Fuzzy cold DM [76, 77] is another hypothetical light form of cold DM, which was initially proposed to amend the distribution of DM found in the galaxy rotation curves when compared to the results produced by n-body simulations, these particles have an expected mass of $\approx 10^{-22}$eV. Sterile neutrinos [78] are another potential candidate for DM, active neutrinos already contribute to the abundance of DM, although marginally. If sterile neutrinos exist, they carry no Standard Model (SM) quantum numbers and primarily interact through mixing with active neutrinos, leading to extremely weak interactions beyond just gravity. Their

masses can vary widely, from as massive as 10^{15}GeV to as small as 1eV. In some cases, they may also help resolve issues related to neutrino mass generation. *Weakly interacting massive particles* (WIMPs) [79, 80] are another popular DM candidate with a mass of approximately $\approx$ 100GeV, it is hypothesised that the WIMPs get froze-out as the universe cools and a relic abundance remains which can play the role of DM. Another potential candidate is self-interacting dark matter (SIDM) [81, 82], which can include WIMPs. Some SIDM models feature a Yukawa-like potential, where a force carrier mediates interactions between the dark matter particles, though other interaction mechanisms are possible.

Many of these particles can arise from extensions of the SM, with an extremely popular extension being *supersymmetry* [83, 84], where the SM is expanded to include particles which are superpartners of the SM species. There are multiple particles that arise from supersymmetry that could play the role of DM, with the lightest supersymmetric particle (LSP) being a favoured potential candidate from supersymmetry. The neutralino could be the LSP, and it is thought that decays of the LSP into SM particles are forbidden, because the supersymmetric particles have different R-parity compared to the SM particles. Potential DM particles can also arise from extensions which include extra dimensions [85] and other exotic physics. Another possibly is the little Higgs [86] model, where it is thought that the Higgs boson is a pseudo-Goldstone boson which arises from global symmetry breaking at high energy levels, perhaps at the TeV scale. Potential dark matter candidates can also couple to the Standard Model through effective field theories (EFTs) [87, 88], which can be minimal extensions of the SM. The downside of EFT's is that they are approximations of a *UV-complete* theory at higher energy scales.

2.4 Neutrino Dark Matter

Neutrinos are the only fermionic particles in the Standard Model that are electrically neutral and remain stable over the vast age of the universe. These facts coupled with the revelation that neutrinos do in fact have mass, made them ideal early candidates for a DM particle. Neutrinos only partake in the weak interaction; therefore, it is these interactions that kept the neutrino in thermal equilibrium in the early universe; after a certain time these interactions cease and the neutrinos effectively freeze-out at temperatures of a few MeV, prior to nucleosynthesis. This process is thought to create the CνB,

as touched upon previously. The number density for such a particle is given by[9] [78]

$$n_\alpha = \frac{3}{2}\frac{\zeta(3)}{\pi^2}T_\nu^3, \tag{2.2}$$

where we have $T_\nu \sim (4/11)^{1/3}T_\gamma \sim 1.96K \sim 10^{-4}$eV. At later times in the universe's history, the neutrinos have cooled sufficiently and their velocities drop below relativistic speeds, they transition to a non-relativistic regime. In this phase, their matter density is governed by the sum of their rest masses, such that $\rho_\nu \approx n_\alpha \sum_i m_i$, where m_i represents the masses of individual neutrinos. The sum of neutrino masses is required to be around 11.5eV if one wants the neutrinos to account for the DM, which is much greater than the upper limit from neutrino mass experiments involving β-decay [78]. There are other problems with active neutrinos playing the role of DM, one is that the neutrinos decouple whilst relativistic and only become nonrelativistic late in the matter-dominated epoch, around when $T \sim m_\nu c^2/k_B$, which for $m_\nu \approx 0.05\,\text{eV}$ gives $T \sim 0.6\,\text{K}$, which is far too late for them to cluster and form the observed structure. This means that the neutrinos would be hot DM when they decouple and therefore in conflict with structure formation due to their free-streaming damping any density fluctuations in the universe[10].

Another constraint is *Tremaine-Gunn bound*[11] which provides a lower bound on fermionic particle masses, or in this instance neutrino masses, from a phase-space study of high-speed neutrinos within a galaxy's DM halo, requiring their masses to be above a few hundred eV to prevent overpopulation of phase space and ensure consistency with fermion degeneracy.

Even though the active neutrinos of the SM are not capable of accounting for all the DM within the universe, it has not stopped physicists' attempts at

[9] Where α is the flavour index and result includes both helicity states.

[10] The free-streaming scale is given by

$$\lambda_{\text{FS}} \sim 20\left(\frac{30\,\text{eV}}{m_\nu}\right)\,\text{Mpc}. \tag{2.3}$$

Assuming a free-streaming length of $\lambda_{\text{FS}} \sim 300\,\text{Mpc}$, we estimate $m_\nu \sim 2\,\text{eV}$. However, current experimental bounds on the sum of neutrino masses, $\Sigma m_\nu < 0.12\,\text{eV}$, suggest that the free-streaming length is likely even larger, leading to neutrino masses well below 1 eV.

[11] Which has recently been extended to particles with a varying mass [89].

explaining DM with neutrino physics. As we shall discuss later, neutrinos give the only clear indication of beyond SM (BSM) physics due to their flavour oscillations which ultimately stem from them having a mass. Typically, to introduce neutrino masses to the SM one must introduce RH neutrino fields to the SM, which are strongly motivated by *grandunified theories* (GUTs), such as extensions based on $SO(10)$[90]. These extensions involving the addition of RH neutrinos are attractive as they are quite minimal and can not only account for the neutrino masses but also in some scenarios these sterile neutrinos can account for DM[12], and the baryon asymmetry of the universe. One popular extension which gained much traction in the 2000s is the *neutrino minimal SM* (νMSM) [78, 91, 92, 93] which introduces RH neutrino fields (also called sterile neutrino as they are essentially sterile to SM interactions) to the SM along with around 18 new parameters (seesaw parameters) [92]. These new parameters are typically three Majorana masses, three diagonal Yukawa couplings for neutrinos, six mixing angles (left and right), and six CP violating phases. The νMSM extends the SM Lagrangian by[13]

$$-\mathcal{L}^{\nu}_{Y+M} = \overline{L_{\alpha}} h_{\alpha J} N_{RJ} \tilde{\Phi} + \frac{1}{2} \overline{N^{c}_{RI}} D_{MIJ} N_{RJ} + \text{h.c.}, \tag{2.4}$$

where we have added a Yukawa term for neutrinos and a Majorana mass term for the RH neutrino fields, where we have neglected the kinematic term. Within these νMSM the neutrino masses are typically explained via the type-I seesaw, dark matter is often explained through active-sterile neutrino mixing[14], whilst the matter-antimatter asymmetry is produced due to leptogenesis from sterile-sterile neutrino mixing [19]. In much of the literature, the lightest sterile neutrino N_1, which plays the role of DM, typically has a mass of $m_{\text{DM}} \sim \mathcal{O}(1)$ keV and is often classified as warm dark matter,

[12] As originally proposed in [14].

[13] If the RH neutrino is a Dirac particle the second term on the RHS (the Majorana mass term) would not be present.

[14] Which can be resonant [94] or non-resonant production [14], as two early examples. To expand on this, typically the RH neutrinos have small couplings to the SM particles, yet if they mix with the active neutrinos which are in thermal equilibrium when the universe is over a few MeV in temperature, then the RH neutrinos can be produced through neutrino oscillations. If the neutrino total lepton number vanishes then one has a Dodelson-Widrow process, if the total lepton number does not vanish, then one has a Shi-Fuller process, where the asymmetry results in a resonant enhancement.

although this depends on its production mechanism[15]. Within this model low-energy neutrino data can be satisfied [92], however, astrophysical constraints from X-ray observations and computational constraints from N-body simulations require that a large lepton asymmetry is present for efficient resonant production [94]. It is possible that this large lepton asymmetry is produced through one of the two heavier seesaw sterile neutrinos decaying (not the DM neutrino), without the need of any additional physics, providing there is a strong degeneracy of the two heavier seesaw RH neutrinos. Perhaps the most interesting feature is that a 7keV sterile neutrino could be responsible for producing the 3.5keV X-ray anomaly [16] [96], with recent numerical simulations showing this scenario is capable of fulfilling all requirements including the 3.5keV anomaly [97]. Unfortunately, a problem with this scenario is that the high degree of fine-tuning requires the degeneracy of the heavier RH neutrinos to be of $\sim \mathcal{O}(10^{-16})$. Finally, it is expected that the XRISM satellite is capable of resolving the 3.5keV anomaly or alternatively provide strong constraints on the decay of warm neutrino DM [98], thus potentially ending the hope that νMSM is capable alone of explaining the origin of matter in the universe. Another interesting possibility is the scope of this work, RHINO DM [99, 1], that we have mentioned briefly, where the νMSM is extended to also include Higgs portal operators along with a larger DM RH neutrino mass than is present in typical νMSM models.

[15] Although a keV mass is commonly discussed, sterile neutrinos could also exist at other mass scales.

[16] This due to a suppressed secondary decay channel of the DM RH neutrino, $N \to \nu + \gamma$, which produces a photon with energy $E = M_{\rm DM}/2$ [95].

3 The Standard Model and Neutrinos

> "I have done a terrible thing. I have postulated a particle that cannot be detected." - Wolfgang Pauli

In this section, important properties of the SM are divulged with a particular emphasis on leptons, starting with the Lagrangian, before next introducing neutrinos, which is then followed by the Dirac equation. Chirality and helicity are then introduced along with discrete symmetries and the Higgs mechanism, before finally briefly discussing the weak interaction.

3.1 The Lagrangian

The *Lagrangian* is the starting point of theories in QFTs, in classical physics the Lagrangian is given by

$$L = T - V, \tag{3.1}$$

where T is the kinetic energy and V the potential energy. Integrating this overtime yields the action such that

$$S = \int dt\, L = \int dt\, dx\, \mathcal{L}, \tag{3.2}$$

where the Lagrangian density $\mathcal{L}$ has been introduced. The Lagrangian density is integrated over spatial dimensions to yield the Lagrangian. Nature favours the path that minimises or maximises the action; these are stationary points where the function is at an extrema. The stationary points of the action functional can be found through the calculus of variations, and upon doing so one arrives at the famous Euler-Lagrange equation, which for a Dirac field is[17]

[17] There are many different forms of the Euler-Lagrange equation depending on the system and thus the Lagrangian being studied.

$$\frac{\partial \mathcal{L}}{\partial \overline{\psi}} = \partial_\mu \left(\frac{\partial \mathcal{L}}{\partial \left(\partial_\mu \overline{\psi} \right)} \right), \tag{3.3}$$

where ∂_μ is the four-derivative and $\overline{\psi}$ is the field which takes a space-time input and outputs the relevant field value(s), fields are more fundamental than particles, with particles representing excitations of the underlying fields. When a Lagrangian is plugged into its correct Euler-Lagrange equation, we obtain the equations of motion for the system. An example of a Lagrangian is the Dirac Lagrangian which takes the form

$$\mathcal{L} = \overline{\psi}(x)(i\partial\!\!\!/ - m)\psi(x), \tag{3.4}$$

which upon insertion into the Dirac Euler-Lagrange equation, eq. (3.3), produces the *Dirac equation*

$$(i\partial\!\!\!/ - m)\psi(x) = 0, \tag{3.5}$$

which is the equation of motion for a Dirac field. Lagrangians are at the heart of particle physics and the SM, additional terms in the Lagrangian can represent different particles and their interactions, with the SM Lagrangian containing all particles and their interactions, however, it is typically convenient to only include the terms of interest, this is because the other terms add no relevant physics when studying a specific process.

3.2 Introduction to Neutrinos

First postulated by Wolfgang Pauli in 1930 the neutrino was introduced to ensure conservation of properties such as energy, momentum, and angular momentum (spin) in *beta decay* (β-decay). The neutrino was initially named the neutron; however, in 1932 James Chadwick discovered a much more massive neutral particle, which today is known as the neutron. The name neutrino was first termed by Enrico Fermi and Edoardo Amaldi, which in Italian means 'little neutral one'. The Fermi beta decay process [100] is

$$n \to p + e^- + \overline{\nu}_e, \tag{3.6}$$

where the heavy neutral neutron decays into a proton, an electron, and an antineutrino (as this conserves *lepton number*[18]). In the SM, neutrinos are thought to be massless and do not participate in electromagnetic interactions or strong interactions, but they do participate in weak interactions such as beta decay. Neutrinos are extremely elusive particles, and for a period it was thought that they would not be detected, so as an example of how weakly neutrinos interact with matter let us compare the cross section of two similar processes. In the first instance, if we collide a photon with a proton, the cross section is $\sigma_{\gamma+p\to\gamma+p} \simeq 10^{-25}\text{cm}^2$, while if we collide an antineutrino with a neutron, the cross section for this process is $\sigma_{\bar{\nu}_e+n\to\bar{\nu}_e+n} \simeq 10^{-45}\text{cm}^2$. Thankfully, neutrinos were directly detected in 1956 by Cowan and Reines in an inverse β-decay [101], $\bar{\nu}_e + p \to n + e^+$. The antineutrinos detected were emitted from uranium fission fragments undergoing β decay. The antineutrino energy spectrum that was detected peaked at a few MeV, with the neutrino detector located roughly 10m away from the reactor underground to reduce the noise from other particles and their interactions. Another important moment for neutrino physics was the discovery of lepton flavour, initially in charged leptons, which led to understanding why we do not see $\mu \to e + \gamma$ in nature. A similar result was then obtained from the neutrino parallel; why do we not see $\bar{\nu}_\mu + p \to e^+ + n$? It turns out they're different flavours and as such $\nu_e \neq \nu_\mu \neq \nu_\tau$, whereby is it thought that lepton number, L, is mostly a conserved quantity in nature.

Neutrinos have many sources and can be classified as artificial or natural. Artificial or man-made neutrinos are made by nuclear reactors, particle accelerators, and nuclear weapons. Reactor neutrinos are produced by fissile isotopes decaying into neutron-rich daughter nuclides that then undergo rapid beta decays resulting in neutrinos. Accelerator neutrinos are produced in particle colliders, which typically involve colliding protons with some target particles resulting in charged pions, which are then focused using electromagnets. These charged pions then decay whilst the relativistic boost provided by the electromagnets then produce the neutrinos in a beam (not isotropically), whilst the other daughter particles can then be filtered out by some material, which leaves only a neutrino beam. Natural neutrinos are produced through naturally occurring processes such as interactions within the

[18]Where lepton flavour is not always conserved, see neutrino oscillations in Section 4, total lepton number does seem to be mostly conserved, however, processes such as the sphaleron process does not conserve total lepton number, but does conserve $B - L$.

Earth's core, interactions from cosmic rays and the atmosphere, a byproduct of nuclear fusion within the core of a star, or supernovae. The weakly interacting nature of neutrinos allows us to investigate processes without or with minimal noise and effects from other background processes.

3.3 The Dirac Equation

Let us start our description of neutrinos by stating that in the pure SM neutrinos are massless, and for the time being we continue with this notion. The Dirac equation was derived by British physicist Paul Dirac in 1928 and in its free form describes all freely propagating spin-1/2 particles, such as leptons and quarks. An important feature of the Dirac equation is that it is consistent with both quantum mechanics and special relativity, unlike Schrödinger's equation which is not Lorentz invariant. The Dirac equation implied a new type of matter in the form of negative energy solutions; these negative energy solutions are today known as antimatter; this discovery was a major break through in physics with many, including Dirac displaying scepticism. The free form covariant Dirac equation in natural units and making use of the Feynman slash notation is

$$(i\not{\partial} - m)\psi(x) = 0. \tag{3.7}$$

Where ψ is a four-component Dirac spinor field, m is the mass, and $\not{\partial} \equiv \gamma^\mu \partial_\mu$, with γ^μ being the Dirac matrices also known as the gamma matrices which form a matrix representation of the underlying *Clifford algebra*, which is anti-commutative as expected for fermions. The gamma matrices can take on different representations as long as they represent the Clifford algebra, $\mathrm{CL}_{1,3}(\mathbb{R})$. In matrix form, this condition is

$$\{\gamma^\mu, \gamma^\nu\} = 2\eta^{\mu\nu} I, \tag{3.8}$$

with $\eta^{\mu\nu}$ being the Minkowski metric, and I being the 4×4 identity matrix. Some forms or representations of the Dirac matrices are more useful than others, depending on the circumstances. Three important representations are the Dirac-Pauli representation, the chiral/Weyl representation, and the Majorana representation[19]. The Dirac representation is best for dealing

[19]In the Majorana representation the gamma matrices are pure imaginary.

with particle and antiparticle states, with the four entries in the spinor accounting for spin-up and spin-down particle components, and spin-up and spin-down antiparticle components. This basis is often used in the literature. The chiral/Weyl representation is especially useful for dealing with massless neutrinos. The free theory expansion of the Dirac spinor field after quantisation is given by

$$\psi_\alpha(\vec{x}) = \sum_{s=1}^{2} \int \frac{d^3p}{(2\pi)^3} \frac{1}{\sqrt{2E_{\vec{p}}}} a^s_{\vec{p}}\, u^s_\alpha(\vec{p}) e^{-i\vec{p}\cdot\vec{x}} + b^{s\dagger}_{\vec{p}} v^s_\alpha(\vec{p}) e^{+i\vec{p}\cdot\vec{x}}, \tag{3.9}$$

with $a^s_{\vec{p}}$ being the annihilation operator for a particle and u^s_α being the corresponding spinor, whilst $b^{s\dagger}_{\vec{p}}$ is the creation operator for an antiparticle with v^s_α corresponding to its spinor[20]. The α subscript labels the component of the spinor and the s superscript indicates the helicity indices. To form a probability four-current we must introduce the Dirac adjoint, which is given by $\overline{\psi} \equiv \psi^\dagger \gamma^0$, where γ^0 is the time-like gamma matrix.

3.4 Chirality and Helicity

A general Dirac spinor field in the Weyl/chiral representation can be decomposed into left-handed and right-handed chiral components (denoted by subscripts L and R, respectively) with the use of a chirality projector operator [102], such that

$$\psi = \psi_{\mathrm{L}} + \psi_{\mathrm{R}} \equiv P_{\mathrm{L}}\psi + P_{\mathrm{R}}\psi, \tag{3.10}$$

with the right- and left-handed chiral projection operators given by

$$P_R = \frac{1+\gamma^5}{2}, \quad P_L = \frac{1-\gamma^5}{2}. \tag{3.11}$$

Here, the matrix γ^5 has been introduced and can be expressed by the other gamma matrices as $\gamma^5 = i\gamma^0\gamma^1\gamma^2\gamma^3$. The fifth gamma matrix is also the chirality operator such that

[20]Note that † indicates the Hermitian conjugate of a matrix, which for real observables we have $A^\dagger = A$.

$$\gamma^5\psi_L = -\psi_L \,, \text{and}\, \gamma^5\psi_R = +\psi_R. \tag{3.12}$$

The chiral representation has advantages over the Dirac representation discussed earlier as the top two elements in the spinor are defined as spin-up and spin-down left-handed chiral fields, and the bottom two elements are spin-up and spin-down right-handed chiral fields, which is unlike the Dirac representation in which the left- and right-handed fields are in combination within the spinors entries. This means that in the chiral basis the four-spinor takes the form $\psi = (\psi_{\rm L}, \psi_{\rm R})^T$, known as a bispinor which contains two (two-component) Weyl spinors, $\psi_{\rm L}$ and $\psi_{\rm R}$. It is important to note that both Weyl spinors transform independently under Lorentz transformations, and as such they form an irreducible basis for the Lorentz group and thus are fundamental building blocks to the SM. More accurately they transform as fundamental representations of the Lorentz group SO(1,3), such that the left- and right-handed fields transform as $(1/2, 0)$ and $(0, 1/2)$ respectively, and together they form the elements of a four-dimensional complex vector space $(1/2, 0) \bigotimes (0, 1/2)$ representation of the Lorentz group[21]. Chirality is a property of the field and in the massless limit a left-handed chiral field destroys a negative helicity particle state (left-handed) and creates a positive helicity antiparticle state. On the other hand, a right-handed chiral field destroys a positive helicity particle state (right-handed) and creates a negative helicity antiparticle. The helicity of a particle is defined by [102]

$$\hat{\lambda} = \frac{\vec{S} \cdot \vec{p}}{|\vec{p}|}, \tag{3.13}$$

where $\vec{S}$ is the spin vector and $\vec{p}$ is the momentum. From the helicity operator a positive helicity state is that in which the spin direction is the same as the momentum, whilst a negative helicity state is one in which the spin and momentum are in opposing directions. Let us also explicitly state that in the massless limit both helicity and chirality coincide.

[21]The Dirac spinor is reducible, as evidenced by the γ^5 matrix, which distinguishes between left-handed and right-handed components.

3.5 Discrete Symmetries

There are three discrete symmetries [103, 104] within particle physics, these are time reversal symmetry or T symmetry, parity symmetry or P symmetry, and charge symmetry or C symmetry. These discrete transformations are often representation-dependent. Discrete symmetries are noncontinuous symmetries, an example of a noncontinuous symmetry is a square which features symmetry only with $\pi/2$ rotations around the centre, which is unlike a circle as a circle has a continuous symmetry upon rotation by any angle. P-symmetry involves flipping the spatial coordinates

$$\psi(t,\vec{x}) \mapsto P\psi(t,\vec{x}) = \psi(t,-\vec{x}). \tag{3.14}$$

Functions that are unchanged by parity transformations are called even functions, while those that change their sign under a parity transformation are known as odd functions. Parity transformations swap the chirality of fields so that left-handed fields transform into right-handed fields, and vice versa. The parity operator also changes the sign of a particles momentum, and thus the helicity due to the spin of the particle remaining constant. The T symmetry involves reversing the time so that

$$\psi(t,\vec{x}) \mapsto T\psi(t,\vec{x}) = \psi(-t,\vec{x}). \tag{3.15}$$

Finally, charge conjugation swaps particles with their antiparticles

$$\psi(t,\vec{x}) \mapsto \psi(t,\vec{x})^c = C\overline{\psi(t,\vec{x})}^T, \tag{3.16}$$

similarly to parity, charge conjugation flips the chirality of a field such that $(\psi_L)^c = (\psi^c)_R$ and vice versa, whilst keeping helicity constant. Another interesting discrete transformation is a CP transformation, which leaves chirality unchanged but changes particles into antiparticles whilst also swapping helicity states.

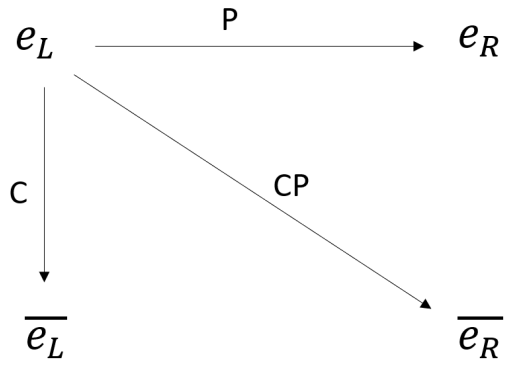

Figure 6: The effect of P, C, and CP transformations on an electron.

3.6 Spontaneous Symmetry Breaking and the Dirac Mass Term

The Higgs boson is the particle excitation of the Higgs field, which is a complex scalar field. Before electroweak spontaneous symmetry breaking (EWSB) [105], the Higgs field is a two-component $SU(2)$ doublet of weak isospin with a neutral and charged component. The Higgs potential is "Mexican hat-shaped" and takes the form

$$V(\phi) = -\mu^2 \phi^\dagger \phi + \lambda \, (\phi^\dagger \phi)^2, \tag{3.17}$$

with λ describing the quartic self-interactions among the scalar fields. Where, due to vacuum stability, it is assumed positive, $\lambda > 0$, and μ is the mass. The Higgs doublet is given by

$$\Phi = \begin{bmatrix} \phi^+ \\ \phi^0 \end{bmatrix}, \tag{3.18}$$

with ϕ^+ being the charged complex scalar component and ϕ^0 the neutral complex scalar component, each having two degrees of freedom (DOF). After EWSB, one degree of freedom of ϕ^0 is absorbed by the Z boson, which provides its longitudinal polarisation. This leaves one physical degree of freedom in the neutral component, which corresponds to a scalar field where Higgs bosons are its excitations. The charged components of ϕ^+ are absorbed

by the $W^{\pm}$ bosons, which provides their longitudinal polarisations and leaves no physical charged scalar. For $\mu > 0$ the scalar Higgs field develops a non-zero vacuum expectation value (VEV) which spontaneously breaks symmetry resulting in[22]

$$\langle \phi_0 \rangle = \frac{1}{\sqrt{2}} \begin{bmatrix} 0 \\ v(= 246\text{GeV}) \end{bmatrix} = \begin{bmatrix} 0 \\ v/\sqrt{2}(= 174\text{GeV}) \end{bmatrix}, \tag{3.19}$$

where due to conservation of electric charge only the neutral scalar field can acquire a VEV. After EWSB, what remains is an unbroken electromagnetism such that

$$SU(2)_L \times U(1)_Y \to U(1)_Q. \tag{3.20}$$

Before EWSB the mass term for fermions within the SM is given by the standard Higgs mechanism via Yukawa couplings. In the case of charged leptons, the Lagrangian is given by

$$\mathcal{L}_Y^l = \overline{L_\alpha} h_{\alpha\alpha}^l \alpha_R \Phi + \text{h.c.}, \tag{3.21}$$

where $L_\alpha^T \equiv (\nu_{L\alpha}, \alpha_L)$ is the left-handed leptonic doublet, with the Greek letters indicating the charged lepton flavours, $\alpha = e, \mu, \tau$. After EWSB the Higgs VEV generates a *Dirac mass* matrix, $m_D = vh$, this results in the charged lepton mass Lagrangian taking the form

$$\mathcal{L}_D^l = \overline{\alpha_L} m_D \alpha_R + \text{h.c.}, \tag{3.22}$$

where similar to the quark sector one can choose the charged lepton Yukawa couplings to be diagonal and thus the Dirac mass matrix is also diagonal. It is clear from this term that both left- and right-handed chiral fields are required for a particle to obtain a mass through Yukawa couplings.

[22]Both 246GeV and 174GeV are used in literature for the Higgs VEV and/or the electroweak scale, however, for our work we use the latter for the Higgs VEV, $\langle \phi_0 \rangle = v = 174\text{GeV}$.

3.7 The Weak Interactions

Within the SM we can divide the particles into two types fermions and bosons, with fermions being matter particles whilst bosons are the force carrying particles. The fermions are divided into two different types of particles, leptons and quarks, each with three generations or flavours. Gauge theories are fundamental to explaining the interactions of fermions which are mediated by gauge bosons. In fact, three of the four fundamental forces, these being the electromagnetic interaction, the weak interaction, and the strong interaction, are described by a different gauge theory. The electromagnetic force is explained through QED and is based on a $U(1)$ gauge symmetry. The strong nuclear force is described by QCD and is based on a $SU(3)$ gauge symmetry, which corresponds to the colour charge and explains interactions between quarks and gluons. Upon quantisation of the gauge fields we get the gauge bosons. The weak force can be unified with the electromagnetic interaction into the electroweak force that is on a $SU(2)_L \times U(1)_Y$ gauge symmetry. There is also hope that the electroweak force can be unified with the strong force at a scale of $\sim 10^{16}$GeV, known as the GUT scale. The electromagnetic force features one massless gauge boson, the photon, and the weak interaction features three massive gauge bosons, two of which are charged the W^+ and W^- bosons, and one neutral the Z boson. However, QCD has eight force-carrying gluons. Overall, the SM is based on a gauge theory with a $SU(3)_c \times SU(2)_L \times U(1)_Y$ symmetry.

The weak interaction [106] is unique compared to the other fundamental forces as it is chiral sensitive and only couples to left-chiral fields. Thus, neutrinos are rather unique amongst fermions, as left-handed neutrinos are part of a $SU(2)_L$ doublet,

$$L_\alpha = \begin{bmatrix} \nu_\alpha \\ l_\alpha \end{bmatrix}, \tag{3.23}$$

and partake in weak interactions, whilst RH neutrinos do not and thus lack all SM quantum numbers. Therefore, should RH neutrinos exist, it is expected that they would be $SU(3)_c \times SU(2)_L \times U(1)_Y$ singlets[23]. This means that all neutrinos detected experimentally are in fact LH helicity neutrino states and that the antineutrinos are only RH helicity states. This lack of RH

[23]This is different to charged leptons as they couple to electromagnetic interactions.

neutrinos also implies a very important fact about neutrinos in the standard model - they are predicted to be massless.

From electroweak theory, we know that neutrinos couple to the Z boson through neutral currents by

$$L_{Z\nu\overline{\nu}} = \frac{e}{2\cos\theta_W \sin\theta_W} Z^\mu [J_\mu^{NC}]_\nu, \tag{3.24}$$

where θ_W is the Weinberg angle or weak mixing angle, e is the charge of an electron, and Z^μ is the Z boson, and one has that the neutral current is given by

$$\left[J_\mu^{NC}\right]_\nu = \sum_{i'=1,\ldots,N_\nu} \overline{\nu_{Li'}} \gamma_\mu \nu_{Li'}, \tag{3.25}$$

with $\nu_{Li'}$ being the neutrino fields, whilst $\overline{\nu}_{Li}$ are the antineutrino fields, while also noting that the primed Latin indices indicate that we are in a generic basis, which does not align with the mass or *flavour basis* and potentially arise from some BSM physics. LH neutrinos also couple to the $W^{+/-}$ bosons through charged currents

$$L_{Wl\nu} = \frac{2}{\sqrt{2}\sin\theta_W} [W_+^\mu J_{-\mu}^{lept} + W_-^\mu J_{+\mu}^{lept}], \tag{3.26}$$

where W_+^μ (W_-^μ) is the positively (negatively) charged W boson, while

$$J_{-\mu}^{lept} = (J_{+\mu}^{lept})^\dagger = \sum_i \overline{l_{Li'}} \gamma^\mu \nu_{Li'}, \tag{3.27}$$

with $\overline{l_{Li'}}$ being the charged lepton field. The number of active neutrino species, N_ν, can be determined from the Z boson line shape, as each neutrino species contributes equally to the Z boson's total decay width. The total decay width of the Z boson is given by

$$\Gamma_{\text{tot}} = \Gamma_{\text{had}} + \Gamma_{\text{chlep}} + \Gamma_{\text{inv}}, \tag{3.28}$$

where Γ_{had} is the decay width into hadrons, Γ_{chlep} is the decay width into charged leptons (of which there are three flavours: e, μ, τ), and Γ_{inv} is the invisible decay width, which is related to the number of neutrino species by

$$\Gamma_{\text{inv}} = N_\nu \cdot \Gamma_\nu \tag{3.29}$$

with N_ν being the number of active neutrino species, and Γ_ν is the decay width into a neutrino species. Experimentalists at the Large Electron-Positron Collider (LEP) have performed highly precise measurements of Γ_{tot}, Γ_{had}, and Γ_{chlep} using processes such as $e^+ + e^- \to \mu^+ + \mu^-$. The decay width for a single neutrino species can be calculated theoretically as

$$\Gamma_\nu = \frac{G_F M_Z^3}{12\sqrt{2}\pi}, \tag{3.30}$$

where G_F is Fermi's constant, and M_Z is the mass of the Z boson. By combining these experimental measurements with the theoretical prediction for Γ_ν, the number of neutrino species can be calculated as

$$N_\nu = \frac{\Gamma_{\text{tot}} - \Gamma_{\text{had}} - 3\Gamma_{\text{chlep}}}{\Gamma_\nu} = 2.9840 \pm 0.0082. \tag{3.31}$$

This result confirms the existence of three active neutrino species, consistent with the SM. [107]

4 Neutrino Oscillations

In this section, it is shown why the assumption of massless neutrinos within the SM is incorrect, starting with the Homestake experiment and the solar neutrino disappearance problem. The solution to this problem is then discussed in the form of neutrino mixing, where matter effects in the Sun (MSW effect) enhance oscillations and require neutrinos to be massive. Then two different approaches to neutrino mixing are considered, starting with the Schrödinger-like formalism. Finally, the density matrix formulation and its vectorial parameterisation are discussed.

4.1 Neutrino Mixing

In the 1960s the Homestake experiment [108] made the first attempt to detect fluxes of electron neutrinos produced from proton-proton nuclear fusion reactions in the Sun; these neutrinos are known as solar neutrinos. This experiment did not yield the expected results, the detected flux being lower than expected by around 30%-50%. This problem was unsolved for around 40 years and became known as the solar neutrino problem. The solution to the solar neutrino problem resulted in the Nobel prize for R. Davis for developing the Homestake experiment, and A.B. McDonald who led the Sudbury Neutrino Observatory (SNO) experiment [109] which played a major role in detecting the missing neutrinos, thus resolving the problem. The solution to this problem is a phenomenon known as neutrino mixing which then results in neutrino oscillations.

To better understand this problem, let us assume that neutrinos are in fact massive, and similarly to how we treat down-type quarks, this would imply that the neutrino states that partake in weak interactions, the weak eigenstates, do not align with the mass eigenstates. To further clarify this, in the case of quarks if we assume that the weak charged currents are diagonal, then we can diagonalise the up-type quarks and then absorb this by redefining the down-type weak interaction quarks, however, in doing so we cannot redefine the down-type mass term; thus, it will not be diagonal. In the quark sector, a mixing matrix exists that performs this transformation from weak eigenfields to mass eigenfields; this matrix is known as the *quark mixing matrix* (Cabibbo-Kobayashi-Maskawa matrix or CKM matrix) [110] such that

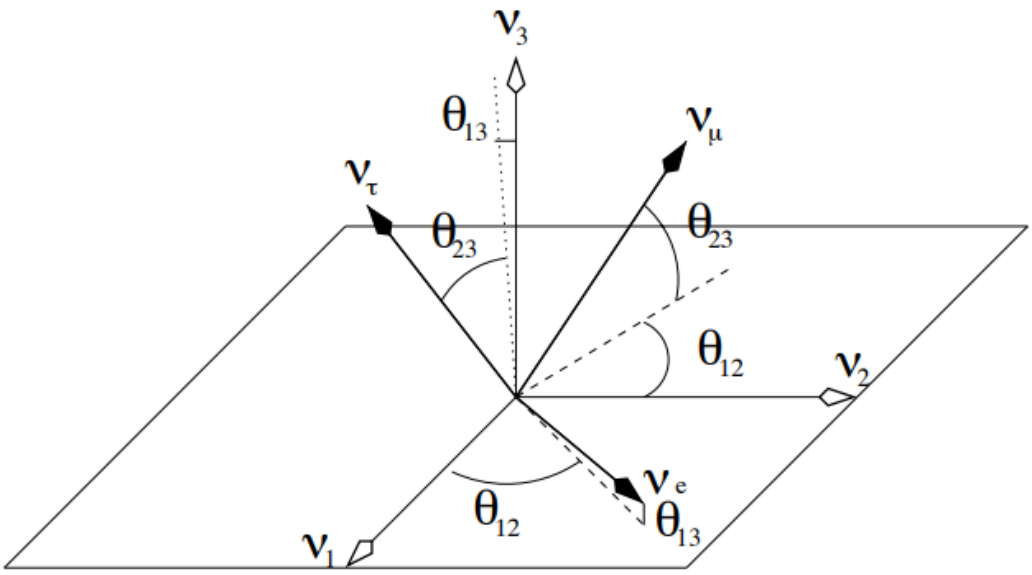

Figure 7: A visualisation of the neutrino mixing angles assuming no CP violation. The mixing angles between ν_i and ν_j, the mass eigenstates are denoted θ_{ij}. The weak interaction states produced from this mixing are denoted by ν_e, ν_μ, and ν_τ. This image is extracted from Ref. [12].

$$\begin{pmatrix} d' \\ s' \\ b' \end{pmatrix} = \begin{pmatrix} V_{ud} & V_{us} & V_{ub} \\ V_{cd} & V_{cs} & V_{cb} \\ V_{td} & V_{tc} & V_{tb} \end{pmatrix} \begin{pmatrix} d \\ s \\ b \end{pmatrix} . \tag{4.1}$$

This CKM matrix which parameterises the mixing of the down-type quark mass eigenstates into the weak eigenstates has been experimentally verified, with values [111]

$$|V_{\mathrm{CKM}}| = \begin{pmatrix} |V_{ud}| & |V_{us}| & |V_{ub}| \\ |V_{cd}| & |V_{cs}| & |V_{cb}| \\ |V_{td}| & |V_{tc}| & |V_{tb}| \end{pmatrix} \simeq \begin{pmatrix} 0.97370 & 0.2245 & 0.00382 \\ 0.221 & 0.987 & 0.0410 \\ 0.0080 & 0.0388 & 1.013 \end{pmatrix} , \tag{4.2}$$

which is almost the identity matrix, and thus displays extremely small mixings. Parallel to the quarks lets introduce the *lepton mixing matrix*

(Pontecorvo-Maki-Nakagawa-Sakata or PMNS matrix) which relates the flavour or weak interactions eigenfields to the mass eigenfields by [112],

$$\nu_\alpha = \sum_{i=1}^{N} U_{\alpha i}\nu_i, \tag{4.3}$$

where the mass eigenfields are indicated by the Latin index and the flavour eigenfields are indicated with Greek letters ($\alpha = e, \mu, \tau$), if we expand this in the case of three mass eigenfields, we get

$$\begin{pmatrix}\nu_e\\ \nu_\mu\\ \nu_\tau\end{pmatrix} = \begin{pmatrix}U_{e1} & U_{e2} & U_{e3}\\ U_{\mu 1} & U_{\mu 2} & U_{\mu 3}\\ U_{\tau 1} & U_{\tau 2} & U_{\tau 3}\end{pmatrix}\begin{pmatrix}\nu_1\\ \nu_2\\ \nu_3\end{pmatrix}. \tag{4.4}$$

with current ranges [113]

$$|U_{\text{PMNS}}| \simeq \begin{pmatrix}0.801-0.845 & 0.513-0.579 & 0.413-0.155\\ 0.234-0.500 & 0.471-0.689 & 0.637-0.776\\ 0.271-0.525 & 0.477-0.694 & 0.613-0.756\end{pmatrix}, \tag{4.5}$$

where upon comparison to the CKM matrix we see that the mixings of the neutrinos are much larger than that of the quarks[24]. The number of mass eigenfields can also be higher than 3, as there are potentially sterile neutrinos that do not couple to the weak interaction [114]. A standard parameterisation for the lepton mixing matrix is[25]

$$U_{\text{PMNS}} = V \cdot P, \tag{4.6}$$

with

$$V = \begin{pmatrix} c_{12}c_{13} & s_{12}c_{13} & s_{13}e^{-i\delta}\\ -s_{12}c_{23} - c_{12}s_{23}s_{13}e^{i\delta} & c_{12}c_{23} - s_{12}s_{23}s_{13}e^{i\delta} & s_{23}c_{13}\\ s_{12}s_{23} - c_{12}c_{23}s_{13}e^{i\delta} & -c_{12}s_{23} - s_{12}c_{23}s_{13}e^{i\delta} & c_{23}c_{13}\end{pmatrix}, \tag{4.7}$$

[24]There is no reason not to expect mixings when compared to the quark sector, however, it is a mystery as to why the mixings are so large when compared to the quark sector. Many ideas have been proposed to try and explain these large mixings; see Ref. [12].

[25]If the discussion is about quarks, one does not include the Majorana phases and thus no P matrix is present.

and

$$P = \text{diag}(e^{i\alpha_1}, e^{i\alpha_2}, 1), \tag{4.8}$$

where $s_{ij} \equiv \sin\theta_{ij}$, and $c_{ij} \equiv \cos\theta_{ij}$. Neutrino mixing, and thus the PMNS matrix, requires the introduction of new parameters to the SM. The new parameters within the leptonic mixing matrix are the three mixing angles $\theta_{12}, \theta_{13}, \theta_{23}$, and the three phases $\delta, \alpha_1, \alpha_2$, where one of these phases is the Dirac phase δ, whilst the other two of these phases are the hypothetical Majorana phases α_1, and α_2. It is also possible that there exists some other basis arising from BSM physics seeking to explain fermionic masses, and as such it can be convenient to introduce a transformation from the mass basis to this new generic basis denoted by the primed indices [115]

$$\nu_{Li'} = \sum_{i=1}^{N} U^{\nu}_{Li'i}\nu_i. \tag{4.9}$$

Due to this, the leptonic mixing matrix can then be regarded as a combination of two transformations, with the first transformation taking the state from the mass basis to the primed basis and the second transformation taking us from the primed state to the flavour basis

$$U = U^l_L U^{\nu}_L. \tag{4.10}$$

4.2 Neutrino Oscillations

In 1957 Bruno Pontecorvo [116] predicted neutrino oscillations [114, 112, 117]. Neutrino oscillations are quantum mechanical phenomena. When neutrinos leave a source as a specific flavour, for example, as an electron neutrino, their state can later be measured as a different flavour. The probability of detecting a particular neutrino flavour oscillates as the neutrino propagates through space. The case of missing solar neutrinos is a more complex situation than neutrino oscillations in a vacuum. Electron neutrinos are produced in the Sun's core, and initially, the flavour eigenstates are almost identical to their matter eigenstates. However, this alignment

changes as they travel outward through the Sun's plasma, where the density gradually decreases with distance from the core. Therefore, one must account for these changes through matter effects, specifically the *Mikheyev–Smirnov–Wolfenstein* (MSW) effect. As the Sun's density decreases, the composition of the matter eigenstates evolves so that it no longer coincides with the flavour eigenstate. This change in the matter eigenstate occurs slowly enough for the adiabatic condition to be satisfied, allowing the neutrinos to track this matter eigenstate without oscillating. After leaving the Sun, electron neutrinos depart from their matter eigenstates and are no longer purely electron neutrinos, resulting in a mixture of neutrino flavours [118].

It is also important to reiterate that neutrino oscillations can occur only if neutrinos are massive, as we shall see. It is important to note that we only know an approximate upper bound on the sum of the neutrino masses with a current bound of approximately $\sum m_\nu < 0.14\text{eV}$ with a 95% confidence level [119]. Let us now proceed with a neutrino oscillation calculation by starting with an ultra-relativistic neutrino state produced at $t = 0$ in flavour α; at a later time, t, the ultra-relativistic neutrino flavour state ket can be related to the mass state ket by

$$|\nu_\alpha(t)\rangle = \sum_i U^*_{\alpha i} \, |\nu_i(t)\rangle \, . \tag{4.11}$$

In charged current interactions the probability that this state α is detected in some state β is given by $P_{\alpha\beta} \equiv |\langle\nu_\beta|\nu_\alpha\rangle|^2$. If the start and end flavours are the same, one has $P_{\alpha\alpha}$, this is called the survival probability, if the start and end flavours are not the same, $P_{\beta\neq\alpha}$, then this is the appearance probability. If we sum all the different possible appearance probabilities and subtract these from unity we get the disappearance probability of the neutrino state α, $\sum P_{\beta\neq\alpha} = 1 - P_{\alpha\alpha}$. The oscillation probability can also be expressed in term of mass eigenstates as

$$P_{\alpha\beta}(t) \equiv |\, \langle\nu_\beta|\nu_\alpha(t)\rangle \,|^2 = |\sum_{i,j} U^*_{\alpha i} U_{\beta j} \langle\nu_j|\nu_i(t)\rangle|^2, \tag{4.12}$$

which can then be computed using the standard plane wave approxima-

tion[26], the ultra-relativistic approximation[27], and the orthonormality condition[28] to obtain a general transition probability in a vacuum

$$\begin{aligned} P_{\alpha\beta}(t) = \delta_{\alpha\beta} - 4\sum_{i<j}^{1,3} \mathrm{Re}[U_{\alpha i}U^{\star}_{\beta i}U^{\star}_{\alpha j}U_{\beta j}]\sin^2\Big(\pi\frac{l}{l^0_{ij}}\Big) \\ +2\sum_{i<j}^{1,3} \mathrm{Im}[U_{\alpha i}U^{\star}_{\beta i}U^{\star}_{\alpha j}U_{\beta j}]\sin\Big(2\pi\frac{l}{l^0_{ij}}\Big). \end{aligned} \tag{4.14}$$

with

$$l^0_{ij} \equiv \frac{4\pi E}{\Delta m^2_{ij}} \approx 2.48\mathrm{km}\frac{E(\mathrm{GeV})}{\Delta m^2_{ij}(\mathrm{eV}^2)}, \quad \Delta m^2_{ij} \equiv m^2_j - m^2_i, \tag{4.15}$$

where l^0_{ij} is the oscillation length, whilst Δm^2_{ij} is the mass squared difference of the mass eigenstates. From this several important conclusions can be determined about neutrino oscillations. Firstly, neutrino oscillations require neutrinos to have mass with the different neutrino generations having different masses, as the oscillation length is inversely proportional to the masses $l^0_{ij} \propto 1/\Delta m^2_{ij}$. Secondly, if $l \ll l^0_{ij}$, then the oscillations do not have enough time to develop, on the other hand if $l \gg l^0_{ij}$, only the averaged oscillation probability can be measured, whilst maximum sensitivity is when $l \approx l^0_{ij}$. The second term in Eq. eq. (4.14) is CP conserving, whilst the third term is CP violating[29]. Finally, with three neutrino masses there are only two independent differences in squared masses, Δm^2_{ij}, which are typically chosen to be Δm^2_{12} and Δm^2_{23}, with $\Delta m^2_{31} = \Delta m^2_{12} + \Delta m^2_{23}$. Neutrino oscillation

[26]The standard plane wave approximation is given by $|v_i(t)\rangle = e^{iE_i t}\,|v_i(0)\rangle$.

[27]Using Taylor expansion, the ultra relativistic approximation is given by

$$E_i = \sqrt{|\vec{p}|^2 + m^2_i} \simeq |\vec{p}| + \frac{m^2_i}{2|\vec{p}|}. \tag{4.13}$$

[28]The orthonormality conditions is defined as $\langle\nu_i|\nu_j\rangle = \delta_{ij}$.

[29]More specifically the CP violating parameter is known as the Jarlskog invariant and is defined as

$$J_{\mathrm{CP}} \equiv \mathrm{Im}[U_{\alpha i}U^{*}_{\alpha j}U^{*}_{\beta i}U_{\beta j}] \tag{4.16}$$

$$\equiv J^{\mathrm{max}}_{\mathrm{CP}} \sin\delta_{\mathrm{CP}} = \cos\theta_{12}\sin\theta_{12}\cos\theta_{23}\sin\theta_{23}\cos^2\theta_{13}\sin\theta_{13}\sin\delta_{\mathrm{CP}}, \tag{4.17}$$

experiments can give us detailed information on the difference between the masses; however, they cannot determine the absolute mass of the states. The hierarchy of the states' masses can be inferred by studying the sign of Δm^2_{32}, particularly in experiments involving matter effects. This is due to matter effects breaking the symmetry in the oscillation probability.

Another method for calculating neutrino oscillations is the Hamiltonian formulation, which we will not strictly compute; however, we will mention an important point about how a portion of the Hamiltonian does not contribute to the mixing. Starting in the mass eigenstate basis the Hamiltonian is given by

$$H_{ij} = \begin{pmatrix} E_1 & 0 \\ 0 & E_2 \end{pmatrix}, \tag{4.19}$$

which can then be decomposed into two terms

$$H_{ij} = \frac{E_1 + E_2}{2}\delta_{ij} + \Delta H_{ij}, \tag{4.20}$$

with ΔH_{ij} defined as[30]

$$\Delta H_{ij} = -\frac{\Delta m^2_{12}}{4E}\begin{pmatrix} 1 & 0 \\ 0 & -1 \end{pmatrix} = -\frac{\Delta m^2_{12}}{4E}\sigma_3. \tag{4.22}$$

This decomposition allows one to separate the Hamiltonian into a part that contributes to the mixing and the part proportional to the identify which only contributes an overall phase factor that is cancelled when calculating the probability of a transition from one flavour to another. *Matter*

where for NO (IO) at 1σ (3σ) we currently have [113]

$$J^{\max}_{\rm CP} = 0.0332 \pm 0.0008(\pm 0.0019). \tag{4.18}$$

[30]Where in the ultra relativistic approximation one has that $E_1 \approx E_2 \approx p \approx E$, and therefore

$$E_2 - E_1 = \frac{E_2^2 - E_1^2}{E_2 + E_1} = \frac{m_2^2 - m_1^2}{E_2 + E_1} \simeq \frac{m_2^2 - m_1^2}{2E} \equiv \frac{\Delta m^2_{12}}{2E}. \tag{4.21}$$

.

effects have not been considered, yet they can and do affect the mixing substantially; an example of this is the Mikheyev–Smirnov–Wolfenstein (MSW) effect [120] which played a substantial role in the solar neutrino problem. If matter effects are considered, these matter effects can contribute an *effective potential*, which is found on the diagonal elements of the flavour basis of the Hamiltonian and arises from charged current interactions. The neutral current interactions occur for all flavours and are proportional to the identity part of the Hamiltonian; thus, they have no influence on the mixing.

4.3 The Density Matrix

There are multiple ways of describing neutrino oscillations, another important method being the density matrix formulation [121, 122], which could be viewed as advantageous as it allows the evolution of mixed states and to deal with decoherence; however, we will assume a pure state $|\psi(t)\rangle$, with the density matrix given by

$$\rho(t) = |\psi(t)\rangle \langle\psi(t)| , \tag{4.23}$$

which is idempotent, hermitian, and possesses a unitary trace, with all entries in the density matrix required to be $0 \leq \rho_{ij} \leq 1$[31]. The time evolution of the density matrix is given by the von Neumann equation

$$\frac{\partial \rho(t)}{\partial t} = -i[\rho(t), \Delta H(t)], \tag{4.24}$$

where $H(t)$ is the time-dependent Hamiltonian. The expectation of an observable, A, can also be calculated from the density matrix such that

$$\langle A \rangle = \mathrm{Tr}[\rho A]. \tag{4.25}$$

In the case of two-neutrino mixing in the flavour basis, the probability that a state starting in some state α is later detected in some state β is given by

[31] To be idempotent requires that $\rho = \rho^2$, whilst a unitary trace (or of purity one) requires that $\mathrm{Tr}(\rho^2) = 1$, and to be Hermitian requires that $\rho = \rho^\dagger$.

$$\rho_{\alpha\beta} = \langle\beta|\psi\rangle \langle\psi|\alpha\rangle \,. \tag{4.26}$$

Using the von Neumann equation one can track the evolution of the density matrix, which is simpler to solve in the mass eigenstate basis. The mass eigenstate basis can be related to the flavour basis by

$$\begin{aligned} \rho_{ij} &= \langle i|\psi\rangle \langle\psi|j\rangle & (4.27)\\ &= \langle i|\beta\rangle \langle\beta|\psi\rangle \langle\psi|\alpha\rangle \langle\alpha|j\rangle & (4.28)\\ &= (U^\dagger)_{i\beta}\, \rho_{\beta\alpha}\, U_{\alpha j}. & (4.29) \end{aligned}$$

If we assume that all neutrinos are produced in a single flavor eigenstate, then initially one has

$$\begin{aligned} \rho_{ij} &= (U^\dagger)_{i\beta}\, \rho_{\beta\alpha}(0)\, U_{\alpha j} & (4.30)\\ &= \begin{pmatrix} \cos^2\theta_{ij} & \sin\theta_{ij}\cos\theta_{ij} \\ \sin\theta_{ij}\cos\theta_{ij} & \sin^2\theta_{ij} \end{pmatrix}, & (4.31) \end{aligned}$$

where the two-neutrino mixing matrix is given by the two-dimensional rotation matrix

$$U_{\alpha j} = \begin{pmatrix} \cos\theta_{ij} & -\sin\theta_{ij} \\ \sin\theta_{ij} & \cos\theta_{ij} \end{pmatrix}, \tag{4.32}$$

where θ_{ij} is the mixing angle between state i and state j. The von Neumann equation in the mass basis is then given by

$$\frac{\partial \rho_{ij}(t)}{\partial t} = -i[\rho(t), \Delta H(t)]_{ij}. \tag{4.33}$$

From the von Neumann equation in the mass eigenstates basis it is then possible to evolve the density matrix to some time t and in doing so one arrives at the following

$$\rho_{ij} = \begin{pmatrix} \cos^2\theta_{ij} & \sin\theta_{ij}\cos\theta_{ij} e^{i(E_j - E_i)t} \\ \sin\theta_{ij}\cos\theta_{ij} e^{-i(E_j - E_i)t} & \sin^2\theta_{ij} \end{pmatrix}. \tag{4.34}$$

From this expression, it is possible to find an expression for the probability of, say, the survival chance of a neutrino species by $P_{\alpha\alpha}(t) = \rho_{\alpha\alpha} = U_{\alpha i}\,\rho_{ij}\,(U^{\dagger})_{j\alpha}$. In doing this calculation, one should find agreement with the Schrödinger like method and the Hamiltonian method.

4.4 Vectorial Parameterisation

There exists an alternative and convenient way to express the von Neumann equation through the utilisation of the Pauli matrices, known as *vectorial parameterisation* [123]. Starting with the von Neumann equation in the flavour basis and noting that the term in the Hamiltonian proportional to the identity cancels out in the commutator and the dynamics of the density matrix including the quantum state one has

$$\frac{\partial \rho_{\alpha\beta}(t)}{\partial t} = i[\rho(t), \Delta H(t)]_{\alpha\beta}. \tag{4.35}$$

The proportion of the Hamiltonian which contributes to the dynamics can be recast as

$$\Delta H_{\alpha\beta} = \frac{1}{2}\vec{V}\cdot\vec{\sigma}, \tag{4.36}$$

where $\vec{\sigma}$ is the Pauli matrix vector defined as $\vec{\sigma} \equiv (\sigma_x, \sigma_y, \sigma_z)$, while the *effective potential vector* $\vec{V}$ is defined as

$$\vec{V} \equiv (E_2 - E_1)(\sin 2\theta_{ij}, 0, -\cos 2\theta_{ij}). \tag{4.37}$$

It is also possible to express the density matrix through the Pauli matrices with the use of a polarisation vector $\vec{P}$, which results in

$$\rho = \frac{1}{2}(1 + \vec{P}\cdot\vec{\sigma}), \tag{4.38}$$

with components

$$\rho_{\alpha\alpha} = \frac{1}{2}(1 + P_z), \tag{4.39}$$
$$\rho_{\beta\beta} = \frac{1}{2}(1 - P_z), \tag{4.40}$$
$$\rho_{\alpha\beta} = P_x - iP_y, \tag{4.41}$$
$$\rho_{\beta\alpha} = P_x + iP_y. \tag{4.42}$$

The components of the polarisation vector are given by

$$P_x = \mathrm{Re}[\rho_{\alpha\beta}], \tag{4.43}$$
$$P_y = -\mathrm{Im}[\rho_{\alpha\beta}], \tag{4.44}$$
$$P_z = \rho_{\alpha\alpha} - \rho_{\beta\beta}. \tag{4.45}$$

This parameterisation is useful as the polarisation vector describes the evolution of the density matrix by recasting the von Neumann equation in a form which describes the precession of the polarisation vector around the potential vector, given by

$$\frac{\partial \vec{P}}{\partial t} = \vec{V} \times \vec{P}, \tag{4.46}$$

which can be solved and upon doing so, one finds agreement with the methods discussed previously.

5 Neutrino Masses

Neutrinos having mass is the major takeaway from neutrino oscillations. In this section, we explore neutrino masses, starting with the neutrino mass hierarchy, followed by a Dirac mass term for neutrinos. Majorana particles are then introduced along with a Majorana mass term for neutrinos. Finally, the seesaw model of neutrino masses is discussed, with a particular emphasis on the type-1 seesaw model.

5.1 Neutrino Mass Hierarchy

There are two possible *neutrino mass hierarchies*, these are known as normal ordering (NO) and inverted ordering (IO) [113], these two hierarchies are shown diagrammatically in Fig. 8. In the case of NO, the solar mass, m_{sol}, is related to the difference between m_2 and m_1. From neutrino oscillation experiments the squared difference is given by $m^2_{\text{sol}} = (7.49^{+0.19}_{-0.17}) \times 10^{-5}\text{eV}^2$, where $m^2_{\text{sol}} = m^2_2 - m^2_1$. Also for NO, the atmospheric mass difference, m_{atm}, is related to the difference between m_3 and m_2, where one has that $m^2_{\text{atm}} = (2.477^{+0.042}_{-0.042}) \times 10^{-3}\text{eV}^2$, where $m^2_{\text{atm}} = m^2_3 - m^2_2$. In the case of IO one has $m^2_{\text{sol}} = m^2_3 - m^2_2$, with m^2_{sol} taking the same value as in the NO case; however, m_{atm} is different and given by $m^2_{\text{atm}} = (2.465^{+0.041}_{-0.043}) \times 10^{-3}\text{eV}^2$ and related to the mass eigenstates by $m^2_{\text{atm}} = m^2_2 - m^2_1$. The mixing matrix U given in Eq. 4.6 is for NO such that one has

$$U^{(\text{NO})} = \begin{pmatrix} c_{12}c_{13} & s_{12}c_{13} & s_{13}e^{-i\delta} \\ -s_{12}c_{23} - c_{12}s_{23}s_{13}e^{i\delta} & c_{12}c_{23} - s_{12}s_{23}s_{13}e^{i\delta} & s_{23}c_{13} \\ s_{12}s_{23} - c_{12}c_{23}s_{13}e^{i\delta} & -c_{12}s_{23} - s_{12}c_{23}s_{13}e^{i\delta} & c_{23}c_{13} \end{pmatrix} \cdot \text{diag}(e^{i\rho}, e^{i\sigma}, 1). \tag{5.1}$$

The mixing matrix can be obtained in the IO scheme by cyclically permuting the NO mixing matrix by

$$U^{(\text{IO})} = U^{(\text{NO})} \begin{pmatrix} 0 & 1 & 0 \\ 0 & 0 & 1 \\ 1 & 0 & 0 \end{pmatrix}. \tag{5.2}$$

In this work we assume NO and therefore one has that $m_1 \leq m_2 \leq m_3$.

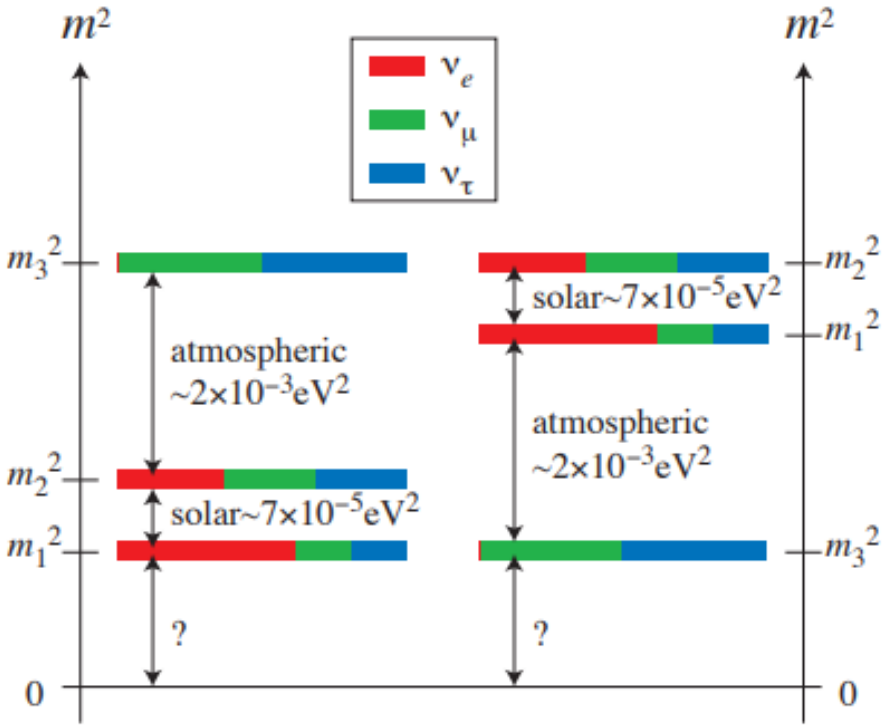

Figure 8: A visualisation of "how much" (the probability) a particular neutrino flavour (interaction) eigenstate contributes towards each mass eigenstate. The left corresponds to NO, whilst the right corresponds to IO, the question mark indicates the unknown magnitude of the smallest neutrino mass eigenstate m_1. This image is extracted from Ref. [12].

5.2 Dirac Mass for Neutrinos

Clearly from our description of neutrino oscillations, neutrinos are massive. As stated in Section 3, this is not predicted in the pure SM and as such provides definitive evidence that the standard model has problems. The other fermions; charged leptons and quarks, gain mass from a Dirac mass term, which after symmetry breaking is given by [124]

$$-\mathcal{L}_{\text{Dirac mass}} = m\overline{\psi}\psi = m(\overline{\psi}_L\psi_R + \overline{\psi}_R\psi_L), \tag{5.3}$$

which is invariant under the transformation, $\psi \to e^{i\alpha}\psi$ and $\overline{\psi} \to \overline{\psi}e^{-i\alpha}$, thus ensuring that the particles and the antiparticles have the same mass, $m_\psi = m_{\overline{\psi}}$. For charged particles which carry $U(1)$ quantum numbers, this is the only possible mass term as it preserves the $U(1)$ quantum numbers through particle-antiparticle interactions. It would be minimal and not be too outlandish if one were to simply add a Dirac mass term for neutrinos to the SM Lagrangian by introducing RH neutrinos, which are, of course, sterile in SM interactions. The Lagrangian for this simple extension of the SM would yield $\mathcal{L} = \mathcal{L}^{\text{SM}} + \mathcal{L}^{\nu}_{\text{Dirac Mass}}$, with

$$-\mathcal{L}^{\nu}_{\text{Dirac mass}} = \overline{\nu_{Li'}} m^{\nu}_{Di'j'} \nu_{Rj'} + \text{h.c.}, \tag{5.4}$$

where, as before, the primed basis is some basis that potentially arises from some new BSM physics, and, as previously, we can change between bases with unitary operators. The neutrino Dirac mass matrix can be diagonalised by a bi-unitary transformation such that

$$m^{\nu}_{Di'j'} = \left(V^{\nu\dagger}_{L} D_{m_D} U^{\nu}_{R}\right)_{i'j'}, \tag{5.5}$$

where $D_{m_D} \equiv \text{diag}(m_1, m_2, m_3)$ (assuming that there is no Majorana term). The basis where the mass matrix is diagonal is the mass or *Yukawa basis*. The introduction of this term to the SM Lagrangian also means that lepton flavours are no longer conserved; however, the total lepton number is still conserved. Unfortunately, the neutrino Yukawa couplings are much smaller than the Yukawa couplings for other SM fermions $h^{\nu} \approx 10^{-12} \ll h^{\text{other fermions}}$, and would require an explanation via some form of fine-tuning.

5.3 Majorana Neutrinos

In 1937 Italian theoretical physicist Ettore Majorana theorised the *Majorana particle* [125]. A Majorana particle is its own particle and is different in nature from our typical Dirac type fermions; because Majorana particles being their own antiparticle they must be electromagnetically neutral, and therefore the only fermionic particle in the SM capable of being a Majorana particle is the neutrino. Majorana showed that it was possible to explain mass generation with bispinors constructed from a Weyl spinor in the chiral

representation. To do this, we must decompose a Majorana field into left- and right-chiral components where $\psi_R = (\psi_L)^c = (\psi^c)_R$, which is known as the Majorana relation and states that the RH field is nothing more than the charge conjugated component of the LH field. The chiral decomposition therefore results in

$$\psi = \psi_L + \psi_R = \psi_L + (\psi_L)^c = \psi_L + (\psi^c)_R, \tag{5.6}$$

where an arbitrary phase factor $\eta = e^{i\phi}$ has been neglected. Evidently, a Majorana field is constructed from one Weyl field and, as such, only features two degrees of freedom, which can be viewed as a LH neutrino and a RH neutrino. Majorana fields are intrinsically neutral as upon charge conjugation you arrive back at the same field up to a phase factor[32]. There is much debate over whether neutrinos are Dirac particles, Majorana particles, or perhaps something more complicated. Further to this, distinguishing whether they are Dirac or Majorana in nature is rather difficult as they are indistinguishable kinematically, thus leaving no evidence within neutrino oscillation experiments; however, it is expected that they could be distinguished in interactions where a LH neutrino is flipped into a RH neutrino, which would only be possible if neutrinos are Majorana particles, since for Dirac neutrinos the RH component, ν_R, is completely sterile. Perhaps our best chance of seeing such a process would arise in neutrinoless double beta decay, which is discussed in more detail in Section 9.

5.4 Majorana Mass for Neutrinos

It is possible and attractive on first inspection to produce a neutrino mass term without the need to introduce RH neutrinos, which is achieved by slightly modifying the Dirac neutrino mass Lagrangian through the Majorana relation [127]

$$-\mathcal{L}^{\nu}_{\text{Left}} = \frac{1}{2}\left[\overline{\nu_{Li'}} m^{\nu}_{Li'j'} \nu^{c}_{Lj'} + \text{h.c.}\right], \tag{5.7}$$

[32]Majorana fields are perhaps best understood in the Majorana basis of the gamma matrices where the Dirac equation is real. In the Majorana basis all the gamma matrices are imaginary. In this basis the Majorana fields correspond to real solutions of the Dirac equation, thus one can impose the reality condition $\psi = \psi^*$ [126].

where the factor 1/2 ensures that the free Majorana field obeys the Dirac equation as the hermitian conjugate is identical, while $m^{\nu}_{Li'j'}$ is the left-left *Majorana mass* matrix which is symmetric. The left-left Majorana mass term is a Lorentz scalar which violates lepton number by two, and similar to the Dirac mass matrix, fine-tuning is required to reproduce the extremely light neutrino masses. The rather naive assumption that this extension is more economical when compared to adding a Dirac mass term is also incorrect, and must be regarded as an effective theory which implies there is some UV-complete extension, which is further discussed in Section 7.

	ν_L	$(\nu_L)^c$	$\overline{(\nu_L)^c}$	$\overline{\nu_L}$
Y	+1	-1	+1	-1
I_3	+1/2	-1/2	+1/2	-1/2
L	1	-1	1	-1

Table 1: Table of the hypercharge, Y, third component of isospin, I_3, and lepton number, L, for different LH neutrino fields.

5.5 Type-I seesaw Model

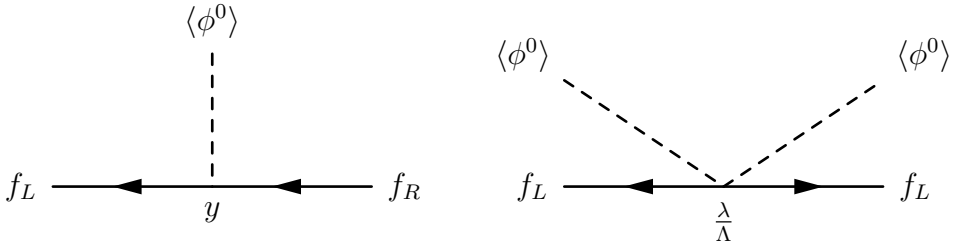

Figure 9: The left diagram corresponds to a Dirac mass term generated by the typical SM Higgs doublet. The right diagram corresponds to a Majorana mass generation from a higher dimensional operator such as the Weinberg operator of Eq. 7.35. In these diagrams the arrows indicate not charge but chirality [128].

Let us now present the type-1 seesaw mechanism of neutrino masses first proposed by Tsutomu Yanagida in [129] at the Tokyo conference in 1981. This mechanism is capable of explaining why neutrino masses are so small

compared to other SM fermions even when the neutrino Yukawa couplings are comparable to other SM fermions. If one again adds singlet RH neutrino fields, ν_R, to the SM along with a right-right Majorana mass term and a Dirac mass term for neutrinos, then after EWSB one has [130]

$$-\mathcal{L}^{\nu}_{\text{Dirac + Right}} = \overline{\nu_{Li'}} m^{\nu}_{Di'j'} \nu_{RJ'} + \frac{1}{2} \overline{\nu_{RI'}} M^{\nu}_{RI'J'} \nu^{c}_{RJ'} + \text{h.c.}, \tag{5.8}$$

where the small Latin indices range from 1 to 3 and indicate the LH neutrino fields, and the capital Latin indices range from 1 to N and indicate the RH neutrino fields. The right Majorana mass term violates lepton number by two due to the Yukawa interaction defining the RH neutrino fields to have lepton number $L = +1$, with this knowledge see Tab. 1, where of course RH or sterile neutrinos carry no isospin or hypercharge quantum numbers. In fact, the RH neutrinos are totally sterile to SM interactions and as such do not feature any SM quantum numbers bar a global charge. As mentioned, the number of RH fields is not required to be three and could be any amount N, however, there must be at least N = 2 as there are two independent mass splittings, also if the lightest neutrino mass, $m_1 > 0$, then one has that $N \geq 3$. Suppressing indices the total neutrino mass term can be expressed as [115]

$$-\mathcal{L}^{\nu}_{\text{Dirac + Right}} = \frac{1}{2} \left[(\overline{\nu_L}, \overline{\nu^{c}_R}) \begin{pmatrix} 0 & m_D \\ m_D^T & M \end{pmatrix} \begin{pmatrix} \nu^{c}_L \\ \nu_R \end{pmatrix} \right] + \text{h.c.}, \tag{5.9}$$

where the relation $\overline{\nu_L} m_D \nu_R = \overline{\nu^{c}_R} m_D^T \nu^{c}_L$ has been used, it is also possible to define $n'^{T}_R \equiv (\nu^{c}_L, \nu_R)^T$, which allows the neutrino mass term to be expressed in a more condensed form

$$-\mathcal{L}^{\nu}_{\text{Dirac + Right}} = \frac{1}{2} \overline{n'^{c}_R} \mathcal{M}_{\nu} n'_R + \text{h.c.}, \tag{5.10}$$

which resembles the form of a Majorana mass term. The mass matrix is symmetric and therefore can be diagonalised[33], resulting in Majorana mass

[33] As Majorana mass matrices are symmetric they can be *Takagi diagonalised* [131] by $A = VDV^T$, where D is a real nonnegative diagonal matrix, while V is a unitary matrix that can be complex.

eigenstates. In instances where $m_D = 0$ one recovers the Majorana mass instance, if $M = 0$ one recovers the Dirac mass instance. To reach the seesaw limit, one takes $M \gg m_D$. Neglecting active-sterile neutrino mixing, diagonalisation of the mass matrix $\mathcal{M}_\nu$ requires finding a unitary matrix $\mathcal{U}_\mathcal{B}$ that block diagonalises the matrix up to mixing terms of the order $\xi \equiv m_D M^{-1}$ such that

$$\mathcal{M}_\nu \simeq \mathcal{U}_B^T D^B_{M_\nu} \mathcal{U}_B, \tag{5.11}$$

where $\mathcal{D}^B_{\mathcal{M}_\nu} = \text{diag}(m_\nu, M)$ is a block diagonal matrix, with m_ν being the $(3,3)$ light neutrino mass matrix, while M is the (N,N) heavy neutrino mass matrix. The block diagonalising matrix up to $\mathcal{O}(\xi)$ is defined by

$$\mathcal{U}_B \simeq \begin{pmatrix} 1 & -\xi^\star \\ \xi^T & 1 \end{pmatrix}, \tag{5.12}$$

which results in the light neutrino masses m_ν given by the seesaw formula

$$m_\nu = -m_D \frac{1}{M} m_D^T = -\xi M \xi^T. \tag{5.13}$$

After all this the neutrino mass Lagrangian features a light-mass term and a heavy-mass term

$$-\mathcal{L}^\nu_{\text{Dirac + Right}} = \frac{1}{2}\left[\overline{\nu_L} m_\nu \nu_L^c + \overline{N_R^c} M N_R\right], \tag{5.14}$$

where the light neutrino mass matrix m_ν is a $(3,3)$ matrix that is a complex and symmetric matrix and therefore can be further diagonalised by Takagi diagonalisation such that

$$\text{Diag}(m_1, m_2, m_3) = V_L^\nu m_D \frac{1}{M} m_D^T V_L^{\nu T}. \tag{5.15}$$

If the mixing matrix that brings the charged leptons from the generic prime basis to the flavour basis where the charged lepton mass matrix is diagonal is reintroduced, U_L^l, then the leptonic mixing matrix is $U = U_L^l V_L^{\nu\dagger}$.

Instead, one could start in the flavour basis and one could identify that $U_L^l = I$, which results in the leptonic mixing matrix given by $U = V_L^{\nu\dagger}$, which would result in the light neutrino masses given by [9]

$$D_{m_\nu} = \text{Diag}(m_1, m_2, m_3) = U^\dagger m_D \frac{1}{M} m_D^T U^\star. \tag{5.16}$$

A useful parameterisation is the orthogonal seesaw matrix which can be obtained by manipulating the light neutrino masses as [132]

$$\frac{1}{\sqrt{D_{m_\nu}}} D_{m_\nu} \frac{1}{\sqrt{D_{m_\nu}}} = \frac{1}{\sqrt{D_{m_\nu}}} U^\dagger m_D \frac{1}{\sqrt{M}} \frac{1}{\sqrt{M}} m_D^T U^\star \frac{1}{\sqrt{D_{m_\nu}}}. \tag{5.17}$$

which results in

$$1 = \left[\frac{1}{\sqrt{D_{m_\nu}}} U^\dagger m_D \frac{1}{\sqrt{M}}\right] \left[\frac{1}{\sqrt{D_{m_\nu}}} U^\dagger m_D \frac{1}{\sqrt{M}}\right]^T = \Omega\Omega^T. \tag{5.18}$$

This orthogonal seesaw matrix Ω encompasses the properties of both the RH neutrinos, light neutrino masses, along with the CP asymmetries which are contained within the leptonic mixing matrix U. The type I seesaw model discussed here is a fundamental aspect of the RHINO model and allows us to address neutrino masses.

6 Thermal Physics and the Early Universe

In this section we start by discussing the early universe followed by the effective degrees of freedom in the radiation dominated universe along with a short insight into the equilibrium number densities for both fermions and bosons, at both relativistic and nonrelativistic velocities. After which normalisations of particle abundances in the early universe are discussed, followed by the Boltzmann equation, starting with the Liouville operator before moving on to the collisional operator that together formulates the Boltzmann equation. Two common thermal dark matter production methods are then discussed as examples of using the Boltzmann equation, these DM candidates are weakly interaction massive particles (WIMPs) and feebly interaction massive particles (FIMPs) which result in freeze-out and freeze-in scenarios, respectively. Finally, leptogenesis, a form of baryogenesis, is discussed, which seeks to solve the matter-antimatter asymmetry.

6.1 The Early Universe

Evidence suggests that the universe has existed through three distinct eras, these epochs in chronological order are the radiation-dominated era, the matter-dominated era, and finally the dark-energy-dominated era in which we inhabit. The general gist is that the scale factor of the universe, $a(t)$, has not always consistently increased proportional to time[34]. In fact, the three eras of the universe are defined by how the scale factor changes with time. The scale factor arises from the solution of the Friedmann equations with the *Friedmann–Lemaître–Robertson–Walker* (FRW) metric. The regime which is of particular interest to us is the *radiation-dominated epoch* when the kinetic contribution to the energy of particle dominates their mass, the scale factor scales with time[35] as $a(t) \propto t^{1/2}$. The radiation-dominated era begins after the reheating of the universe, which is thought to occur at the end of the inflationary period. Reheating is thought to occur through the

[34]The scale factor of the universe at current time is defined as $a(0) \equiv a_0 = 1$ and increases with time. This allows one to relate the distances of a comoving universe measured by a comoving ruler to the proper distance, which takes into account the expansion of the universe by $d_p = ad_c$. The scale factor is also related to the red shift of an astronomical object as a(t) = 1/(1 + z), and thus the Hubble expansion constant by $H \equiv \dot{a}/a$

[35]The matter-dominated era and the dark-energy-dominated era scale as $a(t) \propto t^{2/3}$ and $a(t) \propto \exp(H_0 t)$ respectively.

decay of the inflationary scalar field, which drives inflation, into Standard Model particles. This process increases the temperature of the universe. The upper limit on the reheat temperature is model-dependent; in our model, it is given by $T_{\rm RH} \lesssim 10^{15}$ GeV. Various constraints arise depending on the specific model, such as avoiding gravitino overproduction in supersymmetric theories or considering the scale of primordial gravitational waves.

An extremely useful cosmological parameter is the density parameter Ω, which determines the overall geometry of the universe and is defined as the ratio of the observed density of some cosmological component(s) ρ to the critical density ρ_c by

$$\Omega_{\rm X} \equiv \frac{\rho_{\rm X}}{\rho_c} = \frac{8\pi G \rho_{\rm X}}{3H^2}. \tag{6.1}$$

In our universe, the density parameter is measured to be extremely close to unity, indicating that we live in an essentially flat universe. This is a remarkable observation, suggesting that the universe is finely tuned. The question of why this is the case, and how such fine-tuning arises, is known as the *flatness problem*. The contributions to the density parameter within the favoured $\Lambda_{\rm CDM}$ model are from baryonic matter (B), dark mater (DM), and dark energy (Λ). Therefore, the density parameter can be expressed as $\Omega_0 = \Omega_{\rm B} + \Omega_{\rm D} + \Omega_\Lambda$, with values $\Omega_\Lambda = 0.73$, $\Omega_{\rm D} = 0.23$, and $\Omega_{\rm B} = 0.04$. In the radiation-dominated universe right after inflation the SM particles were in full thermal equilibrium, both kinetic and chemical equilibrium, then as the universe cooled and expanded, some species drop out of equilibrium, depending on how reactive the species are, i.e, what fundamental interactions do the particles partake in (hence neutrinos decouple early, fuelling the search for the CνB). It is useful to relate the interaction rate[36] Γ, with the Hubble expansion rate[37] H, whereby processes are said to be 'on' and in thermal equilibrium if $\Gamma/H > 1$, or 'off' and out of thermal equilibrium if $\Gamma/H < 1$.

[36]With the interaction rate given by, $\Gamma = n\sigma v$, where n is the number density, σ is the cross section, and v is the relative velocity.

[37]In the radiation dominated universe the Hubble rate is given by

$$H = 1.66 (g_*^\rho)^{\frac{1}{2}} \frac{T^2}{m_{\rm Pl}}. \tag{6.2}$$

6.2 Degrees of Freedom and Equilibrium Number Densities

In the radiation-dominated epoch of the universe the energy density can be expressed in terms of the effective degrees of freedom [133, 134]

$$\rho = \frac{\pi^2}{30} g_*^{\rho}(T) T^4, \tag{6.3}$$

where T is the temperature and g_*^{ρ} is the effective degrees of freedom energy

$$g_*^{\rho}(T) = \sum_{i=\text{bosons}} g_i \left(\frac{T_i}{T}\right)^4 + \frac{7}{8} \sum_{i=\text{fermions}} g_i \left(\frac{T_i}{T}\right)^4. \tag{6.4}$$

When there is no change in the number of particles, the entropy density of the radiation dominated universe can be expressed as

$$s = \frac{2\pi^2}{45} g_*^{s}(T) T^3, \tag{6.5}$$

where g_*^s are the effective degrees of freedom of entropy

$$g_*^{s}(T) = \sum_{i=\text{bosons}} g_i \left(\frac{T_i}{T}\right)^3 + \frac{7}{8} \sum_{i=\text{fermions}} g_i \left(\frac{T_i}{T}\right)^3. \tag{6.6}$$

If the particles are in thermal equilibrium, then $g_*^{\rho} = g_*^{s}$, as $T_i = T$, where T_i is the temperature of the particle and T is the temperature of the ambient radiation. If the particles are not in thermal equilibrium, then $(T_i/T)^4 \neq (T_i/T)^3$, thus $g_*^{\rho} \neq g_*^{s}$ and the effective degrees of freedom is then the combination of the degrees of freedom for the particles in thermal equilibrium and the decoupled particles given by

$$g_*^{(\rho,s)} = g_*^{\text{eq}(\rho,s)} + g_*^{\text{dec}(\rho,s)}. \tag{6.7}$$

The expressions for the number densities [135] can be derived by integrating the Fermi-Dirac or Bose-Einstein distributions in the relativistic or

nonrelativistic regime. Starting with relativistic bosons and fermions, the expressions are derived using the approximation that $E \approx p$ for relativistic particles yields

$$n_{\text{rel}} = \frac{\zeta(3)}{\pi^2} g_{\text{eff}} T^3, \tag{6.8}$$

where g_{eff} is the effective internal degrees of freedom, $g_{\text{eff}} = g_i$ for bosons and $g_{\text{eff}} = \frac{3}{4} g_i$ for fermions, T is the temperature and ζ is the Riemann zeta function. The nonrelativistic number density expression is derived using the approximation $E \approx m$, and results in

$$n_{\text{nrel}} = g_{\text{eff}} \left(\frac{mT}{2\pi} \right)^{\frac{3}{2}} e^{\frac{-m}{T}}. \tag{6.9}$$

6.3 Normalisation of Particle Abundances

Kinetic theory is commonly used to calculate abundances in the early universe, however, this calculation does not result in the absolute particle number at some time, and instead calculates the particle abundance in a portion of comoving volume[38]

$$N_X = n_X a^3 R_0^3, \tag{6.10}$$

where n_X is the number density of particle X, a is the typical scale factor of the universe, and R_0^3 is a normalisation factor. The conversion from a proper volume to a comoving volume is $V_{\text{P}} = a^3 V_{\text{C}}$. If entropy is conserved, then it is typical to normalise the box in such a way that $S = s a^3 R_0^3 = 1$ which results in

$$Y_X = \frac{n_X}{s} = \frac{n_X}{(2\pi^2/45) g_*^s(T) T^3}. \tag{6.11}$$

Unfortunately, processes in the early universe that result in entropy generation can occur due to BSM physics, leaving Y_X as a rather inconvenient

[38]The comoving number density is defined by $N \equiv a^3 n$.

quantity to deal with. Perhaps the most graceful normalisation is to normalise the comoving box so that it contains one particle of species X in ultra-relativistic thermal equilibrium, such that $1 = n_X^{\rm eq}(T \gg m_X)a^3R_0^3$. With this normalisation, one arrives at

$$\overline{N_X} = \frac{N_X}{N_X^{\rm eq}(T \gg m_X)} = \frac{n_X}{n_X^{\rm eq}(T \gg m_X)}, \tag{6.12}$$

which does not depend on particle X being ultrarelativistic.

6.4 The Boltzmann Equation

The Boltzmann equation [133, 134] is an integro-differential equation that is often employed to calculate macroscopic thermodynamic properties, such as energy and number density for a system that is not in thermal equilibrium. The number density of a particle species can be calculated from

$$\hat{L}[f_X] = \sum_r C_r[f_{X_i}](f_{X_{j\neq i}}) \tag{6.13}$$

with $\hat{L}[f_X]$ being the Liouville operator and $C_r[f_X]$ the collisional integral operator(s), in which all the different collisions, elastic and inelastic, are considered. In theory, there exists one equation for each species of particle in which particle X will react with; however, the particles considered here are in thermal equilibrium, which dramatically simplifies the system of equations to only one equation for the species of interest. Both the Liouville operator and the collisional operators depend on the phase space distribution function, which describes the occupancy number for a given particle species and is a function of momentum, position, and time such that $f_X(\vec{p}, \vec{r}, t)$. The thermal equilibrium phase space distribution function for a particle species is given by

$$f_X^{\rm eq} = \frac{1}{e^{\beta(E-\mu_X)} \pm 1}, \tag{6.14}$$

where E is the energy, μ_X is the so-called pseudochemical potential that vanishes at chemical equilibrium, and T is the temperature. The +1 in the denominator corresponds to Fermi-Dirac statistics for fermionic particles, whilst the -1 corresponds to Bose-Einstein statistics for bosonic particles.

6.5 The Liouville Operator (LHS)

The left hand side of the Boltzmann equation is the Liouville operator which in tensor notation is given by

$$\hat{L} = p^{\mu}\frac{\partial}{\partial x^{\mu}} - \Gamma^{\mu}_{\rho\sigma}p^{\rho}p^{\sigma}\frac{\partial}{\partial p^{\mu}}, \tag{6.15}$$

where p^{μ} is the four-momentum, $\partial/\partial x^{\mu}$ is the partial derivative with respect to spacetime coordinates, $\Gamma^{\mu}_{\rho\sigma}$ are the Christoffel symbols, $\partial/\partial p^{\mu}$ is the partial derivative with respect to the components of the four-momentum. The Liouville operator acts on a phase space distribution function. It is assumed that the universe is homogeneous and isotropic at large scales, and therefore in the FRW universe the phase space distribution function can be simplified such that $f(x^{\mu}, p^{\mu}) = f(t, E)$, where the position dependence has been dropped. This results in the Liouville operator acting on f_X taking the form

$$\hat{L}[f_X] = E_X\frac{\partial f_X}{\partial t} - H|\vec{p}|^2\frac{\partial f_X}{\partial E_X}, \tag{6.16}$$

where E is the energy, p is the momentum, $p^0 = E_X$, H is the Hubble parameter, and $f_X(t, E)$ is the distribution function only dependent on the energy and time. It is important to note the relation $\dot{a}/a = H$. The number density of a particle species is obtained by integrating the distribution function over momentum space, such that

$$n_X = g_X\int\frac{d^3p}{(2\pi)^3}f_X, \tag{6.17}$$

with n_X being the number density, g_X the number of internal degrees of freedom, and as previously f_X is the distribution function of the particle X. Integrating the Liouville operator gives

$$g_X\int\frac{d^3p}{(2\pi)^3}\frac{1}{E_X}\hat{L}[f_X] = g_X\int\frac{d^3p}{(2\pi)^3}\frac{\partial f_X}{\partial t} - g_X H\int\frac{d^3p}{(2\pi)^3}\frac{|\vec{p}|^2}{E_X}\frac{\partial f_X}{\partial E_X}. \tag{6.18}$$

which results in

$$g_X \int \frac{d^3p}{(2\pi)^3} \frac{1}{E_X} \hat{L}[f_X] = \dot{n}_X + 3Hn_X. \tag{6.19}$$

It is important to note that the second term $3Hn_X$ is the cosmological dilution due to the expansion of the universe. At this point it is useful to define[39] $N_X(t) = n_X(t)R(t)^3$, where $R(t) = a(t)R_0$, and as such

$$g_X \int \frac{d^3p}{(2\pi)^3} \frac{1}{E_X} \hat{L}[f_X] = \frac{1}{R(t)^3} \frac{dN_X(t)}{dt}. \tag{6.21}$$

It is important to note that this redefinition has allowed us to remove the dilution term. Often in literature, one will see the number density normalised by introducing s the entropy density, as in Eq. 6.11. To investigate this normalisation let us derive the evolution of Y. We start with the definition $Y = n/s$ and then we differentiate it with respect to time as

$$\frac{dY}{dt} = \frac{1}{s}\frac{dn_X}{dt} - \frac{n_X}{s^2}\frac{ds}{dt}. \tag{6.22}$$

.

If one assumes that the universe expands isoentropically such that $a^3 s =$ constant, then this implies that $ds/dt = -3Hs$, where H is again the Hubble parameter. Substituting this into 6.22, we arrive at

$$\frac{dY}{dt} = \frac{1}{s}\frac{dn_X}{dt} + 3HY, \tag{6.23}$$

where this normalisation has resulted in the removal of the dilution term (the term containing H).

[39] With this parameterisation the relativistic equilibrium number density Eq. 6.8 is given by

$$N_{\rm rel} = \frac{\zeta(3)}{\pi^2} g_{\rm eff} T^3 R^3. \tag{6.20}$$

6.6 The Integral Collisional Operator (RHS)

The integral collisional operator contains terms for both elastic and inelastic collisions. The elastic collisions do not change the number of particles and can therefore be neglected; the collisional operator, which only considers number-changing processes, then takes the form

$$\begin{aligned} g_X \int \frac{d^3p}{(2\pi)^3}\frac{C[f_X]}{E} = \int d\Pi_X d\Pi_A d\Pi_B ... d\Pi_1 d\Pi_2 d\Pi_3 ... (2\pi)^4 \\ \times\delta^4(p_X + p_A + p_B ... - p_1 - p_2 - p_3 ...) \\ \times \Big[|M_{1+2+3...\to X+A+B...}|^2 f_1 f_2 f_3 ... (1 \pm f_X)(1 \pm f_A)(1 \pm f_B) ... \\ - |M_{X+A+B...\to 1+2+3...}|^2 f_X f_A f_B ... (1 \pm f_1)(1 \pm f_2)(1 \pm f_3) ... \Big], \end{aligned} \tag{6.24}$$

where δ^4 is the four-dimensional Dirac delta function that ensures energy-momentum conservation, $M_{X+A\to 1+2}$ signifies the amplitude of the process $X + A \to 1 + 2$, as an example, and Π_i is the Lorentz-invariant phase space for each particle and is given by

$$d\Pi_i = \frac{g_i}{(2\pi)^3}\frac{d^3p_i}{2E_i}. \tag{6.25}$$

6.7 The Freezing-Out of WIMP Dark Matter

The freeze-out production of the hypothesised WIMP particles [136] is IR-dominated[40] which is attractive to physicists, as it does not depend on the uncertain cosmological history of the universe. WIMPs arise in many BSM models that have tried to solve the *gauge hierarchy problem*[41] and as such can be viewed as rather natural DM candidates, that in some ways generalise the idea of neutrino DM. WIMPs are expected to have been in kinetic

[40]The use of IR or infrared for low energy solutions and UV or ultraviolet for high energy solutions stems from the ultraviolet catastrophe.

[41]The hierarchy problem relates to the issues of quantum stability of the Higgs boson mass against radiative corrections that arise from many BSM extensions, for the Higgs mass to be the value it is, typically requires fine-tuning unless there is a natural symmetry breaking [137].

equilibrium with the SM particles in the thermal bath. As mentioned previously, the elastic collisions are neglected as they do not change the number of particles. An elastic collision is of the form $X + B \leftrightarrow X + B$. For simplicity in the derivation that follows, only pair productions and annihilation's are considered, $X + \bar{X} \leftrightarrow B + \bar{B}$. It is also assumed that the bath particles are in full thermal equilibrium (kinetic and chemical equilibrium). Realistically, the annihilation mechanism could be far more complex. Going forward, X is the dark matter particle assumed to be in kinetic equilibrium as mentioned, whereas the SM particles in the thermal bath are denoted by B. The first step in the WIMP calculation is defining the collisional operator for pair-productions and annihilation's of the WIMP particles. The collision operator for the $X + \bar{X} \leftrightarrow B + \bar{B}$ process is defined as

$$\begin{aligned} g_X \int \frac{d^3p}{(2\pi)^3} \frac{C_r[f_X]}{E_X} = \int d\Pi_X d\Pi_{\bar{X}} d\Pi_B d\Pi_{\bar{B}} (2\pi)^4 \delta^4(p_X + p_{\bar{X}} - p_B - p_{\bar{B}}) \\ \times \Big[|\mathcal{M}_{B+\bar{B}\to X+\bar{X}}|^2 f_B f_{\bar{B}} (1 \pm f_X)(1 \pm f_{\bar{X}}) \\ - |\mathcal{M}_{X+\bar{X}\to B+\bar{B}}|^2 f_X f_{\bar{X}} (1 \pm f_B)(1 \pm f_{\bar{B}}) \Big]. \end{aligned} \tag{6.26}$$

This expression can be simplified by making a few rational assumptions. The first assumption is that the process is reversible $|M| = |M_{X+\bar{X}\to B+\bar{B}}| = |M_{B+\bar{B}\to X+\bar{X}}|$, known as the principle of detailed balance. The next assumption is that we can neglect quantum mechanical effects, with these effects represented by the $(1 \pm f_i)$ terms, where specifically the negative term relates to Fermi-blocking factors and the positive term relates to the Boson-enchantment factors. Disregarding these quantum effects allows us to use Maxwell-Boltzmann statistics $1 \pm f_i = 1$. One can also assume that the bath particles are in thermal equilibrium (kinetic and chemical equilibrium), whilst the WIMPs are only in kinetic equilibrium, as mentioned previously. It is also expected that for the bath particles $E > T$, which allows the quantum effects of the distribution functions to be disregarded, similarly for the WIMPs, $E - \mu > T$, resulting in their distribution functions being expressed as

$$f_X \simeq \exp\left(\frac{-E_X}{T}\right) \exp\left(\frac{\mu_X}{T}\right), \tag{6.27}$$

where at chemical equilibrium $\mu = 0$ (i.e. $\mu_B = 0$). Then finally assuming energy conservation $E_X + E_{\bar{X}} = E_B + E_{\bar{B}}$ results in the WIMP collisional operator taking the form

$$g_X \int \frac{d^3p}{(2\pi)^3} \frac{C_r[f_X]}{E_X} = \int d\Pi_X d\Pi_{\bar{X}} d\Pi_B d\Pi_{\bar{B}} (2\pi)^4 \delta^4(p_X + p_{\bar{X}} - p_B - p_{\bar{B}}) \times |\mathcal{M}|^2 \exp\left(\frac{-E_X - E_{\bar{X}}}{T}\right) \left[1 - \exp\left(\frac{\mu_X - \mu_{\bar{X}}}{T}\right)\right]. \tag{6.28}$$

We can now further simplify the integro-differential equation by utilising the definition of the number density defined in Eq. 6.17, in the following manner

$$\exp\left(\frac{\mu_X}{T}\right) = \frac{n_X}{n_X^{\text{eq}}}, \tag{6.29}$$

which results in the collisional operator now being expressed as

$$g_X \int \frac{d^3p}{(2\pi)^3} \frac{C_r[f_X]}{E_X} = \int d\Pi_X d\Pi_{\bar{X}} d\Pi_B d\Pi_{\bar{B}} (2\pi)^4 \delta^4(p_X + p_{\bar{X}} - p_B - p_{\bar{B}}) \times |\mathcal{M}|^2 \exp\left(\frac{-E_X - E_{\bar{X}}}{T}\right) \left[1 - \frac{n_X n_{\bar{X}}}{n_X^{\text{eq}} n_{\bar{X}}^{\text{eq}}}\right], \tag{6.30}$$

with the thermally averaged cross section defined as[42]

$$\langle \sigma v \rangle = \frac{1}{n_X^{\text{eq}} n_{\bar{X}}^{\text{eq}}} \int d\Pi_X d\Pi_{\bar{X}} d\Pi_B d\Pi_{\bar{B}} (2\pi)^4 \delta^4(p_X + p_{\bar{X}} - p_B - p_{\bar{B}}) \times |\mathcal{M}|^2 \exp\left(\frac{-E_X - E_{\bar{X}}}{T}\right). \tag{6.32}$$

[42]Where one has that v is the relative velocity also known as the Møller velocity

$$(v_{\text{Møl}})_{ij} = \frac{\sqrt{(p_i \cdot p_j)^2 - (m_i m_j)^2}}{E_i E_j}. \tag{6.31}$$

This results in the collisional operator for the WIMPs becoming

$$g_X \int \frac{d^3p}{(2\pi)^3} \frac{C_r[f_X]}{E_X} = -\langle \sigma v \rangle \left[n_X n_{\bar{X}} - n_X^{\rm eq} n_{\bar{X}}^{\rm eq} \right], \tag{6.33}$$

and finally we arrive at the rate equation

$$\frac{dN_X}{dt} = -\frac{\langle \sigma v \rangle}{R(t)^3} \left[N_X^2 - (N_X^{\rm eq})^2 \right], \tag{6.34}$$

where we have assumed no asymmetry between X and $\bar{X}$. If this rate equation is normalised as in Eq. 6.10, such that $\overline{N_X} \equiv N_X/N_X^{\rm in}$ (where $N_X^{\rm in}$ is given by Eq. 6.20 and assuming that X is fermionic), along with using the approximation that $\langle \sigma v \rangle \approx \sigma_0$, and introducing the dimensionless quantity $z = m_X/T$, which allows the comoving number density to depend on z which is ultimately temperature dependence $s \propto T^3$ and $a \propto T^{-1}$ such that

$$\frac{d}{dt}(a^3 s) = 0 \rightarrow \frac{d}{dt}(aT) = 0 \rightarrow \frac{d}{dt}\left(\frac{a}{z}\right) = 0, \tag{6.35}$$

from this one can then find dz/dt using the product and the chain rule

$$\frac{\dot{a}}{z} - \frac{a}{z^2}\frac{dz}{dt} = 0, \tag{6.36}$$

thus

$$\frac{dz}{dt} = Hz \rightarrow \frac{dN_X}{dt} = \frac{dN_X}{dz}\frac{dz}{dt} = \frac{dN_X}{dz} Hz. \tag{6.37}$$

Finally, we arrive at *Lee-Weinberg equation*

$$\frac{d\overline{N_X}}{dz} = -\frac{A_0}{z^2} \left[\overline{N_X}^2 - (\overline{N_X^{\rm eq}})^2 \right], \tag{6.38}$$

where A_0 contains the Hubble constant[43]

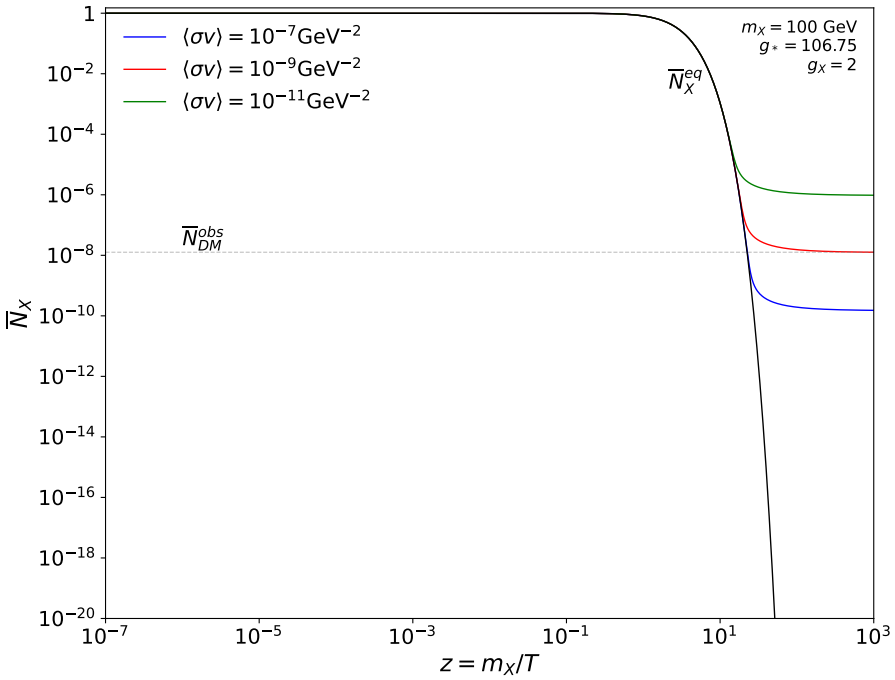

Figure 10: Evolution of the WIMP abundance for different values of thermally averaged cross section as indicated. Clearly one can see the freeze-out mechanism. The dotted grey line indicates the observed DM abundance for a mass of 100GeV. The abundances are normalised according to Eq. 6.12.

$$A_0 = \frac{3}{4}\frac{\zeta(3)}{\pi^2}\sqrt{\frac{90}{8\pi^3}}\frac{g_X}{\sqrt{g_*^\rho}}\sigma_0 m_X m_{\mathrm{Pl}}. \tag{6.40}$$

[43]The Hubble constant as a function of z is given by

$$H(z) = \sqrt{g_*^\rho}\sqrt{\frac{8\pi^3}{90}}\frac{m_X^2}{m_{\mathrm{Pl}}}\frac{1}{z^2}. \tag{6.39}$$

.

This expression for $H(z)$ is derived from the Friedmann equation during the radiation-dominated era of the universe. Where, as previously, we have made the substitution $T = m_X/z$.

An approximate solution to the Lee-Weinberg equation can be found analytically, and the freezing temperature can also be obtained. The freezing-out of the WIMPs is plotted in Fig. 10. In our work on RHINO DM, pair production of one of the three RH neutrino states, termed the source RH neutrinos, is modelled by an equation very similar to the Lee-Weinberg equation.

6.8 The Freezing-In of FIMP Dark Matter

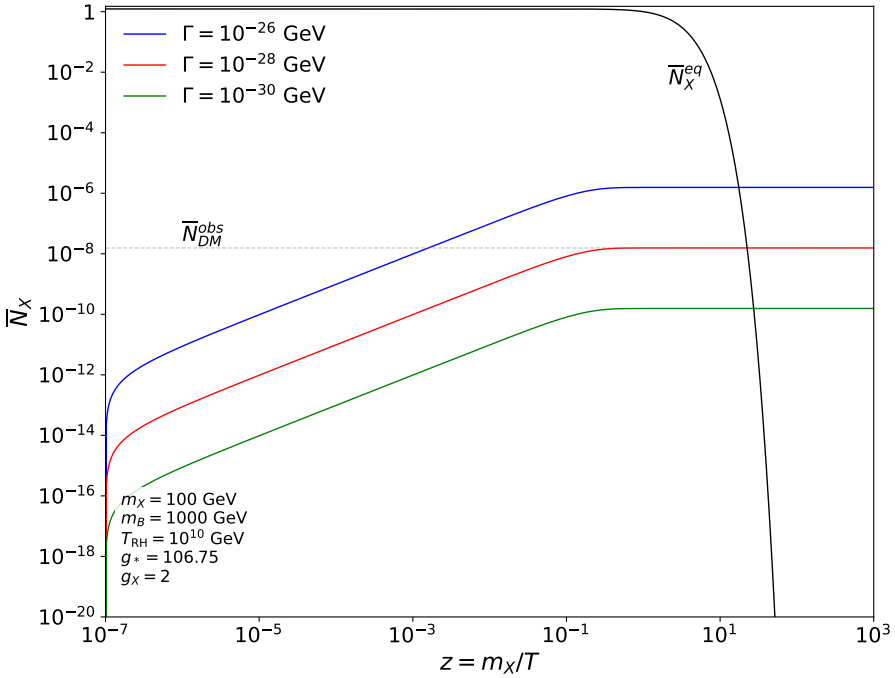

Figure 11: Evolution of the FIMP abundance for different values of the decay rate as indicated. Clearly one can see the freeze-in mechanism. The dotted grey line indicates the observed DM abundance for a mass of 100GeV. The abundances are normalised according to Eq. 6.12.

Unlike WIMPs, the initial abundance of feebly-interacting massive particles (FIMP) particles [138, 139, 140] in the early universe is thought to be negligible, and this could partially be due to their extremely weak interactions with the SM particles in the thermal bath. The exact mechanism of

why the proposed FIMPs start with such a low abundance is unknown and would likely depend on some exotic physics in the early universe. FIMP DM is thought of as the opposite of WIMP DM, the FIMPs abundance starts at a negligible quantity, production then starts, but the particles never get a chance to thermalise and as such are froze-in. Within FIMP DM the couplings of the dark sector to the SM are extremely small, and production can occur through decays of SM particles and/or scatterings. Let us briefly derive perhaps the simplest case involving decays of a massive bath particle, B_1, into a lighter bath particle, B_2,and a DM particle, X, such that $B_1 \to B_2 + X$. The Boltzmann equation for such a process is given by

$$\begin{aligned} \dot{n}_X + 3Hn_X = \int & d\Pi_X d\Pi_{B_1} d\Pi_{B_2} (2\pi)^4 \delta^4(p_X + p_{B_2} - p_{B_1}) \\ & \times \left[|\mathcal{M}|^2_{B_1 \to B_2 + X} f_{B_1}(1 \pm f_{B_2})(1 \pm f_X) \right. \\ & \left. - |\mathcal{M}|^2_{B_2 + X \to B_1} f_{B_2} f_X (1 \pm f_{B_1}) \right], \end{aligned} \tag{6.41}$$

where $d\Pi_i$ is the phase space element defined in Eq. 6.25. It is assumed that the initial abundance of X is negligible, such that $f_X = 0$. This simplifies the equation as the second term on the RHS of Eq. 6.41 can be neglected. As with the WIMP case, this can be further simplified by neglecting the Pauli-blocking/simulated emission effects. This enables the FIMP Boltzmann equation to be expressed as

$$\dot{n}_X + 3Hn_X \approx 2g_{B_1} \int d\Pi_{B_1} \Gamma_{B_1} m_{B_1} f_{B_1} = g_{B_1} \int \frac{d^3 p_{B_1}}{(2\pi)^3} f_{B_1} \frac{\Gamma_{B_1}}{\gamma_{B_1}}, \tag{6.42}$$

where $\gamma_{B_1} = E_{B_1}/m_{B_1}$ and the partial decay width is given by

$$\Gamma_{B_1 \to B_2 + X} = \frac{1}{2E_{B_1}} \int d\Pi_{B_2}\, d\Pi_X\, (2\pi)^4 \delta^4(p_{B_1} - p_{B_2} - p_X) |\mathcal{M}|^2. \tag{6.43}$$

This equation can then be further simplified by assuming that the bath particles are in thermal equilibrium and thus using the approximation that $\exp(E_{B_1}/T) \pm 1) \approx \exp(E_{B_1}/T)$. This can then be integrated by converting the integral from an integral over momentum space to an integral over energy, which yields

$$\dot{n}_X + 3n_X H \approx g_{B_1} \int_{m_{B_1}}^{\infty} \frac{m_{B_1}\Gamma_{B_1}}{2\pi^2}(E_{B_1}^2 - m_{B_1}^2)^{1/2} e^{-E_{B_1}/T} dE_{B_1} \\ = \frac{g_{B_1} m_{B_1}^2 \Gamma_{B_1}}{2\pi^2} T K_1(m_{B_1}/T), \tag{6.44}$$

where K_1 is the first modified Bessel function of the second kind. We can make use of $N_X(t) = n_X(t)R(t)^3$, $z_{B_1} = m_{B_1}/T$, and the normalisation given by Eq. 6.12 to arrive at

$$\frac{d\overline{N_X}}{dt} = \frac{g_{B_1} m_{B_1}^3 \Gamma_{B_1} R^3}{2\pi H z_{B_1} N_X^{\rm in}} K_1(z_{B_1}), \tag{6.45}$$

where, as in the WIMP scenario, $N_X^{\rm in}$ is given by Eq 6.20 and H is given by 6.39. It is also possible to use $z_X = m_X/T$, which can be achieved in the above equation by substituting $z_{B_1} = m_{B_1} z_X/m_X$. The evolution of the FIMP number density (solved computationally) is displayed in Fig. 11. This freeze-in solution is very important to the RHINO model we propose, as the dark neutrino that plays the role of the DM effectively freezes-in.

6.9 Leptogenesis

Currently we cannot explain the matter-antimatter asymmetry of the universe, which is observed in the form of a baryon asymmetry. It appears as though the universe and specifically the SM, contain all the ingredients required to produce the asymmetry; baryon number violations, C and CP violation, and departure from thermal equilibrium, with the asymmetry potentially occurring during the electroweak phase transition. The favoured explanation involves the production of the asymmetry after the inflationary stage. The current baryon abundance measured by the Planck satellite is $\Omega_{B,0}h^2 = 0.022$ [4]. The baryon-to-photon ratio is defined as

$$\eta_{B,0} = \frac{n_B - n_{\bar{B}}}{n_\gamma} = (6.12 \pm 0.04) \times 10^{-10}, \tag{6.46}$$

which is a convenient way to express the baryon asymmetry of the universe and is related to Ω_B by $\eta_{B,0} \approx 280\Omega_{B,0}h^2 \times 10^{-10}$. Before introducing leptogenesis[44] let us start by briefly discussing the sphaleron process

[44]Which was first proposed by Fukugita and Yanagida in 1986 [141].

[142] followed by baryogenesis. Derived from the electroweak field equations, sphalerons are a static solution, which is non-perturbative and represents a saddle point in the electroweak potential. This process is hypothetical and is theorised to violate baryon and lepton numbers, while leaving $B - L$ conserved, where the process freezes out at $\sim$ 132 GeV [18]. The sphaleron process is capable of converting fermion types in groups of three such that the process can convert three antileptons into quarks, or three leptons into antiquarks and vice versa. Baryogenesis is a hypothetical process thought to take place in the early universe, which produces a baryonic asymmetry and thus the matter-antimatter asymmetry. Baryogenesis can be incorporated into the SM, however, it is thought that within the SM one cannot produce enough of an asymmetry to account for what we see in the universe. Baryogenesis within the SM requires that EWSB is a first-order cosmological phase transition, wherein if the process is not first-order sphaleron transitions would destroy any baryon asymmetry produced. SM baryogenesis is now generally unfavourable [143]. A theory of baryogenesis capable of explaining the matter-antimatter asymmetry must obey the following conditions, known as the *Sakharov conditions* [144]:

- Baryon number B violation - this is vital to produce an excess of baryons over antibaryons.
- C-symmetry violation - this is required so that interactions that produce more baryons over antibaryons are not balanced out by interactions that do the opposite.
- CP-symmetry violation - this is required so that interactions produce more left-handed baryons over right-handed antibaryons.
- Out of thermal equilibrium interactions - this is required as otherwise CPT symmetry would remove a net baryon number.

Unfortunately, as mentioned one struggles to produce a successful model of baryogenesis within the SM, and therefore the asymmetry of the universe acts as a strong hint towards BSM physics. Leptogenesis [19, 145] is a baryogenesis scenario that offers a simple and elegant solution to the observed baryon asymmetry and arises from neutrino physics, with the minimal scenario of thermal leptogenesis relying on the incorporation of the type I seesaw along with the thermal production of heavy RH neutrinos. Within this

model lepton number violating processes occur in the early universe which produce a lepton asymmetry, this lepton asymmetry is then transferred to the baryons via the sphaleron process. The lepton asymmetry is often achieved through the incorporation of the RH neutrinos to the SM, which as we know is attractive as this also allows the seesaw model of neutrino masses to be incorporated. Allowing one to simultaneously explain neutrino masses together with the asymmetry of the universe. Typically, within thermal leptogenesis, decays of the lightest heavy neutrino, denoted by N_1, are ultimately responsible for the asymmetry. The heavy neutrino can decay into a Higgs-lepton pair with the rate at tree-level given by [146]

$$\Gamma_{\mathrm{D}_i} + \bar{\Gamma}_{\mathrm{D}_i} = \Gamma(N_1 \to H + l_L) + \Gamma(N_1 \to H^\dagger + l_L^\dagger) = \frac{1}{8\pi}(hh^\dagger)_{11} M_1. \quad (6.47)$$

The CP asymmetry occurs because of interference between the tree-level amplitude and the one-loop diagrams stemming from the one-loop vertex along with the self-energy corrections. This results in the CP violating parameter which is defined as

$$\varepsilon_i = \frac{\Gamma_{\mathrm{D}_i} - \bar{\Gamma}_{\mathrm{D}_i}}{\Gamma_{\mathrm{D}_i} + \bar{\Gamma}_{\mathrm{D}_i}}, \quad (6.48)$$

where explicitly the CP asymmetry from N_1 is defined as [147]

$$\varepsilon_1 \simeq -\frac{3}{16\pi}\frac{M_1}{(h^\dagger h)_{11}} \mathrm{Im}\left(h^\dagger h \frac{1}{M} h^T h^*\right)_{11}, \quad (6.49)$$

where corrections of $\mathcal{O}(M_1/M_{2,3})$ have been neglected. From this one can then obtain an upper bound on the CP asymmetry [23]

$$|\varepsilon_1| \leq \frac{3}{16\pi}\frac{M_1 m_3}{v^2}. \quad (6.50)$$

These heavy neutrinos feature no SM quantum numbers and are thus SM gauge singlets; this is ideal and allows them to leave equilibrium with the typical SM particles. This is interesting as the Lagrangian used to describe these neutrinos, Eq. 2.4, satisfies all the Sacharov conditions; it has lepton

number violation in the Majorana mass term, C and CP violation within the mass matrices, and finally due to the heavy neutrinos singlet nature, it also has the potential for out of equilibrium decays. Thermal leptogenesis is a favoured form of leptogenesis as at high temperatures $T > M_1$, because it allows any lepton asymmetry that has already accumulated to be erased. As the universe cools below the mass of M_1, these neutrinos drop out of equilibrium, and thus CP violating decays create a $B - L$ asymmetry, which is stored in the lepton sector. The sphaleron process then converts a fraction of this asymmetry to the baryon sector. The final baryon asymmetry is the result of the interplay between the production of the asymmetry and the washout processes that reduce the asymmetry. There are potentially three out of equilibrium processes that can contribute towards the asymmetry, these are [148]

- N_1 decays (D) and inverse-decays (ID) into Higgs bosons and leptons, $N_1 \leftrightarrow \phi l$ along with the opposite $N_1 \leftrightarrow \bar{\phi}\bar{l}$
- $\Delta L = 2$ scatterings which are mediated by the exchange of all the heavy Majorana neutrinos $l\phi \leftrightarrow \bar{l}\bar{\phi}$, $ll \leftrightarrow \bar{\phi}\bar{\phi}$, and $\overline{ll} \leftrightarrow \phi\phi$.
- $\Delta L = 1$ scatterings mediated by Higgs particles $N_1 l(\bar{l}) \leftrightarrow \bar{t}(t)q(\bar{q})$ and $N_1 t(\bar{t}) \leftrightarrow \bar{l}(l)q(\bar{q})$.

The decays, inverse decays and the $\Delta L = 1$ scatterings all contribute in driving the N_1 number density towards its equilibrium number density, $N_{N_1}^{\rm eq}$. The decays alone contribute towards the $B - L$ generation, whilst the other processes seek to washout the $B - L$ number. The leptogenesis process is described by Boltzmann equations, where if one neglects Yukawa couplings and the sum of the three lepton flavours, one has [149]

$$\frac{dN_{N_1}}{dz} = -(D + S)(N_{N_1} - N_{N_1}^{\rm eq}), \tag{6.51}$$

for the N_{N_1} abundance, and then

$$\frac{dN_{B-L}}{dz} = -\varepsilon_1 D(N_{N_1} - N_{N_1}^{\rm eq}) - W N_{B-L}, \tag{6.52}$$

for the rate of $B - L$. Within these equations, one has that $D = \Gamma_D/Hz$ for the decay and inverse decay rates, whilst $S = \Gamma_S/Hz$ for the scattering

rates for the $\Delta L = 1$ processes, and finally $W = \Gamma_W / Hz$ for the washout rates.

7 The Higgs Portal and Effective Theories

In this section, operators in QFT are discussed starting with requirements of operators in QFT, before explaining what an effective field theory (EFT) is. Next, the Higgs portal operator is introduced with emphasis on its ability to connect the hypothetical dark sector to the SM sector. After this, the WIMPzilla cross section for fermions is outlined, which features Higgs-Higgs annihilations into dark sector particles. Finally, the Anisimov operator is introduced, which is a special type of Higgs portal operator involving RH neutrinos.

7.1 Operators in Quantum Field Theory

In quantum field theories, it is typical to work with all fundamental constants equal to unity such that $\hbar = c = 1$, and thus all quantities are then measured in energy with the unit of electron volts (eV). As we have discussed previously in quantum field theories, we typically start with the action, which features a 4-dimensional integral over spacetime of the Lagrangian density such that

$$S = \int d^4x \mathcal{L}, \tag{7.1}$$

with the action being a dimensionless quantity. In a 4-dimensional field theory we require that the Lagrangian density is of energy dimension $[\mathcal{L}] = E^4$, this is because the four dimensions we integrate over have energy dimensions $[d^4x] = E^{-4}$. If we expand operators with perturbation theory, the energy dimensions of the couplings are such that the Lagrangian density has an energy dimension equal to the spacetime dimensions. If we look at the Yukawa couplings of fermions to scalars

$$\mathcal{L} = -y\phi\psi\overline{\psi}, \tag{7.2}$$

we can see that this Lagrangian density has dimension, $[\mathcal{L}] = E^4$, as the spinors have dimensions, $[\psi] = E^{3/2}$, the scalar field has dimensions, $[\phi] = E^1$, while the Yukawa couplings, y, are dimensionless.

An effective theory [150, 151] is the low-energy limit of a theory, an example of this is the Fermi theory of weak interactions and most likely the

SM itself. Effective theories typically involve couplings of negative energy dimensions, $[g] = E^n$, with $n < 0$, in Fermis theory, the Fermi constant is such that $[G_F] = E^{-2}$, and holds for instances where the energies are $E \ll M_W \approx 80\text{GeV}$, above which the complete $SU(2) \times U(1)$ electroweak theory is required as the theory diverges. It is therefore worth looking for potential operators with negative energy dimensions of couplings, $n < 0$, which could give rise to new and interesting physics with new particles and interactions for interactions below some energy threshold $E < \Lambda$, with Λ being the energy in which the effective theory breaks down, at which point we would require the complete theory. It is a requirement that a UV-complete theory cannot have negative energy dimensional couplings, and therefore we must have that $n \geq 0$. In typical QFTs of dimensions $3+1$, this restricts the types of interactions that are possible as only a handful of couplings have $n \geq 0$. The dimensionality of the couplings is given by

$$n = 4 - n_b - \frac{3}{2}n_f - n_\delta, \tag{7.3}$$

where n_x is the number of field types x in the Lagrangian density or operator, with b being bosons, f fermions and δ being derivatives, whilst 4 accounts for our typical 4D field theories. Within the SM all couplings are dimensionless except for the Higgs mass term, $\mathcal{L}^{\text{Higgs mass}} = -\mu^2\phi\phi$, which features a coupling term of energy dimension two, and as such has been called *super-renormalisable*.

7.2 The Higgs Portal Operator

Let us now introduce a potential extension to the SM, which features Higgs-Higgs interactions with the so called 'dark sector'. The dark sector contains particles and interactions that do not feature within the typical SM $SU(3) \times SU(2) \times U(1)$, i.e. particles which are singlets under the SM gauge group, and as such they do not have SM quantum numbers. However, these dark particles are probably coupled to new interactions beyond the SM. There is no reason to think this could not be the case as already within the SM different fermionic fields already couple to different interactions in the SM, for example, the LH quark fields couple to the strong, weak, and the electromagnetic interaction, whilst the RH charged lepton fields only couple to one interaction- the electromagnetic force. One possible candidate that requires

a rather minimal extension is the RH neutrino as we have discussed, which should it exist would be a $SU(3) \times SU(2) \times U(1)$ singlet. Should this hidden sector exist, one could ask the question of why is this sector dark? There are two possibilities as such [152], the first is that the hidden sector is hiding behind a large mass scale, however, this creates a new kind of hierarchy problem; why do these interactions not arise at a comparable mass scale of the visible sector. The other possibility is that the scale of the hidden sector is similar to that of the visible sector with coupling between the dark and visible sector through weakly coupled fields with masses which are naturally close to the visible scale, which would explain why the sector is invisible or dark.

The Higgs Portal operator is an hypothesised operator which allows interactions between the SM Higgs doublets with the hidden sector, and in a generic form is [153]

$$-\mathcal{L} = g\chi\chi\Phi^\dagger\Phi, \tag{7.4}$$

and features the Higgs squared operator, $\Phi^\dagger\Phi$, which is the only two-dimensional SM operator that is both Lorentz and gauge invariant where Φ is the typical Higgs doublet, and χ is some dark sector particle, which could be scalar, fermionic (with an adjoint $\overline{\chi}$ present in the case of a Dirac fermion), or vector particle (where indices would present for a vector particle, χ_μ), and the parameter g contains the coupling constant and other parameters to ensure the Lagrangian is of dimension-4. This operator featuring Higgs-Higgs is an extremely interesting operator and if we assume some fermionic dark particles this operator becomes

$$-\mathcal{L} = \frac{\lambda}{\Lambda}\psi\psi\Phi^\dagger\Phi, \tag{7.5}$$

with ψ being a fermionic field where λ is the dimensionless coupling constant between the dark sector and the Higgs sector, Λ is the scale of new physics above which the theory breaks down and as such it can be viewed as an effective theory. Without the scale of new physics this operator for fermionic dark particles results in a dimension-5 operator, thus the scale of new physics ensures that the Lagrangian density is of dimension-4. As we mentioned in the previous section an effective theory has a coupling constant of negative energy dimension, which we can see by letting

$g = \lambda/\Lambda = [E^0]/[E^1] = [E^{-1}]$. The Higgs portal operator can influence a whole range of physics such as; the EW scale [154], inflationary physics [155] and dark matter interactions with the SM [156, 157, 1].

Field	Higgs	RH Neutrino
Symbol	Φ	N
Mass [GeV]	125	Model Dependent
Electric Charge [e]	0	0
Colour Charge	0	0
Spin	0	$\frac{1}{2}$
Weak Isospin	$\phi^+ = \frac{1}{2}$, $\phi^0 = -\frac{1}{2}$	0
Weak Hypercharge	$\frac{1}{2}$	0

Table 2: Quantum numbers of the fields involved in the 5-dimensional operator, assuming the fermion is a RH singlet neutrino.

7.3 The WIMPzilla Cross Section

One feature of the Higgs portal operator is that Higgs-Higgs annihilations could hypothetically pair produce dark fermions, or more specifically in our case right-handed neutrinos; it is also possible that these dark fermions could themselves play the role of dark matter. A recent paper by Kolb *et al.* extended the WIMPzilla model by introducing thermal production rather than the gravitational production originally proposed [158]. In this more recent paper, the thermally averaged cross section for such a particle was calculated [159], where the leading order interactions occur through a Higgs portal with the SM Higgs doublet square operator. The Lagrangian for this model is of the form[45]

$$\mathcal{L}_{int} = \frac{\lambda}{2}\frac{1}{\Lambda}\psi\psi\Phi^\dagger\Phi, \tag{7.6}$$

with Λ being the scale of new physics and λ is the coupling between the Majorana fermionic fields and the Higgs fields. The thermally averaged cross

[45]We only summarise the key points of the derivation here, for an in-depth derivation please see the original paper Ref. [159].

section for a fermionic WIMPzilla particle was calculated by Kolb *et al.* [159] and is given by

$$\langle \sigma v \rangle_{XX \to \Phi\bar{\Phi}} \equiv \frac{1}{n^{\rm eq} n^{\rm eq}} \int \frac{d^3 p_\Phi}{(2\pi)^3 2E_\Phi} \frac{d^3 p_{\bar{\Phi}}}{(2\pi)^3 2E_{\bar{\Phi}}} \frac{d^3 p_1}{(2\pi)^3 2E_1} \frac{d^3 p_2}{(2\pi)^3 2E_2} \times (2\pi)^4 \delta^4 (p_\Phi + p_{\bar{\Phi}} - p_1 - p_2) \sum_{s_1, s_2} |\mathcal{M}_{XX \to \Phi\bar{\Phi}}|^2 e^{-\frac{(E_1+E_2)}{T}}, \tag{7.7}$$

where $E = \sqrt{\vec{p}^2 + M^2}$, M is the mass of the DM candidate, and $n^{\rm eq}$ is given by Eq. 6.8 or Eq. 6.9 depending on whether the particle is relativistic or not. To solve this integral, it is useful to make use of

$$\sigma_{XX \to \Phi\bar{\Phi}} = \frac{1}{4F(p_1, p_2)} \int \frac{d^3 p_\Phi}{(2\pi)^3 2E_\Phi} \frac{d^3 p_{\bar{\Phi}}}{(2\pi)^3 2E_{\bar{\Phi}}} \times (2\pi)^4 \delta^4 (p_\Phi + p_{\bar{\Phi}} - p_1 - p_2) |\mathcal{M}_{XX \to \Phi\bar{\Phi}}|^2, \tag{7.8}$$

where $F(p_1, p_2) = (1/2)\sqrt{s}\sqrt{(s - 4M^2)}$ is the Lorentz scalar function, and $s = (p_1 + p_2)^2$ is the Mandelstam variable. After averaging over the possible spin projections of the WIMPzilla particles in the initial state, where $g = (2S + 1)$, the spin-averaged cross section is given by

$$\bar{\sigma}_{XX \to \Phi\bar{\Phi}} = \frac{1}{g^2} \sum_{s_1} \sum_{s_2} \sigma_{XX \to \Phi\bar{\Phi}}. \tag{7.9}$$

This results in the thermally averaged cross section given by

$$\langle \sigma v \rangle_{XX \to \Phi\bar{\Phi}} = \frac{g^2}{n^{\rm eq} n^{\rm eq}} \int \frac{d^3 p_1}{(2\pi)^3} \frac{d^3 p_2}{(2\pi)^3} \bar{\sigma}_{XX \to \Phi\bar{\Phi}}\, v_{\rm M\o l}(p_1, p_2) e^{-\frac{(E_1+E_2)}{T}}, \tag{7.10}$$

with the Møller velocity defined as

$$v_{\rm M\o l}(p_1, p_2) = \frac{F(p_1, p_2)}{E_1 E_2} = \sqrt{|\vec{v}_1 - \vec{v}_2|^2 - |\vec{v}_1 \times \vec{v}_2|^2}, \tag{7.11}$$

where $\vec{v} = \vec{p}/E$. Providing $\bar{\sigma}_{XX\to\phi\bar{\phi}}$ is only dependent on s, the momentum integrals over p_1 and p_2 can be evaluated, which yields

$$\langle\sigma v\rangle_{XX\to\Phi\bar{\Phi}} = \frac{g^2}{n^{\rm eq}n^{\rm eq}}\frac{T}{32\pi^4}\int_{4m^2}^{\infty} ds\,(s-4m^2)\sqrt{s}\,K_1(\sqrt{s}/T)\,\bar{\sigma}_{XX\to\Phi\bar{\Phi}}(s) \tag{7.12}$$

where $K_n(x)$ is the modified Bessel function of the second kind, with n defining its order. To proceed, one must select the relevant $|\mathcal{M}_{XX\to\Phi\Phi}|$, which in the case of a fermionic WIMPzilla is given by

$$\sum_{s_1,s_2}|\mathcal{M}_{\Phi^\dagger\Phi\to XX}|^2 = \frac{2\lambda^2}{\Lambda^2}(s-4M^2). \tag{7.13}$$

If we now substitute this into our expression for $\bar{\sigma}_{XX\to\phi\phi}$, we get

$$\bar{\sigma}_{XX\to\Phi\bar{\Phi}} = \frac{1}{4}\frac{1}{4F(p_1,p_2)}\frac{2\lambda^2}{\Lambda^2}(s-4M^2)\,(2\pi)^4\int\frac{d^3p_\Phi}{2E_\Phi}\frac{d^3p_{\bar{\Phi}}}{2E_{\bar{\Phi}}}\delta^4(p_\Phi+p_{\bar{\Phi}}-p_1-p_2), \tag{7.14}$$

where for a Majorana fermion we have $g = 2$. This can be evaluated, which yields

$$\bar{\sigma}_{XX\to\Phi\bar{\Phi}} = \frac{1}{32\pi}\frac{\lambda^2}{\Lambda^2}\frac{1}{s}\sqrt{s-4M^2}\sqrt{s-4m_\Phi^2}. \tag{7.15}$$

This results in the thermally averaged cross section given by

$$\langle\sigma v\rangle_{XX\to\Phi\bar{\Phi}} = \frac{1}{n^{\rm eq}n^{\rm eq}}\frac{1}{256\pi^5}\frac{\lambda^2}{\Lambda^2}T\int_{4M^2}^{\infty} ds\,(s-4M^2)^{3/2}K_1(\sqrt{s}/T), \tag{7.16}$$

where the mass of the Higgs boson has been neglected. Next, if one performs a change of variables, where $\sqrt{s}/T = y$ one arrives at

$$\langle\sigma v\rangle_{XX\to\Phi\bar{\Phi}} = \frac{1}{n^{\rm eq}n^{\rm eq}}\frac{1}{8\pi^5}\frac{\lambda^2}{\Lambda^2}T^6\left[\frac{1}{16}\int_{2M/T}^{\infty} ydy\,(y^2-4M^2/T^2)^{3/2}K_1(y)\right]. \tag{7.17}$$

.

This expression can be integrated with the help of the Meijer G-function [160], with the part in the square brackets yielding

$$[\cdots] = \frac{3\sqrt{\pi}}{8} G^{3,0}_{1,3}\left(\frac{M^2}{T^2}\,\middle|\,\begin{matrix}5/2\\0,2,3\end{matrix}\right) \approx \begin{cases} \frac{3\pi M^2}{8T^2}\left(1+\frac{7T}{4M}\right)e^{-2M/T} & \text{for } T < M \\ 1 - \frac{3M^2}{4T^2} + \cdots & \text{for } M < T. \end{cases} \tag{7.18}$$

In this result, the double exponential suppression arises from the fact that only Φ particles with high energy (particles that reside in the high-energy tail of the Boltzmann phase-space distribution function) can produce χ particles with energy $E = 2M$. Finally, substituting the expression for $n^{\rm eq}$ results in

$$\langle\sigma v\rangle_{XX\to\Phi\bar{\Phi}} = \frac{1}{4\pi}\frac{\lambda^2}{\Lambda^2}\frac{T^4}{M^4 K_2^2(M/T)}\left[\frac{3\sqrt{\pi}}{8} G^{1,3}_{3,0}\left(\frac{M^2}{T^2}\,\middle|\,\begin{matrix}5/2\\0,2,3\end{matrix}\right)\right] \tag{7.19}$$

where a factor two has been included in the above result as there are two potential annihilation channels. In the asymptotic limit for large and small WIMPzilla masses, this results in

$$\langle\sigma v\rangle \approx \frac{1}{16\pi}\frac{\lambda^2}{\Lambda^2} \times \begin{cases} \frac{3T}{M} & \text{for } T \ll M \\ 1 & \text{for } M \ll T \end{cases}. \tag{7.20}$$

where the case $M \ll T$ is of importance for source-source interactions for our RHINO model detailed in Section 11.

7.4 Anisimov Operator

Another interesting Higgs portal-like operator is the Anisimov operator [15], which is not strictly a Higgs portal operator but has similarities, in the sense that it features the Higgs-Higgs dim-2 operator coupled to RH neutrinos. This operator takes the form [8],

$$\mathcal{L}_A = \sum_{I,J}\frac{\lambda'_{IJ}}{\Lambda}\Phi^\dagger\Phi\overline{N_I^c}N_J, \tag{7.21}$$

Let us briefly pause to compare the above Anisimov operator with the WIMPzilla operator of Eq. 7.6. Starting with the similarities, both operators are dimension-5 operators, both include the Higgs squared operator $\Phi^\dagger\Phi$, both couple a fermion bilinear to a scalar bilinear (forming a Lorentz-invariant and gauge-invariant interaction), both operators can contribute to the masses of the fermions involved in the interaction after EWSB, and both are invariant under SM gauge transformations. Now, for the key difference: unlike the WIMPzilla operator, which contains only one flavour, the Anisimov operator features flavour indices that allow for flavour mixing. The WIMPzilla operator serves as a Higgs portal for the production of potential Majorana fermions, whereas the Anisimov operator not only facilitates this production but also incorporates the possibility of flavour mixing, which is vital to the RHINO model, as we shall see.

In previous work [99, 15] the main contributions come from the instance $I \neq J$ and the mixing it induces. However, as we have discussed the Anisimov operator is capable of more than just mixing as it can also pair produce RH neutrinos through Higgs-Higgs annihilations, with the thermally averaged cross section given by Eq. 7.20. In the instance where $I \neq J$, one gets a mixed production of RH neutrino mass eigenstates, and when $I = J$, one gets a pure production of one RH mass eigenstate. Also when $I \neq J$, this rather remarkable operator has two unique qualities, the first is the ability to induce oscillations of a source RH neutrino, N_S which is coupled to the SM, into an uncoupled dark RH neutrino, N_D, which could potentially play the role of DM. The reason this happens is due to the Anisimov operator producing off-diagonal terms in the mixing Hamiltonian, which will be discussed when the model is discussed in more detail in Section 10 onwards. Another consequence of the Anisimov operator will be discussed now and involves its ability to induce decoupled dark neutrino decays. Before EWSB the RH neutrino only Lagrangian takes the form [99]

$$\mathcal{L}^{\text{RH only}} = \overline{N_{RI}} i \not{\partial} N_{RI} + \frac{1}{2}\overline{N_{RI}^c} D_{MIJ} N_{RJ} + \frac{\lambda_{IJ}}{\Lambda}\Phi^\dagger\Phi\overline{N_{RI}^c} N_{RJ} + \text{h.c.}, \quad (7.22)$$

where D_{MIJ} is the diagonal RH neutrino mass matrix as we are working in a basis where the RH neutrino mass matrix is diagonal. After EWSB a correction to the Majorana mass term is generated by the Anisimov operator at zero temperature, $\delta M_\Lambda = 2\lambda_{IJ}v^2/\Lambda$, which results in the RH neutrino only Lagrangian becoming

$$\mathcal{L}^{\text{RH only}} = \frac{1}{2}\overline{N_{RI}^c} D_{MIJ} N_{RJ} + \frac{1}{2}\delta M_{IJ}^{\Lambda} \overline{N_{RI}^c} N_{RJ} + \text{h.c.}, \tag{7.23}$$

which introduces off-diagonal terms in the total Majorana mass term $M_{IJ}^{\lambda} = D_{MIJ} + \delta M_{\Lambda}$. The total Majorana mass term can then be diagonalised with the standard method in which one can diagonalise a symmetric matrix via Takagi diagonalisation. If mixing is assumed between only N_S and N_D, then $\delta M_{\Lambda} = 2\lambda_{\text{DS}} v^2/\Lambda$, and the mixing matrix can be made real and parameterised by only one mixing angle which results in the mixing matrix given by

$$U_R^{\Lambda}(\theta_{\Lambda}^0) = \begin{pmatrix} 1 & 0 & 0 \\ 0 & \cos\theta_{\Lambda}^0 & \sin\theta_{\Lambda}^0 \\ 0 & -\sin\theta_{\Lambda}^0 & \cos\theta_{\Lambda}^0 \end{pmatrix}, \tag{7.24}$$

where corrections to the RH neutrino masses are considered negligible $M_I' \approx M_I$. This mixing has another rather interesting consequence for the Dirac mass matrix, which is now of the form

$$m_D = \begin{pmatrix} m_{De1} & m_{De2} & 0 \\ m_{D\mu 1} & m_{D\mu 2} & 0 \\ m_{D\tau 1} & m_{D\tau 2} & 0 \end{pmatrix}, \tag{7.25}$$

where N_D is decoupled from the SM, hence the column of zeros. However, when we diagonalise the total Majorana mass term by $U_R^{\Lambda}(\theta_{\Lambda}^0)$ the Dirac mass matrix becomes

$$m_{\text{D}}^{\Lambda} = m_{\text{D}} U_R^{\Lambda}(\theta_{\Lambda}^0) = \begin{pmatrix} m_{De1} & m_{De2}\cos\theta_{\Lambda}^0 & m_{De2}\sin\theta_{\Lambda}^0 \\ m_{D\mu 1} & m_{D\mu 2}\cos\theta_{\Lambda}^0 & m_{D\mu 2}\sin\theta_{\Lambda}^0 \\ m_{D\tau 1} & m_{D\tau 2}\cos\theta_{\Lambda}^0 & m_{D\tau 2}\sin\theta_{\Lambda}^0 \end{pmatrix}, \tag{7.26}$$

which introduces small effective Yukawa couplings for N_D. These small couplings are then capable of inducing N_D decays, with the decay rate given by $\Gamma_{\text{D}\to\text{A}+\nu_S} = (\theta_{\Lambda}^0)^2 h_{\text{S}}^2 M_{\text{D}}/4\pi$. One derives the mixing angle θ_{Λ}^0 in as is normally done for calculating mixing angles. The total RH neutrino mass matrix after EWSB is given by

$$M_{IJ}^{\Lambda} = \begin{pmatrix} M_1 & 0 & 0 \\ 0 & M_{\rm S} & \frac{v^2}{\tilde{\Lambda}} \\ 0 & \frac{v^2}{\tilde{\Lambda}} & M_{\rm D} \end{pmatrix}, \tag{7.27}$$

where we have defined $\tilde{\Lambda} = \lambda_{\rm DS}/\Lambda$. Next, focussing only on the lower right square matrix, one can subtract a term proportional to the identity given by $(M_{\rm D} + M_{\rm S})/2 \times I_{2\times 2}$, which yields

$$\Delta M_{\rm DS}^{\Lambda} = \begin{pmatrix} -\frac{\Delta M}{2} & \frac{v^2}{\tilde{\Lambda}} \\ \frac{v^2}{\tilde{\Lambda}} & \frac{\Delta M}{2} \end{pmatrix}, \tag{7.28}$$

where $\Delta M = M_{\rm D} - M_{\rm S}$. If one then finds the eigenvalues of this matrix, then one should have

$$\begin{pmatrix} -\frac{\Delta M}{2} & \frac{v^2}{\tilde{\Lambda}} \\ \frac{v^2}{\tilde{\Lambda}} & \frac{\Delta M}{2} \end{pmatrix} = \begin{pmatrix} \lambda^+ \cos 2\theta_{\Lambda}^0 & \lambda^+ \sin 2\theta_{\Lambda}^0 \\ -\lambda^+ \sin 2\theta_{\Lambda}^0 & -\lambda^+ \cos 2\theta_{\Lambda}^0 \end{pmatrix}, \tag{7.29}$$

where we have used the two dimensional rotation matrix[46] and two trigonometric identities[47]. Then finally, the mixing angle is obtained upon comparison such that

$$\frac{\lambda^+ \sin 2\theta_{\Lambda}^0}{\lambda^+ \cos 2\theta_{\Lambda}^0} = \frac{\frac{v^2}{\tilde{\Lambda}}}{\frac{\Delta M}{2}} = \frac{2v^2/\tilde{\Lambda}}{\Delta M} = \tan 2\theta_{\Lambda}^0 \approx \theta_{\Lambda}^0, \tag{7.31}$$

where the small angle approximation has been used.

[46]The two dimensional rotation matrix is given by

$$R_\theta = \begin{pmatrix} \cos\theta & -\sin\theta \\ \sin\theta & \cos\theta \end{pmatrix}. \tag{7.30}$$

[47]These identities are that $\cos^2\theta - \sin^2\theta = \cos 2\theta$, and $2\cos\theta\sin\theta = \sin 2\theta$.

7.5 Majorana Mass

In Section 5 a left-left Majorana mass term was briefly discussed and it was mentioned that a left-left Majorana mass term would arise as an EFT which implies some UV-complete theory exists [161]. The reason for this is that the SM Lagrangian requires not only Lorentz invariance but also $SU(2)_L \times U(1)_Y$ invariance to ensure renormalisability. A LH neutrino chiral field ν_L has a hypercharge[48], $Y = -1$, therefore the left mass term[49]

$$-\mathcal{L}_{\text{Left mass}} = \frac{1}{2}\left[\overline{\nu_{Li'}} m^{\nu}_{Li'j'} \nu^{c}_{Lj'} + \text{h.c.}\right], \tag{7.34}$$

has a net hyper charge of $Y = -2$, as $\overline{\nu_L}(\nu_L)^c$ has $Y = -2$. One method to resolve this problem is to introduce some $SU(2)$ triplet where $Y = 2$, an example of this is the introduction of an isotriplet Higgs field. Another possible solution is to introduce the lepton number violating dim-5 Weinberg operator [162, 163] which is the lowest dimensional operator capable of preserving SM quantum numbers

$$\mathcal{L}_5 = \frac{\lambda_{\alpha\beta}}{\Lambda}(\overline{L^c_\alpha}\tilde{\Phi}^*)(\tilde{\Phi}^\dagger L_\beta) + \text{h.c.}, \tag{7.35}$$

where $\lambda_{\alpha\beta}$ is a symmetric dimensionless coupling matrix, $\tilde{\Phi} = i\sigma^2\Phi^*$ is the Higgs dual, and Λ is an energy scale at which new physics emerges. This operator can be obtained in the type I seesaw by integrating out the heavy RH Majorana fields [164]. It is theorised that after spontaneous symmetry breaking that this operator generates a left neutrino Majorana mass

[48] See Tab. 1.

[49] The full Lagrangian for such a term is given by

$$\mathcal{L} = \mathcal{L}_{\text{kinetic}} - \mathcal{L}_{\text{Left mass}} \tag{7.32}$$

$$= i\sum_{i'} \overline{\nu_{Li'}}\gamma^\mu \partial_\mu \nu_{Li'} - \frac{1}{2}\left[\overline{\nu_{Li'}} m^{\nu}_{Li'j'} \nu^{c}_{Lj'} + \text{h.c.}\right], \tag{7.33}$$

where $\nu_{Li'}$ is the left-handed neutrino field for the flavour index i', $\nu^c_{Lj'}$ is the charge-conjugated left-handed neutrino field, $m^{\nu}_{Li'j'}$ is the symmetric Majorana mass matrix, $\overline{\nu_{Li'}} = \nu^\dagger_{Li'}\gamma^0$ is the Dirac adjoint of the left-handed neutrino field, γ^μ are the gamma matrices, and ∂_μ is the four-gradient operator.

$$m_{\nu\alpha\beta} = \frac{\lambda_{\alpha\beta} v^2}{\Lambda} \propto \frac{m_D^2}{\Lambda}, \tag{7.36}$$

where the masses can be suppressed if $\Lambda \gg m_D$, which is interesting and has the potential to explain the smallness of the neutrino masses that we detect. At tree-level there are three ways to generate the Weinberg operator[161]:

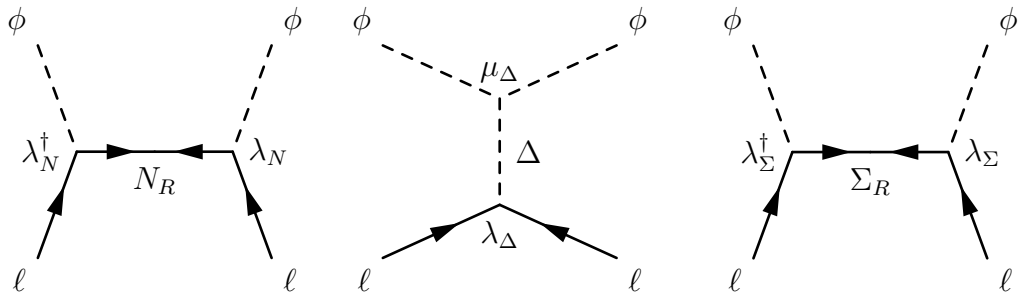

Figure 12: Feynman diagrams of the three seesaw mechanisms. The left corresponds to the type-I seesaw, the middle corresponds to the type-II seesaw, whilst the right corresponds to the type-III seesaw.

1. Type I seesaw mechanism features a $SU(2)$ singlet fermion as the mediator, shown on the left of Fig. 12. This involves heavy RH neutrinos N_R that couple to the LH neutrinos ℓ via the Higgs field ϕ, generating small neutrino masses through a seesaw effect when the RH neutrinos acquire large Majorana masses.
2. Type II seesaw mechanism features a triplet scalar Δ as a mediator, shown in the middle of Fig. 12. Neutrino masses are generated through a scalar triplet that couples with LH leptons ℓ, with the neutral component of the triplet acquiring a small vacuum expectation value. This process is similar to typical mass generation by the Higgs in the SM.
3. Type III seesaw mechanism features a triplet fermion Σ_R as a mediator, shown on the right of Fig. 12. This mechanism introduces fermion triplets that couple to the lepton doublets ℓ and the Higgs field ϕ, producing small neutrino masses when the triplets acquire large masses. This process is similar to the Type-I seesaw.

8 Dark Matter Searches

The detection of DM is a current goal of experimental and theoretical particle physics, with theorists developing models with new interactions typically through extensions of the SM, some of which have been discussed. It is hopeful that proposed extensions of the SM produce signals which can be searched for. There are currently three possible avenues for DM searches, which are categorised as direct searches, indirect searches, and collider searches, all of which will be outlined in this section and are mostly built around detecting WIMP like particles.

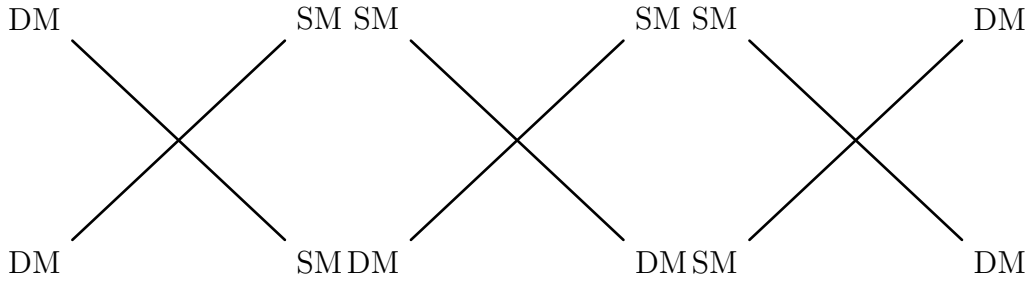

Figure 13: Interaction diagrams for the three DM detection techniques. The left diagram represents indirect detection via DM annihilations, though decays are also possible. The middle diagram shows direct detection, where a DM particle scatters off a SM particle. The right diagram is unlikely to produce a detectable signal due to the weak interactions between DM and SM particles, assuming such interactions exist. This process could also involve a mediator.

8.1 Collider Searches for Dark Matter

It is expected that particle colliders themselves will not be able to identify DM; however, it is extremely hopeful that particle accelerators will at some point identify some missing energy predicted by some novel theory, such as an effective field theory, some simplified model, or some complete model that could lead to us segregating and identifying DM. DM searches in colliders rely on the production of DM particles or novel mediators [165, 166]. Unfortunately, this has some rather difficult problems to overcome. Firstly, many DM models do not produce detectable results, and secondly, if there

are possible signatures, they are typically hidden behind some inaccessible mass scale or are so weakly interacting that the chances of production are minimal. Naturally, as our technology improves, our ability to probe these extensions at colliders becomes more realistic. However, many extensions are still far beyond what is feasibly testable in laboratories in the near future. It is no mystery that particle colliders have been one of the most useful tools for probing the SM and thus have led to the discovery of many fundamental components of our known universe, with the Large Hadron Collider (LHC) being the most powerful particle accelerator amongst the current generation of particle accelerators. As we have previously discussed, it is widely accepted among physicists that DM is a new form of matter, composed of particles not present within the SM. This is unsurprising, given that all known phenomena in the universe can be attributed to interactions between particles through the exchange of mediator particles, with the current exception of gravity.

The Higgs portal discussed in Section 7 or some other unspecified EFT could be the link between the dark realm and the visible realm, which potentially could result in signatures at colliders. It is expected that if DM particles were to be produced in colliders, it would result in missing energy similarly to how neutrinos behave by essentially interacting with almost nothing upon production. The fact that DM is still present implies that it must be extremely stable, which can be imposed by a $\mathcal{Z}_2$ *symmetry*[50] as an example, in which the SM content could be even and the DM particle(s) could be odd. Simple extensions of the SM which could be investigated at colliders capable of accounting for DM are Higgs portal as discussed, or Z boson portal models [167]. As we have seen, Higgs portal models in their simplest form can be constructed by adding only novel DM particles to the SM, where recent generations of colliders have now made it possible to probe these realms albeit without any success. With Z-portal models the situation is similar, but unlike Higgs portals, they are strongly constrained by LEP and direct detection experiments [168]. If DM interactions are mediated by SM bosons, searches for invisible particle production are the key to finding DM. Similarly to what occurs in the production of neutrinos mediated by the W boson in charged current interactions or the Z boson in neutral current interactions, there is a particular emphasis on looking for effects of invisible particles being produced from the decay of Z bosons. Here, the invisible decay width is of

[50]This is similar to what one has with supersymmetery, where some species are even and some are odd. The $\mathcal{Z}_2$ is the cyclic group that has two elements 1 and -1.

importance and has been measured to be 499.1 ± 1.5MeV and has been used to constrain many Z-portal models [168]. A similar situation arises from the invisible Higgs boson decays, which account for around 0. 1% of the total decay width of the Higgs boson[169]. Hopefully, the Higgs-to-invisible rate could become observable and these interactions could be viewed by directly observing the recoil of these decays against other visible particles.

Naturally, EFT interactions are not required to be as simple as the Higgs or Z boson portals and could involve numerous generations of dark particles and the interactions with the SM could also be mediated by a new more massive particle or particles. If this is the case, then there are thought to be two possibilities, whereby one hopes that such a model could provide some insight with which we could build upon. In the case where the mediator is more massive than the collision energy, the DM-SM interaction would appear to be a contact interaction, with the complex high energy interactions integrated out. The other possibility is that the mediator is not massive compared to the kinetics of the collision, in which case one would hope that the full theory could be found. One might also look at supersymmetric models[84, 83], or some other complete theory which features long-lived particles present that could play the role of DM [7]. Supersymmetry has received a fair amount of collider examination, especially from ATLAS and CMS, with many searches for its particles, such as squarks and gluinos. Unfortunately, no conclusive supersymmetric signal has been detected thus far, and rarer processes are now being examined after failure with the most prominent channels[170]. Methods employed to find DM at colliders include searches with jets, searches utilising photons and vector bosons, searches utilising the Higgs boson and related physics, searches with heavy third-generation quarks, Dijet searches, supersymmetric searches, Higgs to invisible decays, and low-energy beam dump experiments [171, 7].

8.2 Direct Detection of Dark Matter

Direct detection of DM involves signatures in laboratories from DM and SM scatterings. These searches depend on DM particles from the Milky Way's DM halo scattering in a detector on Earth (composed of SM particles) and are typically located deep underground. The direct detection rate is likely to depend on the local density of DM and its local velocity distribution, with estimates for the density of DM currently at approximately $\rho \approx 0.39 \pm 0.03\text{GeVcm}^{-3}$, which has a systematic uncertainty of up to 40% when factors

such as DM clumps, streams, or effects of the galactic disk are taken into account [172, 173]. When a DM particle scatters off nuclei in a detector, a recoil energy is induced, which can generate a detectable signal in the form of phonons or photons as examples. WIMP or WIMP-like particles are expected to feature potentially large de Brogile wavelengths, and as such the particles are expected to interact coherently with all nucleons within the target mass of the detector. The expected rate of WIMP scattering off a target nucleus of mass m_N is integrated from the minimal WIMP velocity to induce a nuclear recoil of energy E_{nr}, up to the escape velocity at which the WIMPs are no longer bound to the potential well of the Milky Way [174]

$$\frac{dR}{dE_{\rm nr}} = \frac{\rho M}{m_N m_\chi} \int_{\nu_{\rm min}}^{\nu_{\rm esc}} \nu f(\nu) \frac{d\sigma}{dE_{\rm nr}} d\nu, \tag{8.1}$$

where m_χ is the WIMP mass, σ is the scattering cross section, M is the detector target mass, $f(\nu)$ is the normalised WIMP velocity distribution of the Milky Way, and ρ is the local DM density. The differential cross section is dependent on both spin-independent interactions (SI) and spin-dependent interactions (SD) [173] and is given by

$$\frac{d\sigma}{dE_{\rm nr}} = \frac{m_N}{2\nu^2\mu^2}(\sigma_{\rm SI}F_{\rm SI}^2(E_{\rm nr}) + \sigma_{\rm DS}F_{\rm DS}^2(E_{\rm nr})), \tag{8.2}$$

with μ being the reduced WIMP-nucleus mass given by $\mu = (m_N m_\chi)/(m_N + m_\chi)$, while F_S is the form factors which encode the dependence on momentum transfer and nuclear structure, which avoids explicit details of the dependencies, with an example being the Helm Form Factor which applies to spin independent interactions[175].

Inorganic crystal detectors are used in searches for WIMP DM and include high purity Germanium crystals, with high purity Germanium being an ideal detector as only a small amount of energy is required to create an electron-positron pair, which allows good resolution due to many signal carriers, although this material at large masses can at times be too sensitive to background noise. Other examples of Inorganic crystal detectors involve the use of Si-crystals, NaI(Tl), and also CsI(Tl). Examples of crystal scintillator experiments are DAMA/LIBRA [176], ANAIS [177], KIMS [178], and DM-Ice at IceCube [179]. Another type of DM direct detectors are cryogenic detectors, and these depend on detecting a heat signal in the form of phonons

by measuring a temperature increase after a collision of a DM particle with the detector; example materials used are dielectric crystals such as germanium and silicon in experiments such as Soudan Mine [180], CRESST [181] and CoGeNT [182]. Liquid noble gases are also deployed as DM detectors, known as noble liquid detectors, with the noble gases argon and xenon often employed because they are also excellent scintillators, as they too can be easily ionised. Examples of noble gas scintillators are DEAP [183] and DarkSide [184] which use argon for sensitive WIMP searches; other examples include Zeplin [185], and XENON1T [186] which used xenon, with larger multi-ton detectors proposed for future searches. Other types of DM detector include, but are not limited to, bubble chambers such as the PICO experiment [187], and novel techniques involving quantum dots [188] have also been proposed and are believed to be capable of improving current DM constraints by orders of magnitude, while also employing directional detectors.

8.3 Indirect Detection of Dark Matter

Indirect detection of DM does not involve detection of the DM particles themselves but rather the detection of the products of DM interactions. This typically involves looking for astrophysical and cosmological effects of DM annihilations or decays into SM particles. The idea revolves around scanning the sky seeking an excess or unexplained SM particles that cannot be attributed to known astrophysical processes. Neutral particles are an ideal choice; this is because the signal is not as likely to be influenced by other astrophysical processes resulting in a clearer picture of the process in which they are created. The flux of such neutral daughter particles is given by [189]

$$\Phi(E,\phi) = \frac{\Gamma}{4\pi m_X^a}\frac{dN}{dE}\int \rho[r,(\ell,\phi)]^a d\ell, \tag{8.3}$$

where $a = 2$ for annihilation's, whilst $a = 1$ for decays. Other parameters in the equation are the mass of the DM particles m_X, while dN/dE is the energy spectrum of the parent particles, while ρ is the density parameter of the DM. The expression is integrated over line of sight $d\ell$ and in the case of annihilating DM this yields the J-factor [190]. The final parameter is the rate Γ and takes two forms; in the case of annihilations, it is proportional to the thermally averaged cross section $\Gamma = \langle\sigma v\rangle$, and when decays are involved $\Gamma = 1/\tau$, where τ is the lifetime.

Neutrinos possess unique abilities to probe DM due to their neutral nature and could arise from DM annihilations and decays. One relatively recent and exciting prospect in the search for DM stems from the 3.5keV line which could be a signal from keV-sized sterile neutrinos decaying through the process $\chi \to \nu + \gamma$, however, when using blank sky searches, no 3.5keV line is found [191] which is not expected if this signal is produced by DM decays as the signal should also be detectable everywhere in the halo, thus the signal is disputed [192]. Another possible method is utilising gamma rays [193, 194], where it is believed that any DM model which features hadronic final states should in theory produce strong gamma ray signals, with ongoing searches investigating gamma rays from the Sun, the centre of the Milky Way, in other galaxies, or other extragalacitc gamma ray sources.

Signals from X-rays are investigated with indirect detection experiments at places such as XRISM [98], as X-rays, being neutral particles, can mostly ignore potentially tempestuous astrophysical magnetic fields. It is thought that electrically charged products can be produced from DM annihilating, which can in turn lead to X-ray signatures by inverse Compton scattering with astrophysical magnetic fields. Other forms of electromagnetic radiation are also investigated for DM signals; for example, charged products of DM annihilations can produce synchrotron emission as they pass through astrophysical magnetic fields. An exciting X-ray prospect is, of course, the 3.5keV signal previously discussed. Cosmic rays also have potential in DM searches in the instances that the final states from DM annihilations or decays result in charged leptons, with excitement arising from the high energies available to investigate novel physics that is not possible in lab based colliders. Particles such as positrons and antiprotons are investigated for fluxes of excessive energies. Other possible indirect contributions from DM include effects on the CMB[51] through photon emission and electromagnetic cascades, the production of antimatter via DM interactions, the capture of WIMPs leading to neutrino emission, and various astrophysical and cosmological signatures.

When searching the sky for an indirect DM signal, one typically has to account for known astrophysical processes; these known processes create components that act as noise, which require removing or accounting for, after which an excess or unexpected signal is likely interesting and accounts for

[51]Processes involving DM, such as annihilations and decays, can release energy during recombination. This can, in turn, delay the process of recombination and alter the CMB by damping small-scale anisotropies, shifting acoustic peak positions, and affecting polarisation. Current CMB data places constraints on these interactions [195].

unexplained physics that the model or fit has not accounted for. An example of such a parameter is the spectral index from observational astronomy, often indicated with γ, which characterises the dependence of the flux density on the frequency such that the radioactive flux density for some frequency is proportional to the spectral index, i.e. $\Phi_\nu \propto \nu^\gamma$. Specific examples of indirect experiments include γ-ray observatories such as the Fermi Gamma-ray Space Telescope [196] and the Large High Altitude Air Shower Observatory (LHAASO) [197] which is also capable of detecting cosmic rays. Neutrino telescopes such as IceCube [198] are also involved in indirect searches for DM signals, with their most recent bounds included in our results; see Figs. 19 - 22.

9 Neutrino Experiments

In this section, the current goals of neutrino experiments are discussed. First, the results and methods of neutrino oscillation experiments are divulged, and secondly, β-decay experiments are outlined along with their potential for identifying the nature and mass of neutrinos. Finally, neutrino telescopes are discussed with a particular emphasis on IceCube.

9.1 Neutrino Oscillation Experiments

Neutrino mixing, and thus masses, provided the first definitive evidence that the SM is not a complete description of particles and their interactions (excluding gravitational interactions). Due to this, neutrino oscillation experiments are currently of great interest, with accurate determination of neutrino mixing angles a subject of ongoing research and exploration [113]. The importance of these oscillation experiments lies in their potential to provide crucial insight into the properties and nature of neutrinos. Multiple neutrino oscillation experiments have been created, and they typically involve the production of a beam of neutrinos in some flavour which is then detected at some distance. A comparison of the flavour composition between the created and detected beam is then performed, allowing properties such as neutrino mass differences and mixing angles to be extracted; however, this is difficult due to the multi-variable nature of the equations that govern neutrino oscillations. These experiments can either be appearance or disappearance experiments. As discussed in Section 4 there are three mixing angles, these are $\theta_{12}, \theta_{13}, \text{and}, \theta_{23}$, which are known as the solar mixing angle, the reactor mixing angle, and the atmospheric mixing angle, respectively. If one only includes the dominant oscillations for a given instance, then a simple two-neutrino oscillation description will suffice, where the probability that a neutrino created in flavour α is detected as flavour β is given by

$$P(\nu_\alpha \to \nu_\beta) = P_{\alpha\beta} = \sin^2(2\theta_{ij})\sin^2\left(\frac{1.27\Delta m^2_{ij}\ell}{E_\nu}\right), \tag{9.1}$$

in units GeV for energy and km for distance.

The solar mixing angle determines the mixing angle between the first and second neutrino mass eigenstates, with the SNO [199] and Borexino [200] experiments providing precise values for θ_{12}, at approximately 33.8^o. Matter

effects play an important role and induce conversions of electron neutrinos to muon neutrinos. If matter effects are not included, the parameters $\ell = 10^8$km and electron neutrinos with energies $\mathcal{O}(10\text{MeV})$ imply that $\Delta m^2\text{sol} = 10^{-10}\text{eV}^2$, in contrast to $\Delta m^2_{\text{sol}} = 10^{-5}\text{eV}^2$, which is obtained when matter effects are accounted for. Reactor neutrinos have helped verify the initial solar results with experiments featuring baselines of approximately 100km for the $\mathcal{O}$(MeV) electron neutrinos produced in experiments such as KamLAND [201] in Japan. The results from KamLand have confirmed the conversion of electron neutrinos to muon neutrinos due to the MSW effect and thus reinforced the Δm^2_{sol} obtained from the solar experiments.

The atmospheric mixing angle determines the mixing between the second and third neutrino mass eigenstates, with measurements of the mixing angle currently at 48.6^o, which indicates an almost maximal mixing, with contributions to measuring the mixing angle coming from Super-Kamiokande [202] and IceCube [203]. Atmospheric neutrinos are produced when cosmic ray particles collide with particles in the Earth's atmosphere. This creates a cascade of short-lived mesons, typically pions that then decay into muons and muon antineutrinos, or vice versa. These muons also then typically decay into an electron, anti-electron, and a muon neutrino; thus the flavour composition of the incident neutrinos is normally around 2/3 muon neutrinos and 1/3 electron neutrinos. Less muon neutrinos were detected compared to what was predicted; this observed discrepancy is due to muon neutrinos oscillating into tau neutrinos, with a maximal disappearance coming from atmospheric neutrinos arriving when the baseline is roughly the Earth's diameter relative to the incident neutrino energies. These results were also verified by a disappearance experiment, utilising accelerator muon neutrinos with energies $\mathcal{O}$(GeV) thanks to the T2K experiment [204]. Unlike solar neutrinos, matter effects are not important, and thus the oscillations essentially occur in a vacuum.

Finally, the reactor mixing angle determines the mixing for the first and third neutrino mass eigenstates and has been measured at around 8.6^o by experiments such as the Daya Bay [205], Double Chooz [206], RENO [207], and Tokai-2-Kamioka (T2K) experiments [204]. Due to the small value of θ_{13}, it was initially assumed to be zero. The smallness of θ_{13} also presented additional difficulties in measuring it compared to θ_{12} and θ_{23}. This is because its small magnitude makes it sensitive to interference from the other oscillation channels. The other two angles, θ_{12} and θ_{23}, have relatively large experimental uncertainties, which further complicated the isolation of θ_{13}.

Experiments involving the disappearance of $\overline{\nu_e}$ are generally employed when measuring θ_{13}, with the detector placed roughly 1km allowing one to segregate the reactor oscillation term relative to the neutrino energies. These three mixing angles together with the complex CP violating Dirac phase form the PMNS matrix as also discussed in Section 4. Next generation experiments, such as the Deep Underground Neutrino Experiment (DUNE) in the United States and the Hyper-Kamiokande experiment in Japan, aim to produce even more precise measurements of neutrino mixing angles, especially θ_{13} and the CP violating phase, which has to some extent been examined by T2K [208].

9.2 Neutrino Properties from Decay Experiments

Isotope	$G^{0\nu}$ (10^{-14}y^{-1})	$Q_{\beta\beta}$ (KeV)
^{48}Ca	6.35	4273.7
^{76}Ge	0.623	2039.1
^{82}Se	2.70	2995.5
^{96}Zr	5.63	3347.7
^{100}Mo	4.36	3035.0
^{110}Pd	1.4	2004.0
^{116}Cd	4.62	2809.1
^{124}Sn	2.55	2287.7
^{130}Te	4.09	2530.3
^{136}Xe	4.31	2461.9
^{150}Nd	19.2	3367.3

Table 3: Nuclei which are theorised to undergo $0\nu\beta\beta$-decay, where $G^{0\nu}$ are the phase space factors, and $Q_{\beta\beta}$ are the Q-values which indicate the expected energy peak fo the emitted electrons, adapted from [209].

Results from neutrino oscillation experiments have provided evidence that neutrinos are massive, with a current goal in neutrino physics being measuring the electron neutrino mass. Measurement attempts are typically made by studying β-decay[52], with the energy distribution of emitted electrons roughly

[52]Tritium is a very popular isotope for multiple reasons. It has a relatively short half-life $\sim$ 12.4yrs, it emits electrons with a low energy of only $\sim$ 18.6keV, and a molecular structure simple enough to confidently calculate the energy spectrum of the electrons emitted [210].

given by [211]

$$\frac{dN}{dE_e} = Ap(E + m_e)(E_0 - E_e)\sqrt{(E_0 - E_e)^2 - m_\nu^2}F(E_e)\theta(E_0 - E_e - m_\nu), \tag{9.2}$$

where A is a normalisation constant, m_e is the mass of the electron, E_0 is the maximum allowed electron energy from decay kinematics which is known as the end point, while F is the Fermi function, and θ is the Heaviside function which imposes energy conservation. It is clear from Eq. 9.2 that the maximum allowed electron energy is determined by the neutrino mass since the electron neutrino contains the missing energy from the decay. It is hopeful that electrons in the end points of the distribution are found; however, electrons in the end points are rare occurrences. To help improve the chances of finding these electrons, some techniques can be employed such as using isotopes with a small end point as this increases the number of electrons found towards the end point thus reducing the statistical error. Using a detector with as good as possible energy resolution is also an obvious advantage, along with using a thin β-source to stop the material altering the kinematics of the emitted electron. Attempts are also being made at measuring the mass of the two other neutrino flavours also through decays of particles, with an example being the measurement of the muon neutrino. These muon neutrinos are produced through a process in which a pion decays into a muon and a muon neutrino, $\pi^+ \to \mu^+ + \nu_\mu$ [212]. In doing these types of experiments it has been possible to place upper limits on the masses of all neutrino flavours.

If neutrinos are massive and Majorana in nature, the three CP violating phases remain [213] and as such this opens up a theoretical avenue of experimentation which investigates neutrinoless double beta decay ($0\nu\beta\beta$) [214, 215, 216], which is a modification of the SM double beta decay ($\beta\beta$-decay). $\beta\beta$-decay occurs in rare isotopes where the daughter isotope has a higher binding energy than the parent isotope, $BE(P) < BE(D)$. Not only does $\beta\beta$-decay occur in rare isotopes, but the process itself, if it exists, is also extremely rare. A Feynman diagram for $0\nu\beta\beta$-decay is shown in Fig. 14, and as we have mentioned it is a potential method for testing the nature of neutrinos, since this process can only occur if neutrinos are Majorana particles. The form of this process is defined as [214]

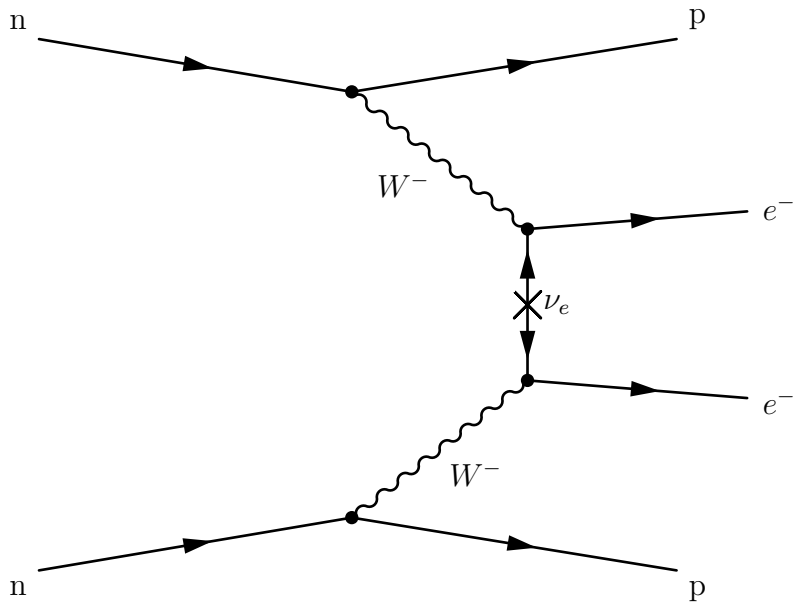

Figure 14: The typical Feynman diagram for neutrinoless double beta decay in which two neutrons decay into two protons and two electrons, with no neutrinos in the final state. The idea is that an antineutrino is emitted from one of the nuclei which is then absorbed by the other.

$$(A, Z) \rightarrow (A, Z+2) + 2e^{-}, \tag{9.3}$$

which clearly violates lepton number by two. If this process were found to exist, it would indicate that lepton number is not a symmetry of nature and would further fuel the speculation that leptons play a major role in the matter-antimatter asymmetry of the universe. Unfortunately, this process is also hypothesised to be extremely rare, as is displayed in Tab. 3, and implies that the chance of detecting such a process is exceptionally slim. The decay rate for $0\nu\beta\beta$ is given by [215]

$$\Gamma^{0\nu}_{\beta\beta} = \frac{1}{T^{0\nu}_{\beta\beta}} = G^{0\nu}|M^{0\nu}|^2\langle m_{\beta\beta}\rangle^2, \tag{9.4}$$

where $T^{0\nu}_{\beta\beta}$ is the lifetime, $G^{0\nu}$ is the phase space factor, $M^{0\nu}$ is the matrix element which is obtained from the relevant Feynman diagram for the process, and $|m_{\beta\beta}|$ is the effective Majorana neutrino mass given by [214]

$$\langle m_{\beta\beta}\rangle = \left|\sum_{i=1}^{3} U_{ei}^2 m_i\right|, \tag{9.5}$$

where m_i are the light neutrino mass eigenstates arising from the type I seesaw, and U_{ei} is the typical leptonic mixing matrix. There are currently many experiments seeking to investigate, or rather detect $0\nu\beta\beta$ such as the Germanium Detector Array experiment (GERDA) [217], the Enriched Xenon Observatory experiment (EXO) [218], Kamioka Liquid Scintillator Antineutrino Detector-Zen experiment (KamLAND-Zen) [219], and the Cryogenic Underground Observatory for Rare Events (CUORE) [220].

9.3 Neutrino Telescopes

Neutrino astronomy is a growing field that uses neutrino telescopes to observe high-energy neutrinos produced from astrophysical sources. Classical telescopes are electromagnetic (EM) telescopes that detect photons in the visible part of the EM spectrum. EM telescopes not only detect photons in the visible part of the EM spectrum but can also be designed to detect photons of other energies; hence, we have the fields of X-ray astronomy and radio

wave astronomy. Typically, a neutrino telescope comprises a large volume of transparent medium that interacts with incident neutrinos, and this interaction then produces detectable particles such as charged leptons or photons. Then, by backtracking these secondary particles, one can infer information about the original incident neutrino and thus the astrophysical processes that produced them. Let us briefly discuss the major advantage of neutrino telescopes when compared to optical telescopes. One large advantage is that neutrinos are not significantly affected by physical phenomena during their propagation; this allows neutrinos to enhance our knowledge of extremely dense regions of space that would be inaccessible to EM telescopes. An exciting research avenue is using neutrino telescopes in combination with other detectors, such as gamma-ray detectors and gravitational wave observatories, known as multimessenger astronomy. This allows a more comprehensive and multidimensional understanding of the universe and its processes.

Currently, the most capable neutrino telescope is the IceCube neutrino observatory, which is located at the South Pole [198]. IceCube is comprised of an array of over 5,000 optical sensors; these sensors are embedded within a cubic kilometre of ice situated approximately 2.5km below the surface. As we have discussed, IceCube relies on high-energy neutrinos interacting with the ice and then producing charged leptons, which are detected directly or through the Cherenkov radiation they emit. IceCube is the most sensitive to muons and neutrinos with energies in excess of 100GeV [221]. High-energy neutrinos enhance the possibility of detection of the muons created, as the muons produced have sufficient energy to travel to the detectors located within the ice. As with other neutrino telescopes, the main objective of IceCube is to improve our understanding of astrophysical processes, particularly processes involving cosmic rays that produce neutrinos during their interaction with the Earth's atmosphere. Although IceCube is primarily a neutrino telescope, it also serves as an excellent cosmic-ray detector. The results of IceCube have produced remarkable insights into high-energy astrophysical processes, including the identification of high-energy neutrino sources, such as blazars and gamma-ray bursts [222].

As we have discussed in previous parts of this thesis, neutrinos could play a large role in DM, with the search for DM signals also of interest at IceCube and other neutrino telescopes. An example of such signals could be the production of neutrinos from decaying DM particles. These DM decays could potentially lead to high-energy neutrino fluxes, and if this is the case, one could potentially expect a signal at IceCube. [223, 224, 225]. IceCube

has been operating for over a decade and has detected multiple very high-energy neutrinos with origins outside of our Solar System. The energies of these neutrinos ranged from 10GeV to several PeV [226, 227, 228]. A recent study by the IceCube collaboration analysed 7.5years of High-Energy Starting Events (HESE) data [223] and delivered the most constrained DM lifetime to date. The analysis found that that $\tau \gtrsim 10^{27} - 10^{28}$s for the energy range of 60TeV to 10PeV. This result is of significance to the RHINO model discussed within this thesis, as the DM particles are expected to decay into SM particles, which could in theory be detected at neutrino telescopes. A proportion of the high-energy neutrinos detected at IceCube could require new physics to fully explain, with one optimistic possibility being a contribution from dark matter. In theory, the mystery of these high-energy neutrinos could be resolved with a clearer understanding of the astrophysical mechanisms that produce them and their cumulative contributions. Interestingly, the observed neutrino flux is isotropic, which suggests a large number of unresolved sources or phenomena, potentially stemming from either astrophysical origins or new physics.

IceCube is not the only neutrino telescope, with the ANTARES [229, 230, 231] detector being another neutrino telescope located off the coast of France about 2.5km deep on the seabed. KM3NeT [232, 233] is a next generation neutrino telescope that is currently under construction (although it is still currently taking data) in the deep waters of the Mediterranean Sea. KM3NeT aims to become the largest neutrino telescope to date, with two sites; one being the Astroparticle Research with Cosmics in the Abyss (ARCA) site which focuses on the detection of high-energy astrophysical neutrinos, and the other is the Oscillation Research with Cosmics in the Abyss (ORCA) which is optimised for studying neutrino oscillations and determining the neutrino mass hierarchy. To summarise, if neutrinos and dark matter are linked, neutrino telescopes would undoubtedly become vital tools in the quest for evidence.

10 RHINO Dark Matter

The RHINO DM model will now be introduced, before introducing two methods of DM production which have previously been explored; this first production method utilises the LZ approximation where source RH neutrinos are resonantly converted to a dark neutrino which can play the role of DM. The second method uses the density matrix, which has a long history in calculations with respect to neutrino oscillations. Finally, leptogenesis within the model is discussed.

10.1 The RHINO Lagrangian

Let us now introduce the RHINO DM model proposed by Di Bari *et al.* [99] starting with the effective Lagrangian for the model, which features the traditional type-1 seesaw Lagrangian [234] with three generations of RH neutrino plus the Anisimov operator, which currently features only a Higgs-inducing neutrino mixing term. The Lagrangian for RHINO DM before spontaneous EWSB is given by ($\alpha = e, \mu, \tau$ and $I, J = 1, 2, 3$)

$$-\mathcal{L}^{\nu}_{Y+M+\Lambda} = \overline{L_{\alpha}} h_{\alpha J} N_{RJ} \tilde{\Phi} + \frac{1}{2} \overline{N^{c}_{RI}} D_{MIJ} N_{RJ} + \frac{\lambda_{IJ}}{\Lambda} \Phi^{\dagger} \Phi \overline{N^{c}_{RI}} N_{RJ} + \text{h.c.}. \tag{10.1}$$

Where $L^{T}_{\alpha} \equiv (\nu_{L\alpha}, \alpha_{L})$ are the leptonic doublets, Φ is the Higgs doublet ($\tilde{\Phi} \equiv i\sigma_2 \Phi^{*}$ is its dual), the $h_{\alpha J}$'s are the neutrino Yukawa couplings in the flavour basis where both charged lepton and Majorana mass matrices are diagonal, with $D_M \equiv \text{diag}(M_1, M_2, M_3)$, noting that $M_1 \leq M_2 \leq M_3$ are the three heavy neutrino masses, with a dark decoupled neutrino identified as the largest neutrino such that $N_3 = N_{\text{D}}$. This Lagrangian currently does not feature Higgs portal interactions when $I = J$. The Higgs VEV generates the neutrino Dirac mass matrix $m_{\text{D}} = vh$ after EWSB. In this model one of the three RH neutrinos, N_3 in this instance, is assumed to have vanishing Yukawa couplings and is therefore decoupled from the seesaw model[53], such that the Yukawa couplings for neutrinos are given by

[53] Perhaps one should at this point refer to N_{D} as a heavy neutral lepton, until the small Yukawa couplings are induced by the Anisimov operator.

$$h = \begin{pmatrix} h_{e1} & h_{e2} & 0 \\ h_{\mu 1} & h_{\mu 2} & 0 \\ h_{\tau 1} & h_{\tau 2} & 0 \end{pmatrix}, \tag{10.2}$$

which, as one can see, results in one of the columns in h and therefore one of the columns of $m_{\rm D}$ to be vanishing and, as such, is decoupled from the seesaw formula, which, for example, can be justified by imposing a $\mathcal{Z}_2$ symmetry. In this model, the light neutrino masses are given the seesaw formula discussed in Section 5 and are defined by

$$D_m = {\rm diag}(m_1 = 0, m_2, m_3) = U^\dagger m_{\rm D} \frac{1}{D_M} m_{\rm D}^T U^*, \tag{10.3}$$

with U being the leptonic mixing matrix, which reduces to the two RH neutrino case, if one has as we do, that the lightest neutrino mass is vanishing, $m_1 = 0$. This ensures that the model predicts hierarchical light neutrino masses. Naturally, in the Yukawa basis, the Yukawa matrix is diagonal, such that $D_h = {\rm diag}(h_A, h_B, h_C)$, with $h_A = 0 < h_B < h_C$. The transformation between the mass basis and the Yukawa basis is given by the bi-unitary transformation

$$m_{\rm D} = V_L^\dagger D_{m_{\rm D}} U_R, \tag{10.4}$$

in which U_R (V_L) is the RH (LH) neutrino mixing matrix that acts only on the RH (LH) neutrino fields. Without the Higgs-induced interactions that are produced by the Anisimov operator (when $\lambda_{IJ} = 0$) U_R given by

$$U_R(\varepsilon) = \begin{pmatrix} \cos\varepsilon & \sin\varepsilon & 0 \\ -\sin\varepsilon & \cos\varepsilon & 0 \\ 0 & 0 & 1 \end{pmatrix}. \tag{10.5}$$

where ε is a complex angle and if one takes $\varepsilon \simeq 0$ this results in $U_R \simeq I$, which maximises the lifetime of the dark neutrino. This mixing matrix is capable of generating a mixing between the seesaw neutrinos (the two neutrinos that are not $N_{\rm D}$), which is necessary if one wishes to have non-vanishing CP asymmetries in these two neutrinos, thus allowing one to generate the baryon

asymmetry via leptogenesis, which is even possible with infinitesimal deviations from $U_R = I$ [148]. The mixing matrix $U_R(\varepsilon)$ results in the dark RH neutrino Majorana mass eigenstate, $N_{\rm D}$, coinciding with the Yukawa eigenstate, N_3, which is completely decoupled and extremely stable, resulting in no possible production mechanism. The lifetime of dark neutrinos can be further maximised by assuming that the dark neutrino mixes only with the seesaw neutrino with the larger Yukawa couplings h_B, which plays the role of a source RH neutrino $N_{\rm S}$ [99]. This neutrino can be either of the seesaw neutrinos; however, we assume that $N_{\rm S} = N_2$ and, therefore, $M_{\rm S} = M_2$. We also assumed NO for the light neutrino masses in order to minimise the source neutrino Yukawa coupling and to maximise the lifetime of the DM. The neutrino Yukawa couplings are given by[54] $h_{\rm S} = h_B = \sqrt{m_{\rm sol} M_{\rm S}}/v$, which means one also has $h_C = \sqrt{m_{\rm atm} M_I}/v$, where either $I = 1$, if $N_{\rm S} = N_2$, or $I = 2$, if $N_{\rm S} = N_1$. However, and this is key, to have successful leptogenesis much below 10^9GeV, one necessarily has $M_1 \simeq M_2$, thus it does not make a difference in our discussion which seesaw RH neutrino is the source neutrino. This means the RHINO Lagrangian Eq. 10.1 simplifies to

$$-\mathcal{L}^{\nu}_{Y+M+\Lambda} = \overline{L_\alpha} h_{\alpha J} N_{RJ} \tilde{\Phi} + \frac{1}{2} \overline{N^c_{RI}} D_{MIJ} N_{RJ} + \frac{1}{\tilde{\Lambda}_{\rm DS}} \Phi^\dagger \Phi \overline{N^c_{\rm D}} N_{\rm S} + \text{h.c.}, \tag{10.6}$$

where we have $\tilde{\Lambda}_{\rm DS} = \Lambda/\lambda_{\rm DS}$. As we have seen in Section 3 after EWSB, the Higgs acquires a VEV, v, which generates a neutrino Dirac mass matrix given by

$$m_{\rm D} = vh = \begin{pmatrix} m_{De1} & m_{De2} & 0 \\ m_{D\mu 1} & m_{D\mu 2} & 0 \\ m_{D\tau 1} & m_{D\tau 2} & 0 \end{pmatrix}. \tag{10.7}$$

Additionally, small off-diagonal corrections from the Anisimov operator to the Majorana mass term are generated, $\delta M^{\Lambda}_{\rm DS} = v^2/\tilde{\Lambda}_{\rm DS}$, this results in the Lagrangian now given by

$$-\mathcal{L}^{\nu}_{D+M+\delta M^{\Lambda}_{\rm DS}} = \overline{\nu_{L\alpha}} m_{D\alpha J} N_{RJ} \tilde{\Phi} + \frac{1}{2} \overline{N^c_{RI}} D_{MIJ} N_{RJ} + \frac{1}{2} \overline{N^c_{\rm D}} \delta M^{\Lambda}_{\rm DS} N_{\rm S} + \text{h.c.}. \tag{10.8}$$

[54] This ensures that the light neutrino masses are given by $m_\nu = (0, m_{\rm sol}, m_{\rm atm})$.

Due to this the mass eigenstates of the RH neutrinos involved in the Anisimov operator are modified as[55]

$$N_{\rm S} \to N^0_{\rm S,\Lambda} = N_{\rm D}\sin\theta^0_\Lambda + N_{\rm S}\cos\theta^0_\Lambda \tag{10.9}$$

$$N_{\rm D} \to N^0_{\rm D,\Lambda} = N_{\rm D}\cos\theta^0_\Lambda - N_{\rm S}\sin\theta^0_\Lambda, \tag{10.10}$$

where one also has that[56]

$$\theta^0_\Lambda = \frac{2v^2/\tilde{\Lambda}_{\rm DS}}{M_{\rm D}(1-M_{\rm S}/M_{\rm D})}, \tag{10.11}$$

which is the effective mixing angle at zero temperature. Due to this, the RH neutrino mixing matrix, which takes us from the new mass eigenstate basis to the flavour basis, is given by

$$U^\Lambda_R(\theta^0_\Lambda) = \begin{pmatrix} 1 & 0 & 0 \\ 0 & \cos\theta^0_\Lambda & \sin\theta^0_\Lambda \\ 0 & -\sin\theta^0_\Lambda & \cos\theta^0_\Lambda \end{pmatrix}. \tag{10.12}$$

The Dirac mass matrix in the new basis is therefore given by

$$m^\Lambda_{\rm D} = m_{\rm D}U^\Lambda_R(\theta^0_\Lambda) = \begin{pmatrix} m_{De1} & m_{De2}\cos\theta^0_\Lambda & m_{De2}\sin\theta^0_\Lambda \\ m_{D\mu1} & m_{D\mu2}\cos\theta^0_\Lambda & m_{D\mu2}\sin\theta^0_\Lambda \\ m_{D\tau1} & m_{D\tau2}\cos\theta^0_\Lambda & m_{D\tau2}\sin\theta^0_\Lambda \end{pmatrix}, \tag{10.13}$$

which shows that the mass eigenstates created by the field $N^\Lambda_{\rm D}$ are what one should identify with the DM. These states are also not 100% stable and can decay with a lifetime [21]

$$\tau_{\rm D} \simeq (\Gamma_{{\rm D}\to A+\ell_{\rm S}} + \Gamma_{{\rm D}\to 3A+\ell_{\rm S}})^{-1}. \tag{10.14}$$

[55] Where the DS subscript has been neglected, such that $\theta_\Lambda \equiv \theta_{\Lambda_{\rm DS}}$.

[56] Where our results are not affected by this approximation as this expression holds for $\theta^0_\Lambda \ll 1$, which is always the case except in the instance of extreme degeneracy, where the mixing angle becomes maximal.

The total two body decay width when $N_{\rm S} > M_{\rm Higgs} \sim 125$GeV is given by $\Gamma_{\rm S} \equiv h_{\rm S} M_{\rm S}/4\pi$ [235], therefore, the decay width of the process $\Gamma_{{\rm D}\to A+\ell_{\rm S}}$ is given by [9]

$$\Gamma_{{\rm D}\to A+\ell_{\rm S}} = (\theta^0_\Lambda)^2 \frac{h^2_{\rm S}}{4\pi} M_{\rm D} = \frac{h^2_{\rm S}}{\pi} \left(\frac{v^2}{\tilde{\Lambda}_{\rm DS}}\right)^2 \frac{M_{\rm D}}{(M_{\rm D} - M_{\rm S})^2}, \tag{10.15}$$

whilst the four-body decay rate $\Gamma_{{\rm D}\to 3A+\ell_{\rm S}}$ is calculated with the narrow width approximation and is given by

$$\Gamma_{{\rm D}\to 3A+\ell_{\rm S}} = \frac{\Gamma_{\rm S}}{15 \cdot 2^{11} \cdot \pi^4} \frac{M_{\rm D}}{M_{\rm S}} \left(\frac{M_{\rm D}}{\tilde{\Lambda}_{\rm DS}}\right)^2, \tag{10.16}$$

where we have $\Gamma_{\rm S} = h^2_{\rm S} M_{\rm S}/4\pi$. Currently, the 7.5-yr IceCube HESE data features the most stringent lower bound on the DM lifetime, where one has $\tau_{\rm D} \gtrsim 10^{27} - 10^{28} s$ in the 60TeV-10PeV energy range [223], which extends previous results[57] [236].

Let us briefly summarise the RHINO model so far, once the Higgs-induced interactions are switched on, $\lambda_{IJ} \neq 0$, a mixing occurs between $N_{\rm D}$ and the other two RH neutrinos that feature couplings. As we shall see when temperatures are finite, the Yukawa and Higgs-induced interactions contribute to the RH neutrino self-energies that produce effective potentials that in general are not diagonal in the same basis, which affects the RH neutrinos propagation and mixing properties as displayed in panel (a) and (b) of Fig. 15. This misalignment between the two bases is responsible for the RH neutrino mixing. Also, as mentioned, it is convenient to assume that the RH neutrino mixing is dominantly between the dark RH neutrino and one of the other two RH neutrinos, the source RH neutrino, as this simplifies the situation and also minimises the constraints from decays [9]. In this scenario, we can consider a simple two-mixing formalism with the coupling between the dark RH neutrino and the source RH neutrino with coupling $\lambda_{\rm DS}$. In this two-neutrino mixing model when, for example, if $\lambda_{\rm DS} = 0$, one has $U^\Lambda_R(\theta^0_\Lambda) = I$ and thus there would be no mixing resulting in $N_{\rm D}$ being completely decoupled.

[57] We later use these results as approximate and indicative lower bounds. This is expanded later in the work, where we discuss how the lower bounds depend on the decay channel along with the DM mass.

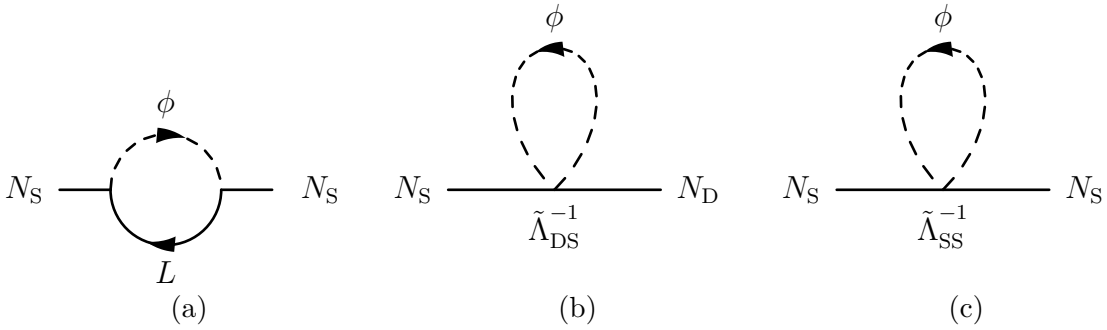

Figure 15: Self-energy diagrams with Yukawa interactions in panel (a), and Anisimov interactions in panel (b) and (c).

Let us now investigate the mixing itself. It is clear that the Yukawa interactions produce a diagonal contribution to the RH neutrino Hamiltonian in the Yukawa basis, such that [237]

$$V_{IJ}^{Y} = \frac{T^2}{8E_J} h_J^2 \delta_{IJ} \quad (I, J = \text{DM, S}), \tag{10.17}$$

with E_J being the energy of the Majorana mass eigenstate N_J, whilst $h_{\rm J} \equiv \sqrt{(h^\dagger h)_{JJ}}$ is the Yukawa coupling of N_J to the SM particles. The potentials V_{IJ}^{Y} are from coherent forward scatterings, with the main contribution stemming from 1-loop self-energy diagrams featuring ordinary lepton and Higgs doublets in the intermediate states. The Higgs-induced interactions which are described by the Anisimov operator, are generally not diagonal in the Yukawa basis and produce an effective potential approximated as [15]

$$V_{IJ}^{\Lambda} \approx \frac{T^2}{12\tilde{\Lambda}_{IJ}} \quad (I, J = \text{DM, S}), \tag{10.18}$$

with again $\tilde{\Lambda} \equiv \Lambda/\lambda$, or explicitly $\tilde{\Lambda}_{\rm DS} \equiv \Lambda/\lambda_{\rm DS}$. In the Majorana mass eigenstate basis, the usual diagonal kinetic contribution must also be considered, which results in the Hamiltonian being expressed as

$$\mathcal{H}_{IJ} = \begin{pmatrix} E_{\rm D} & \frac{T^2}{12\tilde{\Lambda}_{\rm DS}} \\ \frac{T^2}{12\tilde{\Lambda}_{\rm DS}} & E_{\rm S} + \frac{T^2}{8E_{\rm S}} h_{\rm S}^2 \end{pmatrix}, \tag{10.19}$$

remembering that $N_{\rm D}$ has no Yukawa interactions, as $h_{\rm D} = h_A = 0$. One also assumes that the diagonal terms of the Higgs-induced interactions can

be neglected because of their smallness compared to the standard Yukawa interactions. As usual, in this circumstance, it is typical to subtract a contribution proportional to the identity from $\mathcal{H}$ which does not affect the mixing; this results in the effective mixing Hamiltonian becoming

$$\Delta\mathcal{H}_{IJ} \approx \begin{pmatrix} -\frac{\Delta M^2}{4p} - \frac{T^2}{16p}h_{\rm S}^2 & \frac{T^2}{12\Lambda_{\rm DS}} \\ \frac{T^2}{12\Lambda_{\rm DS}} & \frac{\Delta M^2}{4p} + \frac{T^2}{16p}h_{\rm S}^2 \end{pmatrix}, \tag{10.20}$$

where[58] $\Delta M \equiv M_{\rm S}^2 - M_{\rm D}^2$. If a monochromatic approximation is incorporated, such that the momentum is replaced by its average value $p = 3T$, then this results in the effective mixing Hamiltonian in the flavour basis becoming

$$\Delta\mathcal{H}_{IJ} \approx \frac{\Delta M^2}{12T}\begin{pmatrix} -1 - v_{\rm S}^Y & \sin 2\theta_\Lambda \\ \sin 2\theta_\Lambda & 1 + v_{\rm S}^Y \end{pmatrix}. \tag{10.21}$$

Here, a dimensionless effective potential has also been introduced, $v_{\rm S}^Y \equiv T^2 h_{\rm S}^2/(4\,\Delta M^2)$, with an effective mixing angle $\sin 2\theta_\Lambda(T) \equiv T^3/(\tilde{\Lambda}_{\rm DS}\,\Delta M^2)$, which is produced by the misalignment between Yukawa and Higgs-induced interactions.

10.2 Resonant Production

The resonant production of the dark neutrino arises as follows [99]. If $M_{\rm D} \geq M_{\rm S}$, and thus $\Delta M^2 \leq 0$, a resonance occurs for $v_{\rm S}^Y = -1$, which corresponds to a specific temperature, the *resonance temperature*, which can be expressed as

$$T_{res} \equiv \frac{2\sqrt{|\Delta M^2|}}{h_{\rm S}} = \frac{2\sqrt{M_{\rm D}^2 - M_{\rm S}^2}}{h_{\rm S}}. \tag{10.22}$$

Such a production process is highly non-adiabatic, therefore, just a tiny fraction of the $N_{\rm S}$'s produced by the Yukawa interactions are converted at the resonance. Fortunately, large dark RH neutrinos can be considered, and therefore only a tiny amount can suffice to reproduce the DM abundance.

[58] In the ultra-relativistic regime one can write for $N_{\rm D}$ that $E_{\rm D} \simeq p + M_{\rm D}^2/2p$, and similarly for the $N_{\rm S}$ that that $E_{\rm S} \simeq p + M_{\rm S}^2/2p$.

The abundance of DM can be expressed in terms of the conversion fraction of DM ($N_{N_{\rm D}}/N_{N_{\rm S}}$) at the resonance as [99]

$$\Omega_{\rm D}h^2 \approx 1.45\times10^6\left(\frac{N_{N_{\rm S}}}{N_\gamma}\right)_{\rm res}\left(\frac{N_{N_{\rm D}}}{N_{N_{\rm S}}}\right)_{\rm res}\left(\frac{M_{\rm D}}{\rm GeV}\right), \tag{10.23}$$

with $(N_{N_{\rm D}}/N_{N_\gamma})$ being the source RH neutrino-to-photon ratio at the resonance and naturally is determined by the initial conditions, whilst the DM abundance at present day is given by Eq. 1.1. Here, one can see that the measured DM requires a value such that

$$(N_{N_{\rm D}}/N_{N_{\rm S}})_{\rm res} \sim 10^{-10}({\rm TeV}/M_{\rm D})/(N_{N_{\rm S}}/N_\gamma)_{res}, \tag{10.24}$$

it is also worth noting the minute amount required when $M_{\rm D} \geq 1$TeV, which is an imperative feature of this production mechanism. The LZ formula is a simple method to calculate $(N_{N_{\rm D}}/N_{N_{\rm S}})_{res}$, such that [8, 9]

$$\left.\frac{N_{N_{\rm D}}}{N_{N_{\rm S}}}\right|_{\rm res} \approx \frac{\pi}{2}\gamma_{\rm res}, \tag{10.25}$$

with γ_{res} being the *adiabaticity parameter* at the resonance, which is given by

$$\gamma_{res} \equiv \left.\frac{|E^m_{\rm D}-E^m_{\rm S}|}{2|\dot\theta_m|}\right|_{\rm res}, \tag{10.26}$$

in this instance the adiabaticity parameter equates to

$$\gamma_{\rm res} = \sin^2 2\theta_\Lambda(T_{\rm res})\frac{|\Delta M^2|}{12T_{\rm res}H_{\rm res}} \approx 0.4\frac{M_{\rm Pl}\sqrt{|\Delta M^2|}}{\tilde\Lambda^2\sqrt{g_*^{\rm res}}h_{\rm S}^3}, \tag{10.27}$$

with $g_*^{\rm res} = g_*^{SM}+g_*^{N_{\rm S}} = 106.75+g_*^{N_{\rm S}} \approx 106.75$ being the ultra-relativistic degrees of freedom at the resonance, which is essentially the same as the SM contribution, and $H_{res} = 1.66\sqrt{g_*^{\rm res}}T^2_{\rm res}/M_{\rm Pl}$ being the expansion rate at resonance. Constraints on neutrino masses from the seesaw model and

mixing experiments must also be considered; therefore, it is useful to define the effective neutrino mass associated with the source RH neutrino, $\tilde{m}_{\rm S} \equiv v^2 h_{\rm S}^2/M_{\rm S}$. This formalism provides an easy way to normalise the Yukawa couplings, which automatically takes into account the information from the mixing experiments and the seesaw model. Now, if we define $\alpha \equiv \tilde{m_{\rm S}}/m_{\rm sol}$, with $m_{\rm sol}$ being the solar neutrino mass scale, with the seesaw model imposing that $\alpha_{\rm S} \geq 1$, it is worth noting that $h_{\rm S}$ can be expressed in terms $\alpha_{\rm S}$ as

$$h_{\rm S}^2 = \alpha_{\rm S} \frac{m_{\rm sol} M_{\rm S}}{v^2}. \tag{10.28}$$

As usual when dealing with thermal production in the early universe, the variable $z \equiv M_{\rm D}/T$ is introduced, with its value at the resonance being equal to $z_{\rm res} \equiv M_{\rm D}/T_{\rm res}$, which makes it possible to express ΔM^2 in terms of $z_{\rm res}$ resulting in the following

$$\sqrt{|\Delta M^2|} = \frac{h_{\rm S} M_{\rm D}}{2 z_{\rm res}}. \tag{10.29}$$

This expression can then be inserted into Eq. 10.27 along with the definition of $\alpha_{\rm S}$, which allows the adiabaticity parameter at the resonance to be expressed as

$$\gamma_{\rm res} \approx \frac{8}{\alpha_{\rm S}\, z_{\rm res}} \left(\frac{M_{\rm D}}{M_{\rm S}}\right) \left(\frac{10^{16}{\rm GeV}}{\tilde{\Lambda}}\right)^2, \tag{10.30}$$

which allows us to calculate the resonant conversion using the LZ formula Eq. 10.25. This then in turn allows us to calculate the $N_{\rm D}$ abundance using Eq. 10.23 resulting in

$$\Omega_{N_{\rm D}} h^2 \approx \frac{0.1822}{\alpha_{\rm S}\, z_{\rm res}} \left(\frac{N_{N_{\rm S}}}{N_\gamma}\right)_{\rm res} \left(\frac{M_{\rm D}}{\rm GeV}\right) \left(\frac{M_{\rm D}}{M_{\rm S}}\right) \left(\frac{10^{20}{\rm GeV}}{\tilde{\Lambda}_{\rm DS}}\right)^2. \tag{10.31}$$

Imposing that the above expression reproduces the measured value of Eq. 1.1, one obtains the value $\tilde{\Lambda}$ that reproduces the observed DM abundance

$$\tilde{\Lambda}_{\rm DM} \approx {\rm GeV} \sqrt{\frac{1.53}{\alpha_{\rm S}\, z_{\rm res}} \left(\frac{N_{N_{\rm S}}}{N_\gamma}\right)_{\rm res} \frac{M_{\rm D}}{M_{\rm S}} \frac{M_{\rm D}}{\rm GeV}}, \tag{10.32}$$

with five parameters: $z_{\rm res}$, $\alpha_{\rm S}$, $(N_{N_{\rm S}}/N_\gamma)_{\rm res}$, $M_{\rm D}$, and $M_{\rm D}/M_{\rm S}$ (or $M_{\rm S}$). It is also possible by using Eq. (10.29) to express $z_{\rm res}$ in terms of $\alpha_{\rm S}$, $M_{\rm D}$, and $M_{\rm D}/M_{\rm S}$ such that

$$z_{\rm res} = \frac{h_{\rm S}\, M_{\rm D}}{2\sqrt{M_{\rm D}^2 - M_{\rm S}^2}} \approx 0.85 \times 10^{-8} \sqrt{\alpha_{\rm S} \frac{M_{\rm S}}{M_{\rm D}} \left(\frac{M_{\rm D}}{\rm GeV}\right)} \frac{M_{\rm D}/M_{\rm S}}{\sqrt{M_{\rm D}^2/M_{\rm S}^2 - 1}}, \tag{10.33}$$

which shows that there are, in fact, only four parameters. This formulation of $z_{\rm res}$ also displays that $z_{\rm res} \ll 1$ (or $T_{\rm res} \gg M_{\rm D}$), which implies that the reheat temperature cannot be too low, $T_{\rm RH} > T_{\rm res}$. There is an upper bound such that $T_{\rm RH} \lesssim 10^{16}$GeV, which results in further constraints on the allowed parameter space. The dependence on the initial conditions is encoded within the value of $(N_{N_{\rm S}}/N_\gamma)_{\rm res}$. If one assumes that some external mechanism thermalises the source RH neutrinos prior to the resonant conversion, then $(N_{N_{\rm S}}/N_{N_\gamma})_{\rm res} = 3/4$ and in this instance one arrives at

$$\tilde{\Lambda}_{\rm DM} \approx 10^{20}{\rm GeV} \sqrt{\frac{1.15}{\alpha_{\rm S} z_{\rm res}} \frac{M_{\rm D}}{M_{\rm S}} \frac{M_{\rm D}}{\rm GeV}} \tag{10.34}$$

Perhaps the more interesting case which does not rely on any external mechanism is to assume a vanishing initial source RH neutrino abundance, which is then produced by decays from particles in thermal bath through Yukawa interactions. If this is the case, then the production is described by a simple rate equation

$$\frac{dN_{N_{\rm S}}}{dz_{\rm S}} = -(D_{\rm S} + S_{\rm S})(N_{N_{\rm S}} - N_{N_{\rm S}}^{\rm eq}), \tag{10.35}$$

where $z_{\rm S} \equiv M_{\rm S}/T = z\, M_{\rm S}/M_{\rm D}$, as $z = M_{\rm D}/T$, while $D_{\rm S} \equiv \Gamma_{\rm D}^S/(H\, z_{\rm S})$, with $\Gamma_{\rm D}^S$ being the total decay rate, and $S_{\rm S} \equiv \Gamma_{\rm S}^S/(H\, z_{\rm S})$ with $\Gamma_{\rm S}^S$ being the scattering rate. The abundances are normalised in such a way that in the ultra-relativistic equilibrium we have that $N_{N_{\rm S}}^{\rm eq}(z_{\rm S} \gg 1) = 1$, which results in the thermal equilibrium $N_{\rm S}$-abundance being given by [238]

$$N_{N_{\rm S}}^{\rm eq} = \frac{1}{2} \int_{z_{\rm S}}^{\infty} dx\, x \sqrt{x^2 - z_{\rm S}^2}\, e^{-x}. \tag{10.36}$$

The initial vanishing abundance results in the inverse decays being negligible and allows us to simplify the rate equation into

$$\frac{dN_{N_{\rm S}}}{dz_{\rm S}} = (D_{\rm S} + S_{\rm S})N^{\rm eq}_{N_{\rm S}}., \tag{10.37}$$

The decay parameters are defined as $(D+S)(z_{\rm S} \ll 1) \approx K_{\rm S}/5 = 1/z^{\rm eq}_{\rm S}$, with $z^{\rm eq}_{\rm S} \approx 0.5\alpha^{-1}_{\rm S}$ [9, 239] being the value of $z_{\rm S}$ at the time when the $N_{\rm S}$ abundance thermalises. This results in the following solution

$$N_{N_{\rm S}}(z < z^{\rm eq}_{\rm S}) \approx \frac{z_{\rm S}}{z^{\rm eq}_{\rm S}}, \tag{10.38}$$

and therefore at the resonance one has [9]

$$\left(\frac{N_{N_{\rm S}}}{N_\gamma}\right)_{\rm res} = \frac{3}{4}\frac{z_{\rm res}}{z^{\rm eq}_{\rm S}}\frac{M_{\rm S}}{M_{\rm D}}. \tag{10.39}$$

With this result the scale of new physics reproducing the observed DM can be calculated as

$$\tilde{\Lambda}_{\rm DM} \approx 10^{20}{\rm GeV}\sqrt{\frac{1.15}{\alpha_{\rm S} z^{\rm eq}_{\rm S}}\frac{M_{\rm D}}{\rm GeV}}. \tag{10.40}$$

10.3 Density Matrix Formalism

The conversion of source RH neutrinos to dark RH neutrinos has been further investigated by solving the relevant density matrix equations [21]. The density matrix is a generalisation of typical state vectors or wave functions that can represent mixed states instead of just pure states, as discussed previously. Due to the experimental evidence suggesting that neutrino mass eigenstates do not correspond with the flavour eigenstates in which we detect, and from this mixing arise neutrino oscillations, which can be accurately explained by utilising the density matrix equations one would expect to be able to investigate the dark neutrino production in a similar manner as the dark neutrino production occurs from oscillations in the early universe. The density matrix formalism also allows us to consistently describe the decoherence

of the states along with the evolution of the mixed states that occur from neutrino oscillations and collisions. When dealing with a mixture of both pure and mixed states, the Boltzmann equations are not sufficient alone. In fact, previously first-order (or refractive) neutrino matter effects were typically treated on the amplitude level in the form of a Schrödinger equation, whilst the second-order effects were treated with a kinetic equation involving a Boltzmann collision integral, but neither could quantitatively account for a situation where both neutrino oscillations and collisions were important. As mentioned, the use of the density matrix within neutrino physics is no secret and is often employed in the study of active-sterile neutrino mixing in the early universe [240]. Previous studies have found that both the LZ approximation and the density matrix formalism are in quite good agreement [241]. Other uses of the density matrix formalism in neutrino physics are the study of RH neutrino mixing in leptogenesis from neutrino oscillations [19, 20], along with the description of flavour effects in leptogenesis [242].

Without the presence of the Higgs portal interactions, the source RH neutrinos could only have been produced by Yukawa interactions, while the $N_{\rm D}$'s would of been completely decoupled (ignoring a possible third RH neutrino species). It is possible to describe this production of $N_{\rm S}$ using a density matrix normalised in terms of the source RH neutrino abundance that in the Yukawa basis would be diagonal and simply given by $(I, J = DM, S)$

$$N_{IJ}(z) = N_{N_{\rm S}}(z) \begin{pmatrix} 0 & 0 \\ 0 & 1 \end{pmatrix}. \tag{10.41}$$

As with the LZ approximation, a monochromatic approximation is used in which the momentum dependence is integrated away and the abundance of the source RH neutrinos is described by a simple rate equation, which is Eq. 10.35. When the Higgs-induced interactions are turned on, they develop off-diagonal terms that have to be accounted for, along with decoherence effects which must also be investigated. The evolution of this system is described

by the density matrix equation of the form[59]

$$\frac{dN_{IJ}}{dt} = -i[\mathcal{H}, N]_{IJ} - \begin{pmatrix} 0 & \frac{1}{2}(\Gamma_{\rm D} + \Gamma_{\rm S})N_{\rm DS} \\ \frac{1}{2}(\Gamma_{\rm D} + \Gamma_{\rm S})N_{\rm DS} & (\Gamma_{\rm D} + \Gamma_{\rm S})(N_{N_{\rm S}} - N^{\rm eq}_{N_{\rm S}}) \end{pmatrix}, \tag{10.43}$$

where the first term is the Liouville-von Neumann term. The second term is the combination of off-diagonal terms, which features decoherence and damping, along with the repopulation terms on the diagonal. These repopulation terms describe the production of source RH neutrinos. It is worth noting that without the off-diagonal terms in the Hamiltonian, the density matrix equation would simply reduce to Eq. 10.35. As previously, a diagonal term in $\mathcal{H}$ cancels out in the oscillations, and thus we can replace $\mathcal{H} \to \Delta\mathcal{H}$, with $\Delta\mathcal{H}$ given by Eq. 10.20. It is possible to express the matrices in the Pauli matrix basis using vectorial notation. Vectorial parameterisation as discussed previously involves using the Pauli matrix expansion of two by two matrices. This allows us in the pure instance to recast the von Neumann equation (a quantum version of the Liouville equation) and explicitly we can see that the term in the Hamiltonian proportional to the identity cancels out in the commuter and thus ultimately cancels out from the dynamics, and thus the quantum state itself. Vectorial parameterisation results in the effective Hamiltonian in Eq. 10.20 being recast as

$$\Delta\mathcal{H} = \frac{1}{2}\vec{V} \cdot \vec{\sigma}, \tag{10.44}$$

where the effective potential vector $\vec{V}$ for this system is defined as

$$\vec{V} \equiv \frac{\Delta M^2}{6T}(\sin 2\theta_\Lambda, 0, -1 - v_{\rm S}^Y). \tag{10.45}$$

The abundance density matrix is analogously recast, introducing the quantity P_0, and the polarisation vector $\vec{P}$, as [243]

[59] This is equivalent to the popular form of the density matrix, which is expressed through anti-commutators, seen in much of the literature, see Appendix B of Ref [16]. The typical form is

$$\frac{N_{IJ}}{dt} = -i[H, N]_{IJ} - \frac{1}{2}\{\Gamma, N\}_{IJ} + \frac{1}{2}\{\Gamma, N^{\rm eq}\}_{IJ}. \tag{10.42}$$

$$N = \frac{1}{2}P_0(1 + \vec{P} \cdot \vec{\sigma}), \tag{10.46}$$

such that

$$N_{N_{\rm D}} = \frac{1}{2}P_0(1 + P_z), \tag{10.47}$$

$$N_{N_{\rm S}} = \frac{1}{2}P_0(1 - P_z), \tag{10.48}$$

$$N_{N_{\rm D}} + N_{N_{\rm S}} = P_0. \tag{10.49}$$

If we then insert Eq. 10.44 and Eq. 10.46 into the density matrix equation (Eq. 10.43), we then arrive at a set of equations for P_0 and $\vec{P}$

$$\frac{d\vec{P}}{dt} = \vec{V} \times \vec{P} - \left[\frac{1}{2}(\Gamma_{\rm D} + \Gamma_S) + \frac{d\ln P_0}{dt}\right]\vec{P}_T + (1 + P_z)\frac{d\ln P_0}{dt}\vec{z}, \tag{10.50}$$

$$\frac{dP_0}{dt} = -(\Gamma_{\rm D} + \Gamma_{\rm S})(N_{N_{\rm S}} - N^{\rm eq}_{N_{\rm S}}), \tag{10.51}$$

where $\vec{P}_T \equiv P_x\vec{x} + P_y\vec{y}$. If the first equation is unpacked in terms of its components we end up with a set of four coupled differential equations

$$\frac{dP_x}{dt} = -V_zP_y - \frac{1}{2}(\Gamma_{\rm D} + \Gamma_{\rm S})P_x - \frac{P_x}{P_0}\frac{dP_0}{dt}, \tag{10.52}$$

$$\frac{dP_y}{dt} = V_zP_x - V_xP_z\frac{1}{2}(\Gamma_{\rm D} + \Gamma_{\rm S})P_y - \frac{1 + P_z}{P_0}\frac{dP_0}{dt}, \tag{10.53}$$

$$\frac{dP_z}{dt} = -V_xP_y - \frac{1}{2}(\Gamma_{\rm D} + \Gamma_{\rm S})P_x - \frac{P_x}{P_0}\frac{dP_0}{dt}, \tag{10.54}$$

$$\frac{dP_0}{dt} = -(\Gamma_{\rm D} + \Gamma_{\rm S})(N_{N_{\rm S}} - N^{\rm eq}_{N_{\rm S}}), \tag{10.55}$$

then, as usual, if we change the independent variable from t to z, we arrive at

$$\frac{dP_x}{dz} = -\overline{V}_z P_y - \frac{1}{2}(D+S)P_x - \frac{P_x}{P_0}\frac{dP_0}{dz}, \tag{10.56}$$

$$\frac{dP_y}{dz} = \overline{V}_z P_x - \overline{V}_x P_z \frac{1}{2}(D+S)P_y - \frac{1+P_z}{P_0}\frac{dP_0}{dz}, \tag{10.57}$$

$$\frac{dP_z}{dz} = -\overline{V}_x P_y - \frac{P_x}{P_0}\frac{dP_0}{dz}, \tag{10.58}$$

$$\frac{dP_0}{dz} = -(D+S)(N_{N_{\rm S}} - N_{N_{\rm S}}^{\rm eq}), \tag{10.59}$$

where D and S have previously been defined, while $\vec{\overline{V}} = \vec{V}/(Hz)$. It is also worth noting that Eq. 10.59 is essentially a Boltzmann equation as it is responsible for the production of the source RH neutrinos. The other three equations are then responsible for the oscillations, and thus the production of the dark RH neutrinos.

10.4 Leptogenesis and RHINO

Here we do not present anything new and seek to reiterate what was said in the previous RHINO model [99], with respect to the incorporation of leptogenesis, as it is essential for the potential success of the RHINO model. The idea is that for successful leptogenesis, the source RH neutrino should interfere with the third interfering seesaw RH neutrino denoted by $N_{\rm I}$, which is neither the dark nor the source RH neutrino. Leptogenesis also requires that the two neutrinos, $N_{\rm S}$ and $N_{\rm I}$, be quasi-degenerate as this allows resonant enhancement of the CP asymmetry, thus resulting in successful leptogenesis much below the lower bound of $\sim 10^9$GeV present in the hierarchical case. Using the same normalisations as used throughout this work, one can reproduce the observed value of $\eta_{B,0}$, with the baryon-to-photon ratio predicted by leptogenesis by $\eta_{B,0}^{\rm lep} \simeq 0.01 N_{B-L}^{\rm f}$, with $N_{B-L}^{\rm f,obs} \simeq 6.12 \times 10^{-8}$. The evolution of the $B-L$ asymmetry can be calculated as the sum of the six contributions arising from the two heavy quasi-degenerate RH neutrinos, $N_{\rm S}$ and $N_{\rm I}$, along with the three charged lepton flavours, while the asymmetry is generated in the three flavour regime. The takeaway from some rather long calculations and expressions is that the asymmetry $N_{B-L}(z)$ depends on the low-energy neutrino parameters, which include the low energy phases, the degeneracy $\delta \equiv |M_1 - M_2|/M_1$, and a complex angle in the orthogonal matrix (defined

in Eq. 5.18) that parameterises the Dirac neutrino mass matrix. Thus, one can choose parameters that result in successful leptogenesis in which the production of the asymmetry is dominated by the decay of the source RH neutrinos.

Unfortunately, in order to successfully incorporate leptogenesis and DM production, one must assume that the source RH neutrinos are initially thermalised, which requires some other external physics to thermalise $N_{\rm S}$. Solutions to this version of RHINO were found where one could start with an initial vanishing abundance of $N_{\rm S}$, however, efficient production of $N_{\rm D}$ requires one to have $T_{\rm RH} > 10^9$ GeV, and with this requirement one finds that $N_{\rm D}$ can only satisfy $\tau_D \sim 10^{28}$s for $M_{\rm D} \sim 10^7$GeV with $M_{\rm S} \sim 1$GeV when $T_{\rm RH} \sim 10^{15}$GeV. This has some problems, as strong leptogenesis requires that the baryon asymmetry be created by resonant decays of the seesaw neutrinos with roughly twice that of the sphaleron freeze-out temperature. One could still have leptogenesis with $\mathcal{O} \sim 1$ GeV seesaw neutrinos; however, it would be a low-scale leptogenesis in which seesaw neutrinos are relativistic due to the model requiring $T_{\rm RH} > 10^9$GeV. Low-scale leptogenesis, unlike the favourable strong leptogenesis, depends on accurate descriptions of the many processes of the early universe along with the initial conditions. It is also worth mentioning that due to $N_{\rm D}$ production requiring $T_{\rm RH} > 10^9$ GeV a large pre-existing asymmetry is a natural outcome in many different mechanisms. We therefore propose a solution to these problems in which one can incorporate strong leptogenesis, thus circumnavigating many of these issues.

11 Source-Source Higgs Portal Interactions

Let us now extend the RHINO Lagrangian as by introducing Higgs portal interactions for the source neutrinos so that the Lagrangian in Eq. 10.1 is now given by [1]

$$-\mathcal{L}_{M+\Lambda} = \overline{L_\alpha} h_{\alpha J} N_{RJ} \tilde{\Phi} + \frac{1}{2}\overline{N_{RI}^c} D_{MIJ} N_{RJ} + \frac{1}{\tilde{\Lambda}_{\rm DS}} \Phi^\dagger \Phi \overline{N_{\rm D}^c} N_{\rm S} \tag{11.1}$$

$$+ \frac{1}{\tilde{\Lambda}_{\rm SS}} \Phi^\dagger \Phi \overline{N_{\rm S}^c} N_{\rm S} + {\rm h.c.}, \tag{11.2}$$

where the effective scale for the Higgs portal interactions, $\tilde{\Lambda}_{\rm SS} \equiv \Lambda/\lambda_{\rm SS}$, has been introduced. This new term also yields a contribution to $M_{\rm S}$ at zero temperature after EWSB with $\delta M_{\rm S}^\Lambda = v^2/\tilde{\Lambda}_{\rm SS}$, which can be neglected as one obtains $\tilde{\Lambda}_{\rm SS} \geq 10^8$ GeV. The new Higgs portal interactions also give rise to a contribution to the neutrino self-energy, as shown in panel (c) of Fig. 15, and thus to the effective potential at finite temperatures, which is given by

$$V_{\rm SS}^\Lambda = \frac{T^2}{12\tilde{\Lambda}_{\rm SS}}. \tag{11.3}$$

With this new contribution to the effective potential, one must modify Eq. 10.20, and thus the effective Hamiltonian becomes

$$\Delta\mathcal{H}_{IJ} \approx \begin{pmatrix} -\frac{\Delta M^2}{4p} - \frac{T^2}{16p}h_{\rm S}^2 - \frac{T^2}{24\tilde{\Lambda}_{\rm SS}} & \frac{T^2}{12\Lambda} \\ \frac{T^2}{12\Lambda} & \frac{\Delta M^2}{4p} + \frac{T^2}{16p}h_{\rm S}^2 + \frac{T^2}{24\tilde{\Lambda}_{\rm SS}} \end{pmatrix}. \tag{11.4}$$

The influence of the new term in the effective Hamiltonian on the mixing depends on whether $T/\tilde{\Lambda}_{\rm SS} \approx h_{\rm S}^2$ or $T/\tilde{\Lambda}_{\rm SS} > h_{\rm S}^2$. However, because dark neutrino production occurs at temperatures less than the resonant temperatures, the effect of this new term should be limited when $\Lambda_{\rm SS} \gg 10^{10}$GeV. The LZ approximation relies upon neutrino oscillations already occurring at the resonance temperature, $T_{\rm res} \equiv 2\sqrt{|\Delta M^2|}/h_{\rm S}$, however, when solving the density matrix equations one sees that this is not the case, with the neutrino oscillations occurring at temperatures below the resonance temperature, $T_{\rm osc} \ll T_{\rm res}$ [99]. Therefore, these new terms, similar to the Yukawa

effective potentials, can be neglected as they have no major influence on the final abundance, and as such, this produces a subdominant effect compared to the scatterings that allow $N_{\rm S}$ production. These scatterings from the source-source Higgs portal are the main focus of this work.

The interaction diagrams for the Higgs portal interactions are shown in Fig. 16, with the production of $N_{\rm S}$ from Higgs annihilations, $\phi\phi^\dagger \to N_{\rm S}N_{\rm S}$, shown in panel (a).

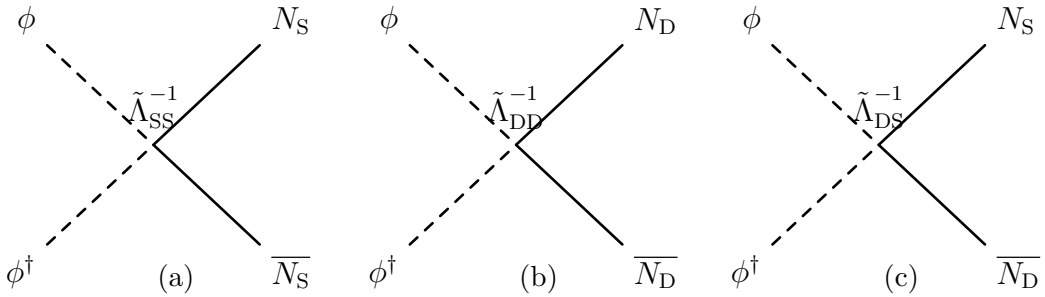

Figure 16: Interaction diagrams for the Higgs portal interactions with source RH neutrino production (a), dark RH neutrino production (b), and mixed production (c).

This novel avenue of source-source production is the most important consequence of this new source-source term in the Lagrangian. This results in a modification of the Boltzmann equation that describes the number density of $N_{\rm S}$, Eq. 10.35, such that

$$\frac{dN_{N_{\rm S}}}{dz_{\rm S}} = -(D_{\rm S} + S_{\rm S})(N_{N_{\rm S}} - N^{\rm eq}_{N_{\rm S}}) - A(N^2_{N_{\rm S}} - N^{\rm eq2}_{N_{\rm S}}), \tag{11.5}$$

where factor A is given by

$$A \equiv \frac{\langle \sigma_{\phi\phi^\dagger \to N_{\rm S}\overline{N^c_{\rm S}}} v_{\rm rel} \rangle}{H(z) z R^3(z)}, \tag{11.6}$$

where $\langle \sigma_{\phi\phi^\dagger \to N_{\rm S}\overline{N^c_{\rm S}}} v_{\rm rel} \rangle$ is the thermally averaged cross section, $R(z)^3$ is the portion of the comoving volume that the abundances inhabit, and $H(z)$ is the Hubble constant, all of which were introduced in Section 6, in this case one has

$$R^3(z) = \frac{4}{3}\frac{\pi^2}{g_{N_\mathrm{S}}\zeta(3)}\frac{z^3}{M_\mathrm{D}^3}. \tag{11.7}$$

For the regime in which we are interested, the thermally averaged cross section for such a process was calculated in Ref. [159], as was divulged in Section 7. The cross section is given by

$$\langle \sigma_{\phi\phi^\dagger \to N_\mathrm{S}\overline{N_\mathrm{S}^c}} v_\mathrm{rel} \rangle \Big|_{M_\mathrm{S} \ll T} = \frac{1}{4\pi \tilde{\Lambda}_{\mathrm{SS}}^2}. \tag{11.8}$$

This results in A being expressed explicitly as

$$A(z) = \frac{A_1}{z^2}, \quad \text{where } A_1 \equiv A(z=1) = \frac{3}{16}\frac{\zeta(3)}{\pi^3} g_{N_\mathrm{S}} \sqrt{\frac{90}{8\pi^3 g_R}} \frac{M_\mathrm{D} M_\mathrm{Pl}}{\tilde{\Lambda}_{\mathrm{SS}}^2}, \tag{11.9}$$

where in numerical form, one arrives at A_1 given by

$$A_1 = 1.0 \times 10^{-11} \left(\frac{M_\mathrm{D}}{100\mathrm{TeV}}\right) \left(\frac{10^{16}\mathrm{GeV}}{\tilde{\Lambda}_{\mathrm{SS}}}\right)^2. \tag{11.10}$$

Whereas previously we have used the SM value for the ultrarelativistic degrees of freedom such that $g_R = 106.75$, whilst $g_{N_\mathrm{S}} = 2$ is the degrees of freedom for the source RH neutrino. If we expect the new scattering term to be dominant in producing N_S, then the Boltzmann equation takes a form similar to that of the Lee-Weinberg equation.

$$\frac{dN_{N_\mathrm{S}}}{dz} = -A(N_{N_\mathrm{S}}^2 - (N_{N_\mathrm{S}}^{\mathrm{eq}})^2), \tag{11.11}$$

which can be trivially solved in the regime $N_{N_\mathrm{S}} \ll N_{N_\mathrm{S}}^{\mathrm{eq}}$ when $z \ll 1$, where due to our normalisation we have $N_{N_\mathrm{S}}^{\mathrm{eq}} \approx 1$, and the initial abundance N_S is negligible, such that $N_{N_\mathrm{S}}(z_\mathrm{in}) = 0$. With these conditions, one can easily arrive at

$$N_{N_\mathrm{S}}(z) \approx A_1 \left(\frac{1}{z_\mathrm{in}} - \frac{1}{z}\right), \tag{11.12}$$

then using Eq. 11.10 in the asymptotic limit and still with $z \ll 1$ one obtains the solution that

$$N_{N_{\rm S}}(z_{\rm in} \ll z \ll 1) \approx \frac{A_1}{z_{\rm in}} \approx \left(\frac{T_{\rm in}}{10^{16}{\rm GeV}}\right)\left(\frac{10^{16}{\rm GeV}}{\tilde{\Lambda}_{\rm SS}}\right)^2, \tag{11.13}$$

where we do not have a dependence on $M_{\rm D}$. We again stress that this result only applies in the case that $N_{N_{\rm S}}(z_{\rm in} \ll z \ll 1)$. From this solution, one can impose a condition on $T_{\rm in}$ and $\tilde{\Lambda}_{\rm SS}$ with respect to the thermalisation of the source RH neutrinos prior to the occurrence of source-dark neutrino oscillations. The condition is such that $\tilde{\Lambda}^2_{\rm SS}/T_{\rm in} = 10^{16}{\rm GeV}$ assuming thermalisation of $N_{\rm S}$, where with our normalisation one has that $N_{N_{\rm S}} = 1$. Another important point regarding the validity of the additional Higgs portal operator is of course, as discussed previously, an effective theory, and as such we require $T_{\rm in} \leq \tilde{\Lambda}_{\rm SS}$.

The new source-source Higgs portal operator also results in a modification of the density matrix, and thus the set of coupled equations one arrives at after vectorial parameterisation is now

$$\frac{dP_x}{dz} = -\overline{V}_z P_y - \frac{1}{2}(D+S)P_x - \frac{P_x}{P_0}\frac{dP_0}{dz}, \tag{11.14}$$

$$\frac{dP_y}{dz} = \overline{V}_z P_x - \overline{V}_x P_z - \frac{1}{2}(D+S)P_y - \frac{1+P_z}{P_0}\frac{dP_0}{dz}, \tag{11.15}$$

$$\frac{dP_z}{dz} = -\overline{V}_x P_y - \frac{P_x}{P_0}\frac{dP_0}{dz}, \tag{11.16}$$

$$\frac{dP_0}{dz} = -(D+S)(N_{N_{\rm S}} - N^{\rm eq}_{N_{\rm S}}) - \frac{A_1}{z^2}(N^2_{N_{\rm S}} - (N^{\rm eq}_{N_{\rm S}})^2). \tag{11.17}$$

12 Results and Discussion

Before discussing the results, let us reiterate that we are neglecting possible pure or mixed production of the dark RH neutrinos, $N_{\rm D}$, directly from dark Higgs portal interactions, which arise from the diagrams shown in panel (b) and (c) of Fig. 16. The way to understand this is by assuming the effective scales[60], $\tilde{\Lambda}_{\rm DD}$ and $\tilde{\Lambda}_{\rm DS}$, are large enough that the production is negligible when compared to the contribution from the neutrino mixing induce by $\tilde{\Lambda}_{\rm DS}$. In fact, a lower bound on $\tilde{\Lambda}_{\rm DD}$ and $\tilde{\Lambda}_{\rm DS}$ can be trivially reached imposing that the DM RH neutrino abundance produced from these interactions is negligible compared to the observed abundance. The DM energy density parameter at present is given by Eq. 1.1, with the abundance for a generic mass or in this instance a dark neutrino, $M_{\rm D}$, given by

$$N_{N_{\rm D}}^{\rm f,\,obs} \approx 1.1 \times 10^{-7} \frac{\rm GeV}{M_{\rm D}}. \tag{12.1}$$

To calculate the abundance arising from these interactions one must follow the same method as that which calculates the abundance from the source-source interactions $\tilde{\Lambda}_{\rm SS}$, which is given by 11.13, obviously replacing $\tilde{\Lambda}_{\rm SS}$ with $\tilde{\Lambda}_{\rm DS}$ or $\tilde{\Lambda}_{\rm DD}$ and then manipulating the expression yields

$$\tilde{\Lambda}_{\rm DD}, \tilde{\Lambda}_{\rm DS} \gg 10^{22}{\rm GeV} \sqrt{\frac{T_{\rm RH}}{10^{16}{\rm GeV}} \frac{M_{\rm D}}{\rm PeV}}. \tag{12.2}$$

Models that can naturally fulfil these two requirements will be discussed in Section 13. We assume that production of the source RH neutrinos starts right after inflation and reheating, thus occurring in the radiation-dominated era[61]. Our initial temperature is therefore the reheat temperature that has been discussed previously, $T_{\rm in} = T_{\rm RH}$. Our results indicate that for $\Lambda_{\rm SS} \leq 10^{16}$GeV it is always possible to thermalise the source RH neutrino by increasing $T_{\rm RH}$. The maximum value possible of the reheat temperature from cosmological observations is $T_{\rm RH} \lesssim 10^{16}$GeV. It is still possible to thermalise the source RH neutrino even in the upper limiting case for the interaction

[60] Where $\tilde{\Lambda}_{\rm DD} = \Lambda/\lambda_{\rm DD}$ and $\tilde{\Lambda}_{\rm DS} = \Lambda/\lambda_{\rm DS}$ as defined previously.

[61] Production between $T_{\rm max} > T_{\rm RH}$ and $T_{\rm RH}$ is not considered since this would only contribute towards minimally relaxing the final constraints [159].

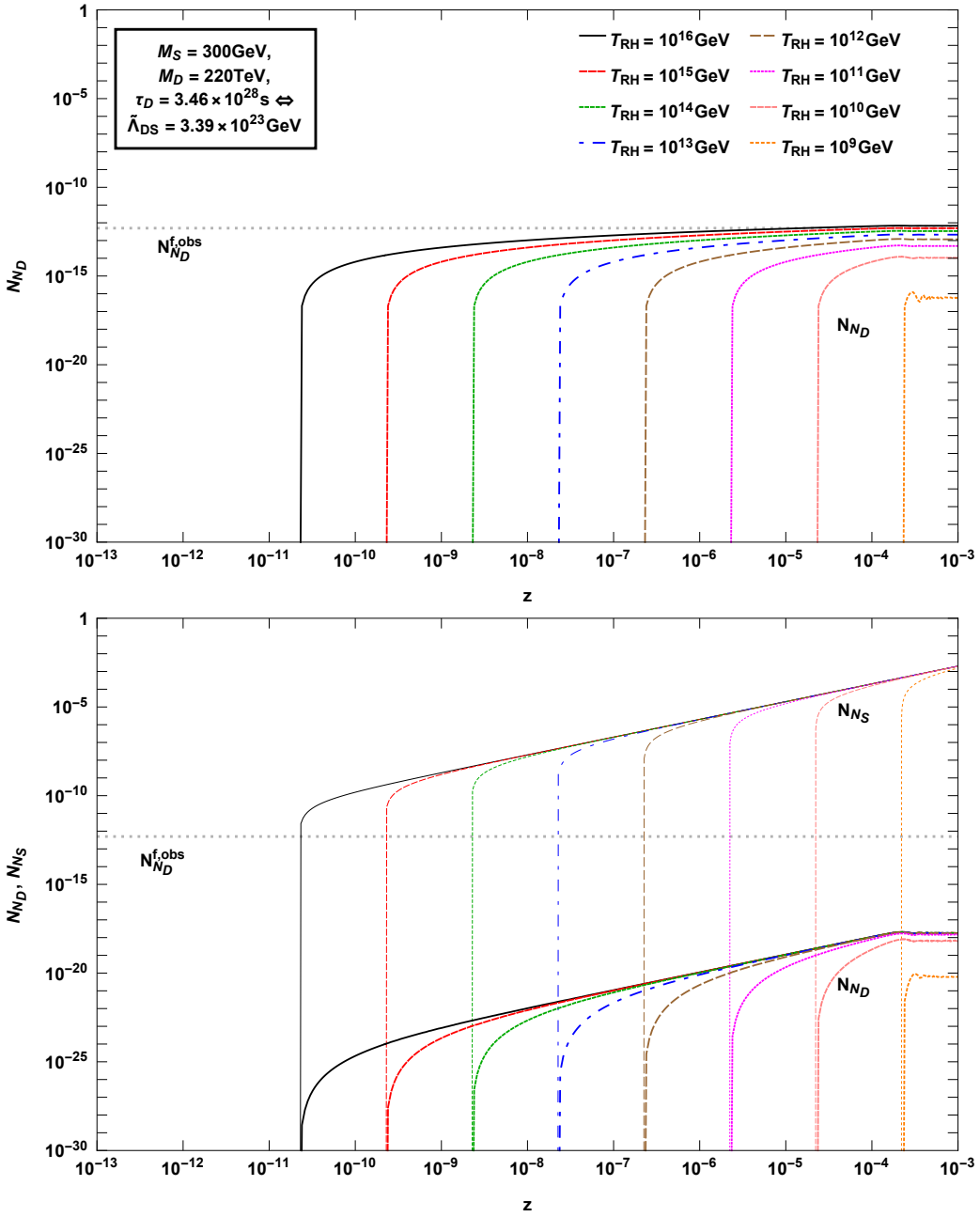

Figure 17: Evolution of the source RH neutrino abundance, $N_{\rm S}$, and the dark RH neutrino abundance, $N_{\rm D}$, for differing values of the initial temperature for the benchmark values of $M_{\rm D} = 220$TeV, $M_{\rm S} = 300$GeV, and $\tau_{\rm D} = 3.46 \times 10^{28}$s as indicated. The top panel corresponds to an initial thermal $N_{N_{\rm S}}$-abundance, whilst the bottom panel corresponds to an initial vanishing $N_{N_{\rm S}}$-abundance.

strength, $\tilde{\Lambda}_{\rm SS} = 10^{16}$ GeV, provided that one assumes maximum reheat temperature, $T_{\rm RH} = 10^{16}$GeV, as shown in Fig. 18.

The first of our results, Fig. 17, displays the evolution of $N_{N_{\rm D}}$ and $N_{N_{\rm S}}$ as in Ref. [99], for the benchmark values $M_{\rm S} = 300$GeV, $M_{\rm D} = 220$TeV, and $\tau_{\rm D} = 3.48\times10^{28}$s. In the top panel, one assumes an initial thermal abundance, whilst in the bottom panel we assume an initial vanishing abundance where the source RH neutrinos are created through Yukawa interactions. The chosen values of $M_{\rm D}$ and $\tau_{\rm D}$ are such that they correspond to the best-fit values obtained from a likelihood statistical analysis of 6 year High Energy Starting Events (HESE) at IceCube. In this analysis neutrinophilic DM decays contribute towards a neutrino flux in addition to an astrophysical component with a fixed spectra index $\gamma = 2.2$, which is favoured at more than $\sim 3\sigma$ when compared to the null hypothesis of no decaying DM[62] [194]. We choose the value $M_{\rm S} = 300$ GeV, as this corresponds to the minimum mass that still allows for successful leptogenesis arising from decays independently of the initial conditions. Unfortunately, from the lower panel of Fig. 17 one must conclude it is not possible to have both strong leptogenesis and the dark neutrino playing the role of DM in a unified picture, however, the source-source Higgs portal interactions are capable of remedying this as we shall see in our next results.

The second set of results shown in Fig. 18 shows the evolution of $N_{N_{\rm S}}$ and $N_{N_{\rm S}}$ for the same toy instance as in Fig. 17, with values of $M_{\rm S} = 300$GeV, $M_{\rm D} = 220$TeV, and $\tau_{\rm DM} = 3.46 \times 10^{28}$s. The difference between Fig. 17 and Fig. 18 is that Fig. 18 features the new extended model featuring the new source-source interactions. The upper panel of Fig. 18 features a fixed $\tilde{\Lambda}_{\rm SS} = 10^{16}$GeV, whilst varying the initial reheat temperature, we have $T_{\rm in} = T_{\rm RH}$. In this case, it is clear that the source RH neutrino thermalises for the maximum $T_{\rm RH}$ value, and is linearly suppressed as $T_{\rm RH}$ decreases. An important feature of these results is that for $T_{\rm RH} = \tilde{\Lambda}_{\rm SS} = 10^{16}$GeV, the maximum $T_{\rm RH}$ value, it is possible to reproduce an excess of the DM

[62] In a different analysis of the 6 year HESE data, where in this instance the astrophysical spectra is varied whilst only one DM decay channel is fixed, it was found that an additional component arising from DM decays in fact improves the fit. In this study the best fit is obtained when the DM particles decay into W bosons, with a DM mass of $M_{\rm DM} = 400$TeV, and a spectral index $\gamma \approx 2.3$, however, these results have a lower statistical significance of $\sim 2\sigma$ [244]. An additional more recent analysis of the 7.5 year HESE data analysis which obtains a maximum statistical significance of $\sim 2\sigma$ is found when multiple decay channels are included. [193]

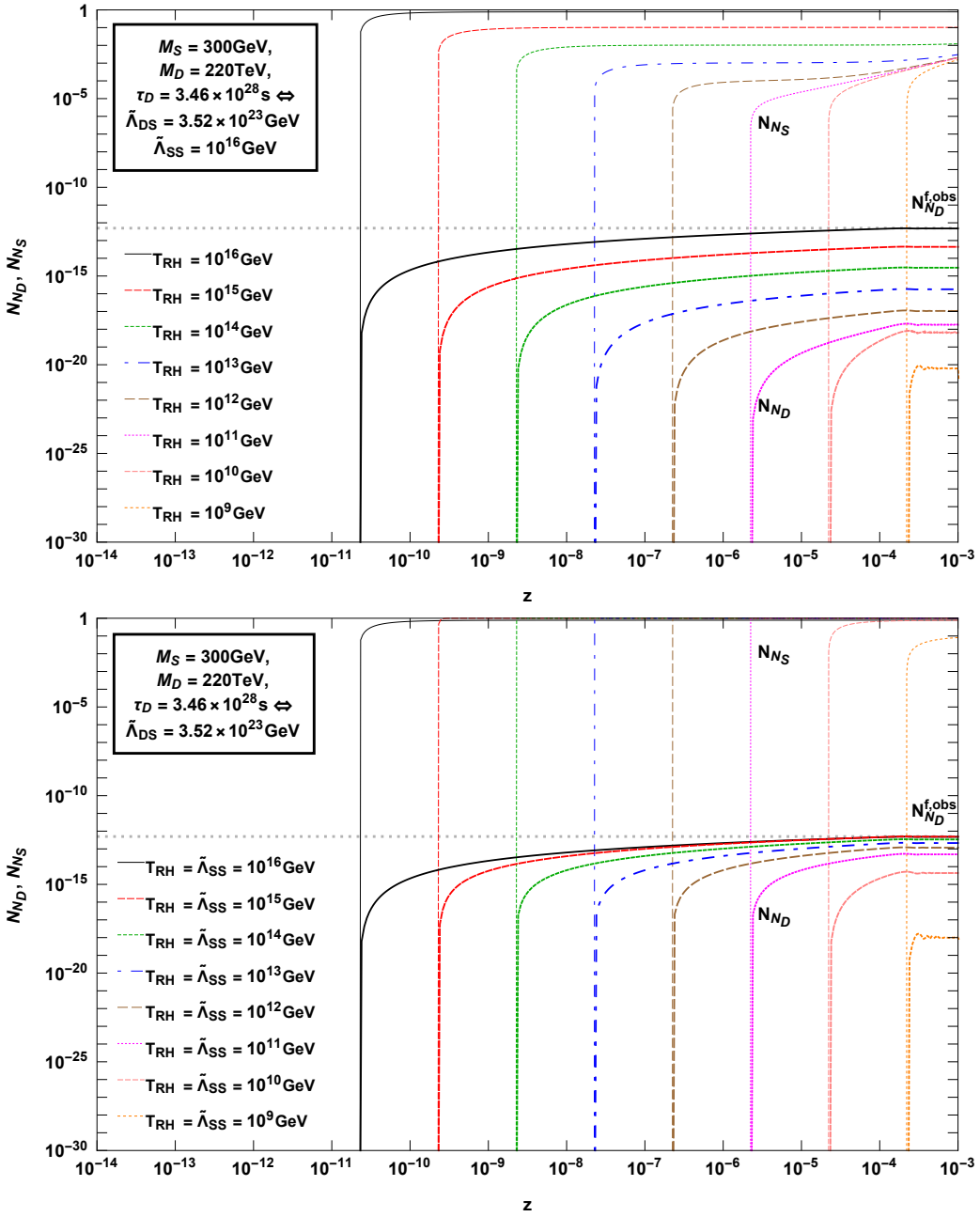

Figure 18: Evolution of the source RH neutrino abundance, $N_{\rm S}$, and the dark RH neutrino abundance, $N_{\rm D}$, for differing values of the initial temperature when the source-source Higgs interactions are introduced for the benchmark values of $M_{\rm D} = 220$TeV, $M_{\rm S} = 300$GeV, and $\tau_{\rm D} = 3.46 \times 10^{28}$s as indicated. The top panel corresponds to $\tilde{\Lambda}_{\rm SS} = 10^{16}$GeV, whilst the bottom panel corresponds to $\tilde{\Lambda}_{\rm SS} = T_{\rm RH}$.

abundance, which indicates that one can always reproduce the DM abundance by carefully selecting the parameters. In the lower panel of Fig. 18 we are more conservative by choosing to impose $T_{\rm RH} = \tilde{\Lambda}_{\rm SS}$ and again displaying the evolution of $N_{N_{\rm S}}$ and $N_{N_{\rm D}}$ for the same toy instance as before, for indicated values of $\tilde{\Lambda}_{\rm SS} \leq 10^{16}$GeV. It is evident from the lower panel that the thermalisation condition is always respected and as such one obtains results that are extremely similar to those displayed in the upper panel of Fig. 17. This means that one does not simply have to assume thermalisation of the source RH neutrinos, as the source RH neutrinos now thermalise due to the additional source-source Higgs portal interactions. Notice how with these new results we can now unify both strong leptogenesis and a dark neutrino playing the role of DM into a single picture.

Our next results are displayed in Figs. 19-22 and show the allowed regions in the dark matter RH neutrino lifetime-mass plane, with the grey shaded region indicating the lower bound of the region that is currently under scrutiny by neutrino telescopes such as IceCube and gamma ray telescopes such as the Fermi Gamma-Ray telescope, with a value of $\tau_{\rm D} \leq 10^{28}$s. In these results, we display some lower bounds on the DM lifetime recently obtained by the IceCube collaboration at 90% C.L. ($\sim 1.65\sigma$) [223]. The thin solid line indicates the lower bound on the DM mass in the range 160TeV-20PeV obtained from the 7.5yr HESE data discussed previously in the energy range 60TeV-10PeV for decays in the DM $\rightarrow$ Higgs $+ \nu$ channel. Our results also show the same lower bound for the decay channel DM $\rightarrow b + \bar{b}$ with a thick solid line. We also indicate a lower bound for lower masses with a dashed line obtained from 2yr cascade events for the decay channel DM $\rightarrow \mu\overline{\mu}$. Even lower masses are shown with a dotted line, with this bound coming from the Fermi gamma-ray telescope for the decay channel DM $\rightarrow \nu\overline{\nu}$ [223]. Additionally, recent lower bounds for different decay channels are also shown, which are still obtained from gamma ray telescopes and observations. The thick dotted line is the lower bound for the decay channel DM $\rightarrow \nu\overline{\nu}$ achieved by combining data from ultra-high energy gamma ray measurements [193]. Finally, the thin dotted line corresponds to the lower bound established by analysing data from the Large High Altitude Air Shower Observatory (LHAASO) [197]. Naturally, many of these decay channels are not directly related to RHINO DM, as the dark RH neutrino can decay both into a Higgs boson and a gauge boson along with a neutrino or charged leptons. This means that all the lower bounds are more suggestive than concrete lower bounds, with a dedicated

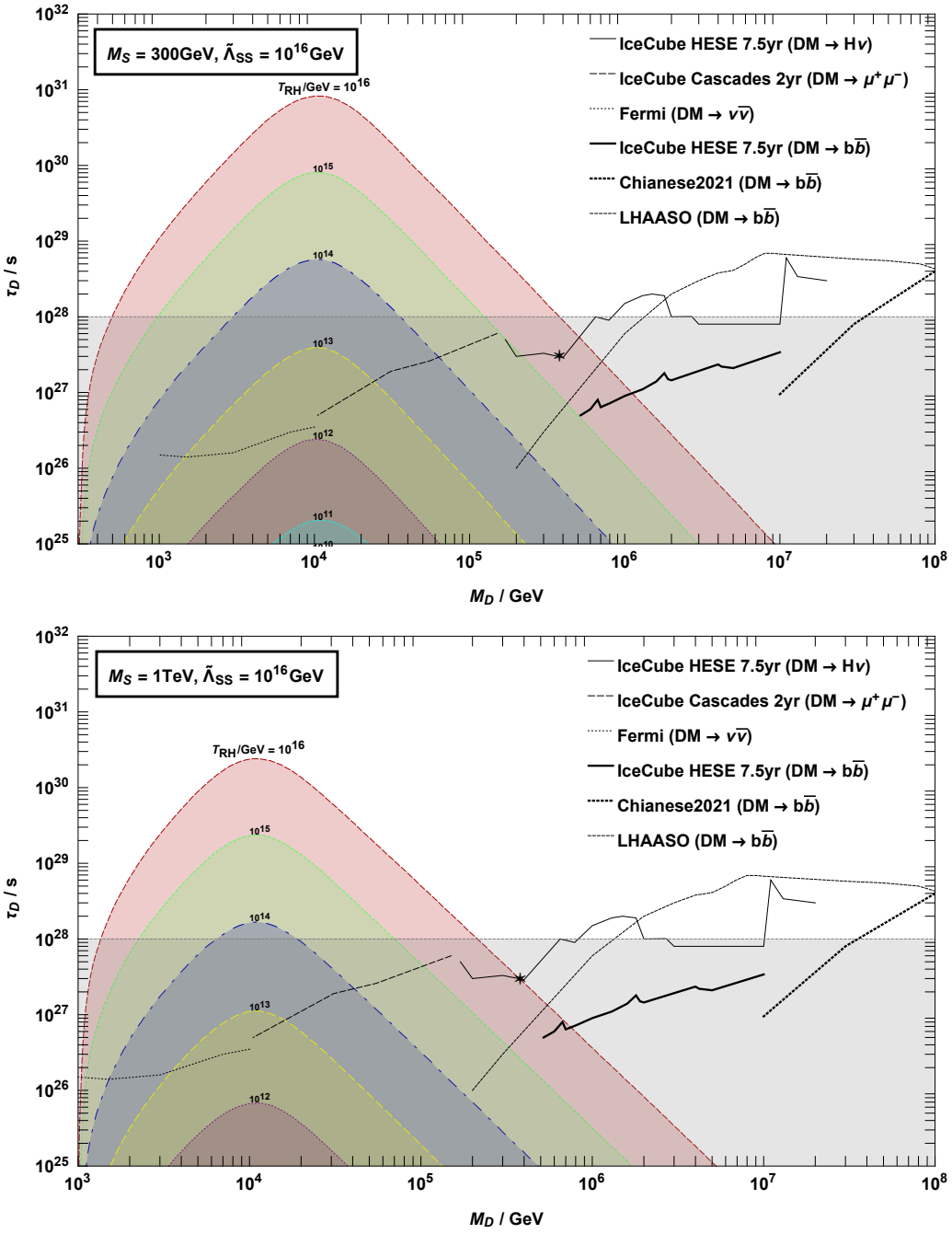

Figure 19: The allowed regions in the lifetime versus mass plane for a constant source-source interaction strength, $\tilde{\Lambda}_{\rm SS} = 10^{16}$GeV, for values of $T_{\rm RH}$ and $M_{\rm S} = 300$GeV in the upper panel, and $M_{\rm S} = 1$TeV in the lower panel.

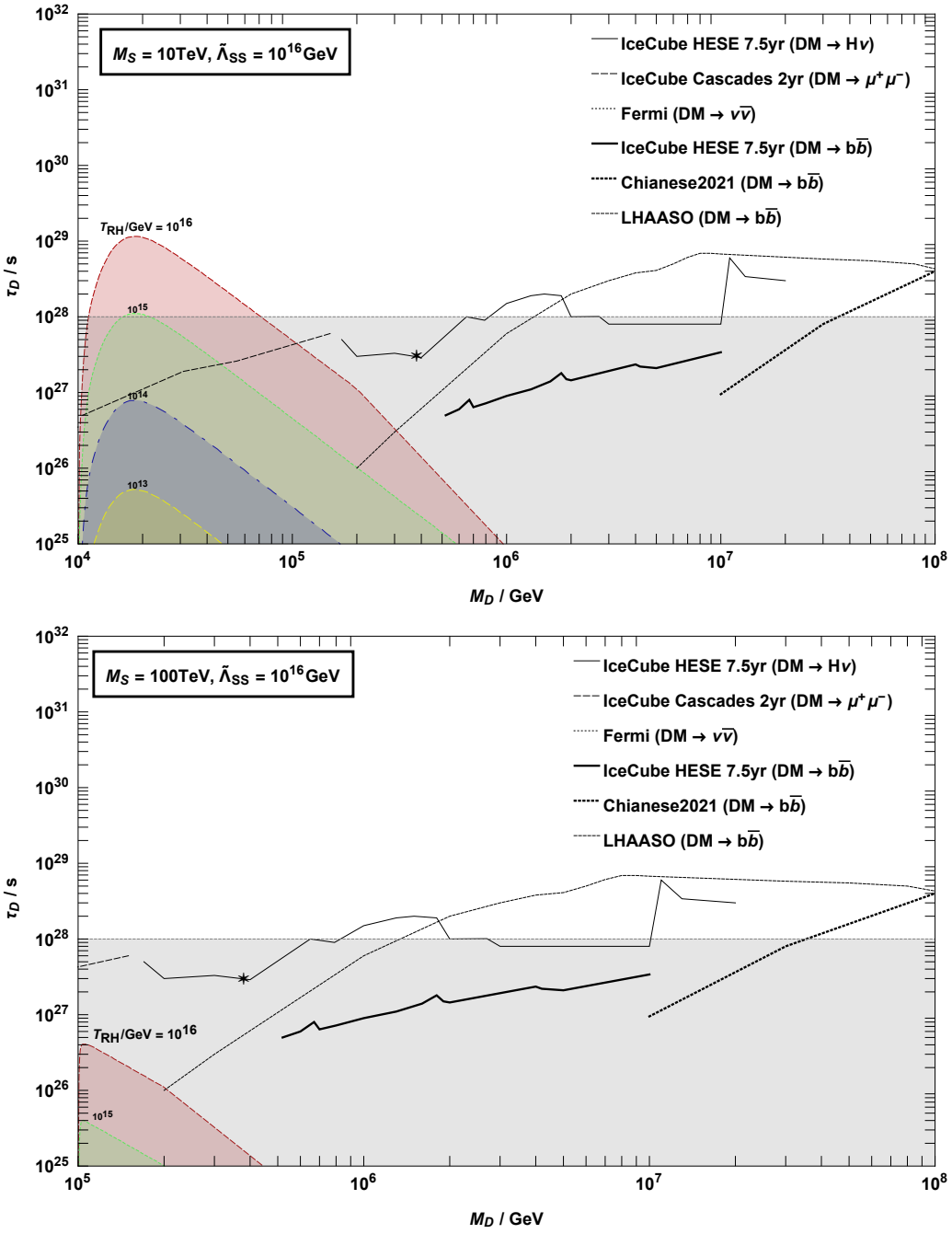

Figure 20: The allowed regions in the lifetime versus mass plane for a constant source-source interaction strength, $\tilde{\Lambda}_{\rm SS} = 10^{16}$GeV, for values of $T_{\rm RH}$ and $M_{\rm S} = 10$TeV in the upper panel, and $M_{\rm S} = 100$TeV in the lower panel.

analysis required. Also of interest is the apparent confirmation of IceCube collaborations of an excess at $\mathcal{O}(100\text{TeV})$ energies compared to the expected astrophysical background, with potential DM decays improving the data fit with a statistical significance of 2.5σ, with the best fit itself deriving from the decay channel DM $\to b + \bar{b}$, with a DM mass $M_{\rm DM} = 289\text{TeV}$, and a lifetime $\tau_{\rm DM} = 2.8 \times 10^{27}\text{s}$. This best fit is indicated by a star, and again this should not be taken as gospel, but rather as informative. It would be interesting to see how a dedicated analysis within the RHINO model could address the excess and thus the statistical significance of the solution.

In the first two figures of these four figures, Figs. 19 and 20, we display results for the case where $\tilde{\Lambda}_{\rm SS}$ is fixed similarly to the results displayed in the upper panel of Fig. 18, where again we have that $\tilde{\Lambda}_{\rm SS} = 10^{16}\text{GeV}$, whilst varying the reheat temperature with $T_{\rm RH} \leq \tilde{\Lambda}_{\rm SS} = 10^{16}\text{GeV}$, which is indicated in the plots. The upper panel of Fig. 19 displays the results for $M_{\rm S} = 300\text{GeV}$, whilst the lower panel displays the results for $M_{\rm S} = 1\text{TeV}$, whereas Fig. 20 displays the results for $M_{\rm S} = 10\text{TeV}$ and $M_{\rm S} = 100\text{TeV}$, in the upper and lower panel respectively. The allowed regions are obtained by requiring that $N_{N_{\rm D}} \geq N_{\rm DM}^{\rm f,obs}$, where on a regions border we reproduce the correct DM abundance, $N_{N_{\rm D}} = N_{\rm DM}^{\rm f,obs}$, while points inside the region correspond to an overabundance of $N_{\rm D}$ which can be lowered by simply increasing the source RH neutrino mass and/or lowering the reheat temperature.

The last two of these four figures, Figs. 21 and 22, show the allowed regions for the instances when $T_{\rm RH} = \tilde{\Lambda}_{\rm SS}$, for the same source RH neutrino masses as Figs. 19 and 20, with the upper panel of Fig. 21 displaying the results for $M_{\rm S} = 300\text{GeV}$, whilst the lower panel displays the results for $M_{\rm S} = 1\text{TeV}$, whereas Fig. 22 displays the results for $M_{\rm S} = 10\text{TeV}$ and $M_{\rm S} = 100\text{TeV}$. It is clear from these results that when $\tilde{\Lambda}_{\rm SS} = T_{\rm RH} \gg 10^{10}\text{GeV}$, the allowed regions only slightly decrease when $\tilde{\Lambda}_{\rm SS}$ is reduced; however, when $\tilde{\Lambda}_{\rm SS} = T_{\rm RH} \lesssim 10^{10}\text{GeV}$ the reduction becomes more significant, while when $\tilde{\Lambda}_{\rm SS} = T_{\rm RH} \lesssim 10^{8}\text{GeV}$ there is essentially no allowed region, indicating that $T_{\rm RH} \gtrsim 10^{8}\text{GeV}$ can essentially be considered as a conservative lower bound for $T_{\rm RH}$, where the dark neutrinos, $N_{\rm DM}$, can account for the dark matter. This result coincides with what we have seen in Fig. 18, where we discussed the dark RH neutrino abundance, and is ultimately a consequence of the onset of the neutrino oscillations and thus the dark neutrino production, which occurs at a temperature of approximately $T \sim 10^{9}\text{GeV}$. Typically in

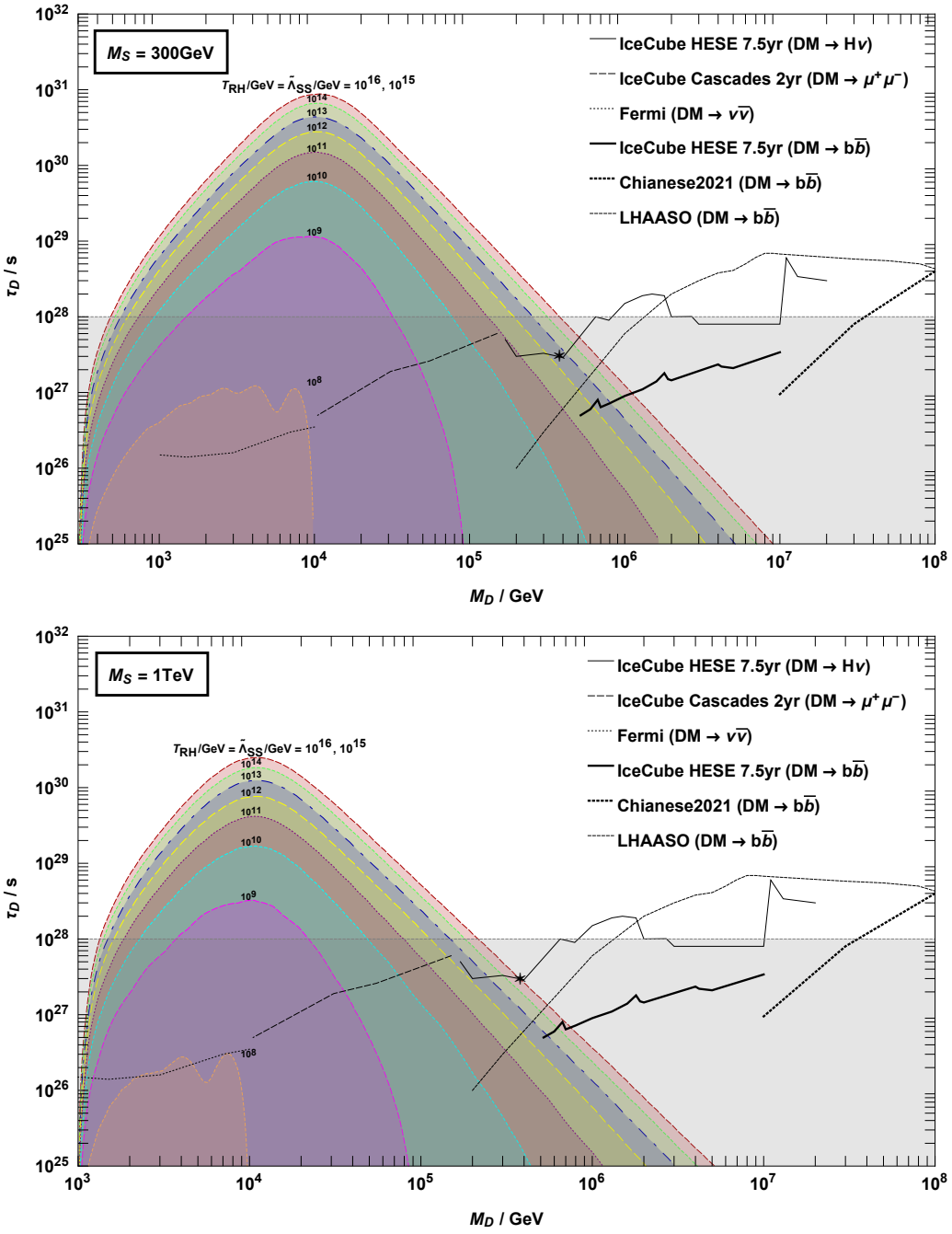

Figure 21: The allowed regions in the lifetime versus mass plane for a varying source-source interaction strength, $\tilde{\Lambda}_{\rm SS} = T_{\rm RH}$, for values of $T_{\rm RH}$ and $M_{\rm S} = 300$GeV in the upper panel, and $M_{\rm S} = 1$TeV in the lower panel.

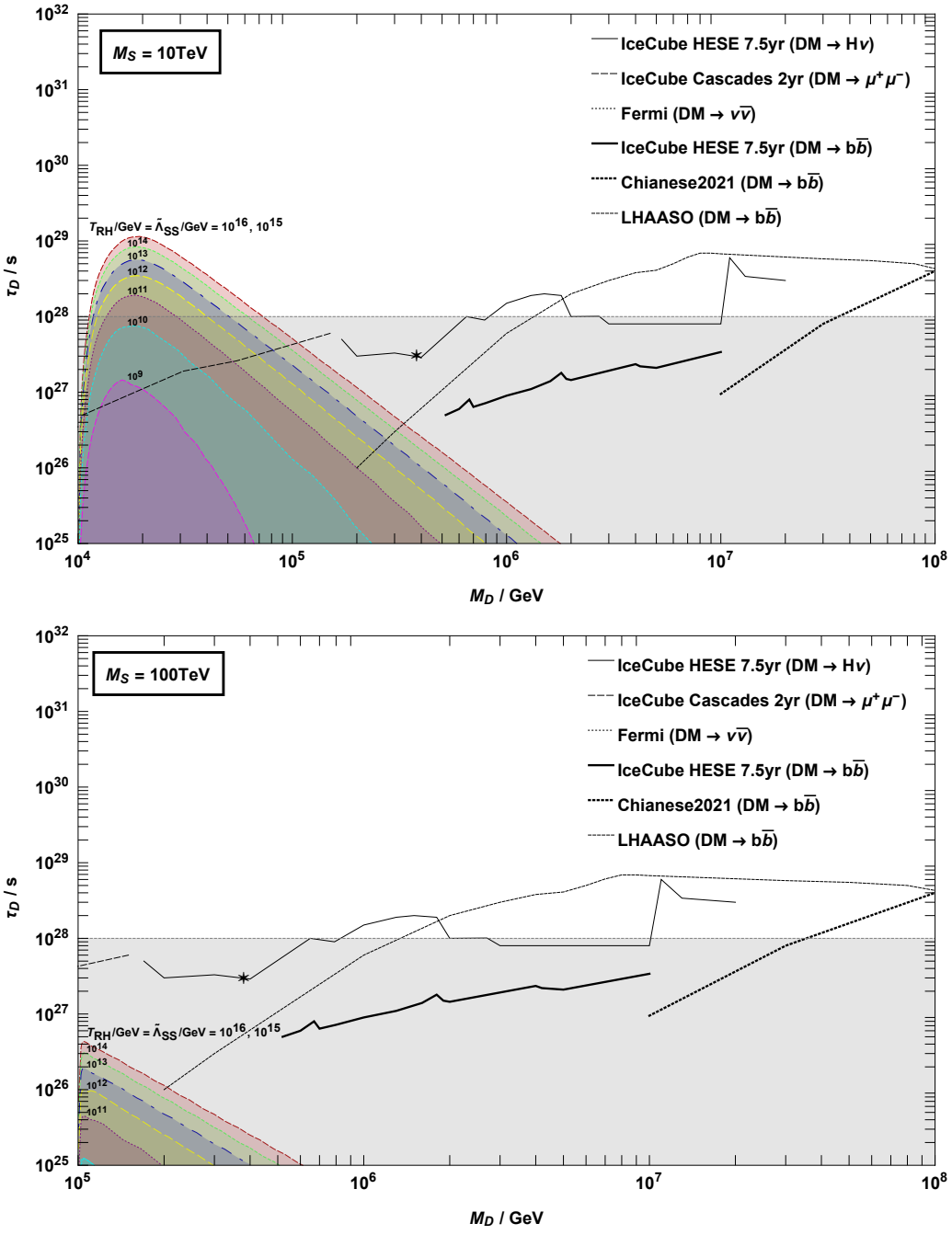

Figure 22: The allowed regions in the lifetime versus mass plane for a varying source-source interaction strength, $\tilde{\Lambda}_{\rm SS} = T_{\rm RH}$, for values of $T_{\rm RH}$ and $M_{\rm S} =$ 10TeV in the upper panel, and $M_{\rm S} = 100$TeV in the lower panel.

our examples where the reheat temperature is much higher than this, the final dark neutrino abundance is not strongly suppressed as it would be if $T \lesssim 10^9$GeV. Another interesting point is that such a lower bound on the reheat temperature is compatible with the well-known upper bound $T_{\rm RH} \lesssim 10^{10}$GeV, from the gravitino problem that arises from gravity-mediated supersymmetric models [245]. The same lower bound also holds for the effective source-source scale $\tilde{\Lambda}_{\rm SS} \gtrsim 10^8$GeV, with this lower bound confirming the decision to neglect the Majorana mass term arising from the source-source Higgs portal term in Eq. 11.2, as one has that $\left|\delta M_{\rm S}^{\Lambda}\right| \lesssim v^2/\tilde{\Lambda}_{\rm SS} \lesssim 0.1$MeV. Finally, one notices that for the value that maximises the DM neutrino abundance, $\Lambda_{\rm SS} = T_{\rm RH} = 10^{16}$GeV, one can only produce the DM abundance when $M_{\rm S} \lesssim 100$TeV, which can be regarded as an upper bound of the model on the seesaw scale.[63]

12.1 RHINO From UV-Complete Theories

Let us now discuss how the effective Higgs portal operators discussed within the RHINO model can arise from UV-complete theories, which has also previously been outlined in Ref. [8]. In the first example, the mediator of the Anisimov operator, Eq. 1.4, is a heavy scalar H with a vanishing VEV, whilst in the second case the mediator is a heavy fermion F.[64]

12.2 Heavy Scalar H as the Mediator

Let us now extend the SM by introducing a heavy real scalar field H, which has a vanishing VEV. This novel field is coupled to the RH neutrinos with Yukawa couplings λ_{IJ} along with couplings to the SM Higgs field by trilinear couplings μ[65]

$$\mathcal{L}_H = \frac{1}{2}\partial_\mu H \partial^\mu H - \frac{1}{2} M_H^2 H^2 - \sum_{I,J} \lambda_{IJ} H \overline{N_I^c} N_J - \mu H \phi^\dagger \phi. \tag{12.3}$$

[63] In this work we assume $M_{\rm D} \geq M_{\rm S}$, and further work needs to be partaken to understand whether there can also be solutions in the potentially interesting case when $M_{\rm S} > M_{\rm D}$.

[64] There is no reason why there cannot be more than one heavy fermion, with the generalisation to multiple generations being straightforward.

[65] This extension of the SM has also been discussed in Ref. [9, 159]

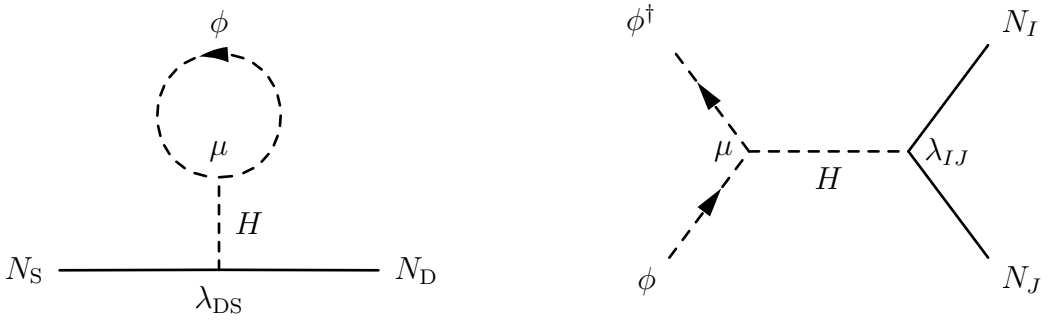

(a) (b)

Figure 23: Feynman diagrams which feature a heavy scalar H as the mediator, with $I, J = D, S$. Upon integrating out H, these correspond to the Feynman diagram shown in panel (b) of Fig. 15, and the interaction diagrams in Fig. 16.

At scales much below M_H one can integrate out H, which results in an effective Lagrangian as

$$\mathcal{L}_H^{\rm eff} = \frac{1}{2}\sum_{I,J,K,L}\frac{\lambda_{IJ}\lambda_{KL}}{M_H^2}(\overline{N_I^c}N_J)(\overline{N_K^c}N_L) + \frac{1}{2}\frac{\mu^2}{M_H^2}(\phi^\dagger\phi)^2 + \sum_{I,J}\frac{\mu\lambda_{IJ}}{M_H^2}\Phi^\dagger\Phi\overline{N_I^c}N_J. \tag{12.4}$$

From this effective Lagrangian one can clearly identify the Higgs portal operators, or the Anisimov operator, as displayed in Eq. 1.4 providing one identifies the interaction cut-off as $\Lambda = M_H^2/\mu$, and then for the effect scale one has that $\tilde{\Lambda} = \Lambda/\lambda_{IJ}$. A Feynman diagram for the self-energy correction is shown in panel (b) of Fig. 15, whilst the scattering diagram is shown in panel (a) of Fig. 16. These effective diagrams arise from the Feynman diagrams displayed in Fig. 23, panel (a) and panel (b) respectively. This model has a rather appealing feature due to its ability to obtain a trans-Planckian[66] value for the Anisimov effective scale, $\tilde{\Lambda}_{\rm DS} \sim 10^{23}$GeV, even with $\lambda = \mathcal{O}(1)$ obtained by choosing $\mu \ll M_{\rm GUT}$, which can be achieved by $M_H \sim M_{GUT} \sim 10^{16}$GeV and $\mu \sim 10^9$GeV as an example. Unfortunately, in this instance one cannot simultaneously produce the source-source Higgs

[66]For more on the Trans-planckian problems see ref. [246].

portal effective scale $\tilde{\Lambda}_{\rm SS} = 10^{16}$GeV. Therefore, it is more reasonable to assume $\Lambda \sim 10^{16}$GeV, which is achieved by $\mu = M_H \sim M_{\rm GUT} \sim 10^{16}$GeV, $\lambda_{\rm SS} \sim 1$GeV, $\lambda_{\rm DS} \sim 10^{-7}$GeV, and $\lambda_{\rm DD} \ll 10^{-7}$GeV which allows $\tilde{\Lambda}_{\rm DD}$ to satisfy the condition of the equation. 12.2.

12.3 Heavy Fermion F as the Mediator

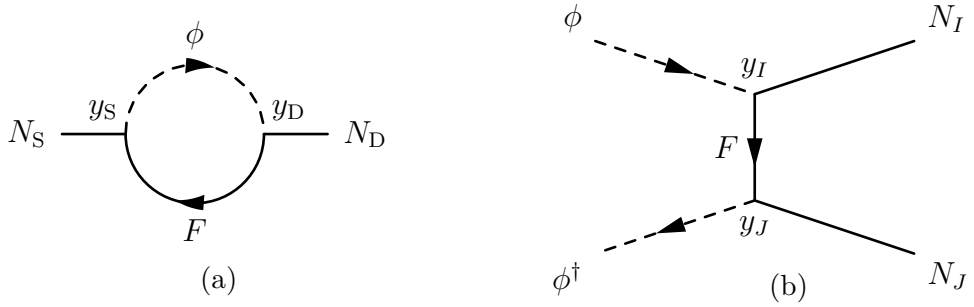

Figure 24: Feynman diagrams which feature a heavy fermion F as the mediator, with $I, J = D, S$. Upon integrating out H, these correspond to the Feynman diagram shown in panel (b) of Fig. 15, and the interaction diagrams in Fig. 16.

There is in fact a much simpler model, where the effective scales feel a little more natural, whilst still allowing one to address DM along with strong leptogenesis and experimental constraints obtained from neutrino telescopes. This time we will instead extend the seesaw Lagrangian by introducing a novel heavy fermion doublet F, which features typical Yukawa couplings y_I to the RH neutrinos, such that

$$\mathcal{L}_F = \overline{F}(i\gamma^{mu}\partial_\mu - m_F)F - \sum_I y_I(\overline{F}\phi N_I + \overline{N_I}\phi^\dagger F). \tag{12.5}$$

Where again at scales much below M_F one can integrate out F, resulting in an effective Lagrangian

$$\mathcal{L}_F^{\rm eff} = \sum_{I,J} \frac{y_I y_J}{M_F}\overline{N}_I N_I \phi^\dagger \phi, \tag{12.6}$$

If in this model one now takes $M_F = M_{GUT}$, $y_{\rm S} \sim 1$, and $y_{\rm D} \sim 10^{-7}$, then one clearly produces the values of $\tilde{\Lambda}_{\rm SS} \sim 10^{16}$GeV, $\tilde{\Lambda}_{\rm DS} \sim 10^{23}$, and $\tilde{\Lambda}_{\rm DD} \sim 10^{30}$. As we have previously seen and discussed, these values are capable of thermalising the source RH neutrinos through source-source Higgs portal interactions before the onset of the oscillations. These values are also capable of producing the observed DM abundance from Higgs-induced RH neutrino mixing, also while suppressing a contribution to the DM neutrino abundance from dark-dark Higgs portal interactions. Compared to the last model, these choices appear less arbitrary, as the three couplings present, λ_{IJ}, are nothing more than the product of two Yukawa couplings, where the third coupling is obtained naturally by the choices of the two Yukawa couplings, thus correctly satisfying Eq. 12.2. It is also interesting that the small DM Yukawa couplings, $y_{\rm D} \sim 10^{-7}$, could be thought of as a small symmetry-breaking parameter that connects the visible and dark sectors, if one imposes a $\mathcal{Z}_2$ symmetry under which all particles are even except the DM neutrino, which is odd.

13 Conclusion

In this work we have completed RHINO DM, by introducing source-source Higgs portal interactions which allow thermalisation of the source RH neutrino, and in doing so we have allowed the RHINO DM model to express its full potential. The RHINO model is capable of producing DM with a mass in the range 1TeV-1PeV that is testable as the DM is expected to decay and these signals can be expected at neutrino telescopes. The model is also compatible with strong thermal leptogenesis and as such it can explain the matter-antimatter asymmetry of the universe, whilst the seesaw model is also incorporated and fundamental to the model, and as such the RHINO model can be regarded as quite minimal. The matter-antimatter asymmetry is also independent of the initial conditions due to the leptogenesis scale potentially being higher than the sphaleron freeze-out temperature. The dark RH neutrino abundance is also independent of any other external contribution that could potentially produce the source RH neutrino, as the source RH neutrino is thermalised regardless from the source-source Higgs portal interactions. This does not disregard an additional component which contributes towards the direct production of the dark RH neutrino, however, if this does occur it must be regarded as sub-dominant or negligible when compared to the Higgs induced neutrino mixing. If another production mechanism does occur then this is likely to be credited to gravitational production, and this is only likely to contribute significantly if the particles are even heavier, as we see in the case of WIMPzillas [158, 159]. One should therefore not regard WIMPzillas and RHINO DM to be competing theories but rather are two solutions that favour different mass ranges. Another attractive feature of RHINO DM derived from cosmological considerations is that the natural fundamental scale of the model that is responsible for the production and the decays of the DM, is that of the GUT scale.

We have also discussed and shown how the Higgs portal operators can arise from UV-complete models, with a particular emphasis on the model where a heavy fermion F has been introduced. This model is favourable, as this UV-complete model can simultaneously yield the correct effective scale for the three Higgs portal interactions when the fundamental scale is close to the scale of a GUT. The results from the RHINO model also display a potential to nicely address the hints from the 7.5-yr HESE IceCube data, which is an excess at approximately 100TeV in the high-energy neutrino flux, when the astrophysical component which features a spectral index of

$\gamma \simeq 2.2$ is taken into account. This is exciting, and if this excess is due to decay DM, then eventually this excess should present anisotropies which align with the DM distribution, as this signal should be proportional to the DM density. Should all this be true, then we propose that RHINO DM could be a favoured solution to this excess due to the predictability this model produces unlike many other models [8], where the same physics is responsible for both the production and the decays of the DM. It has also been suggested, with additional experiments, that there could be reliance on the flavour composition of the primary neutrinos [9]. Finally, it would also be an interesting thought for what the next generation of 100TeV colliders could bring to the forefront regarding possible links with flavour anomalies [247].

Going forward, it would be interesting to investigate the effects of the diagonal source-source term in the effective mixing Hamiltonian. As discussed, these terms are thought to have no major influence on the final abundance; however, it would be interesting to see the effects of this term. It would also be interesting to see the effects of the dark RH neutrino production, either from pure or mixed production, as shown in Fig. 16 (b) and (c), respectively. Perhaps, if the new source-source terms in the Hamiltonian reduce the $N_{\rm D}$ abundance, this could be remedied by one/or both of these interactions. Another compelling avenue is the thought of having hierarchical neutrinos and/or a situation where the dark neutrino could be lighter than the seesaw neutrinos. Finally, it would be interesting to see how the inferring neutrino, $N_{\rm I}$, could potentially influence the picture. The difficulty of including both $N_{\rm D}$ direct production and the influence of $N_{\rm I}$ is that it could spoil the stability that $N_{\rm D}$ requires to play the role of DM.

Bibliography

References

[1] Pasquale Di Bari and Adam Murphy. "Completing RHINO". In: *Journal of High Energy Physics* 2023.3 (Mar. 2023). arXiv:2210.10801 [astro-ph, physics:hep-ph], p. 63. ISSN: 1029-8479. DOI: 10.1007/JHEP03(2023)063.

[2] Gianfranco Bertone and Dan Hooper. "A History of Dark Matter". In: *Reviews of Modern Physics* 90.4 (Oct. 2018). arXiv:1605.04909 [astro-ph, physics:hep-ph], p. 045002. ISSN: 0034-6861, 1539-0756. DOI: 10.1103/RevModPhys.90.045002.

[3] F. Zwicky. "On the Masses of Nebulae and of Clusters of Nebulae". In: *The Astrophysical Journal* 86 (Oct. 1937). Publisher: IOP Publishing, p. 217. ISSN: 0004-637X. DOI: 10.1086/143864.

[4] Planck Collaboration et al. "Planck 2018 results. VI. Cosmological parameters". In: (July 2018). arXiv: 1807.06209.

[5] Chun Yuan Li, Zong Guo Si, and Yu Feng Zhou. "Constraints on dark matter interactions from the first results of DarkSide-50". In: *Nuclear Physics B* 945 (Apr. 2019). arXiv: 1904.02193. ISSN: 05503213. DOI: 10.1016/j.nuclphysb.2019.114678.

[6] Gianfranco Bertone, Dan Hooper, and Joseph Silk. "Particle dark matter: Evidence, candidates and constraints". In: *Physics Reports* 405.5-6 (Jan. 2005). Publisher: North-Holland, pp. 279–390. ISSN: 03701573. DOI: 10.1016/j.physrep.2004.08.031.

[7] Jessica Goodman et al. "Constraints on dark matter from colliders". In: *Physical Review D - Particles, Fields, Gravitation and Cosmology* 82.11 (Dec. 2010). Publisher: American Physical Society, p. 116010. ISSN: 15507998. DOI: 10.1103/PhysRevD.82.116010.

[8] Alexey Anisimov and Pasquale Di Bari. "Cold dark matter from heavy right-handed neutrino mixing". In: *Physical Review D - Particles, Fields, Gravitation and Cosmology* 80.7 (Dec. 2009). arXiv: 0812.5085. ISSN: 15507998. DOI: 10.1103/PhysRevD.80.073017.

[9] Pasquale Di Bari, Patrick Otto Ludl, and Sergio Palomares-Ruiz. "Unifying leptogenesis, dark matter and high-energy neutrinos with right-handed neutrino mixing via Higgs portal". In: *Journal of Cosmology and Astroparticle Physics* 2016.11 (June 2016). arXiv: 1606.06238 Publisher: Institute of Physics Publishing. DOI: 10.1088/1475-7516/2016/11/044.

[10] A. Abada et al. "Low energy effects of neutrino masses". In: *Journal of High Energy Physics* 2007.12 (Dec. 2007). arXiv:0707.4058 [hep-ph], pp. 061–061. ISSN: 1029-8479. DOI: 10.1088/1126-6708/2007/12/061.

[11] Edward Witten. "Lepton Number And Neutrino Masses". In: *Nuclear Physics B - Proceedings Supplements* 91.1-3 (Jan. 2001). arXiv:hep-ph/0006332, pp. 3–8. ISSN: 09205632. DOI: 10.1016/S0920-5632(00)00916-6.

[12] Stephen F. King. *Models of Neutrino Mass, Mixing and CP Violation.* arXiv:1510.02091 [hep-ph]. Nov. 2015.

[13] M. Fukugita and T. Yanagida. "Barygenesis without grand unification". In: *Physics Letters B* 174.1 (June 1986), pp. 45–47. ISSN: 0370-2693. DOI: 10.1016/0370-2693(86)91126-3.

[14] Scott Dodelson and Lawrence M. Widrow. "Sterile Neutrinos as Dark Matter". In: *Physical Review Letters* 72.1 (Jan. 1994). arXiv:hep-ph/9303287, pp. 17–20. ISSN: 0031-9007. DOI: 10.1103/PhysRevLett.72.17.

[15] Alexey Anisimov. "Majorana dark matter". In: *Proceedings of the 6th International Workshop on the Identification of Dark Matter, IDM 2006* (Dec. 2007). arXiv: hep-ph/0612024 Publisher: World Scientific Publishing Co. Pte Ltd ISBN: 9812708529, pp. 439–449. DOI: 10.1142/9789812770288_0058.

[16] P. Di Bari et al. "Density matrix calculation of the dark matter abundance in the Higgs induced right-handed neutrino mixing model". In: (Aug. 2019). arXiv: 1908.00521.

[17] P. Gondolo, G. Gelmini, and S. Sarkar. "Cosmic Neutrinos from Unstable Relic Particles". In: *Nuclear Physics B* 392.1 (Mar. 1993). arXiv:hep-ph/9209236, pp. 111–133. ISSN: 05503213. DOI: 10.1016/0550-3213(93)90199-Y.

[18] Michela D'Onofrio, Kari Rummukainen, and Anders Tranberg. "Sphaleron rate in the minimal standard model". In: *Physical Review Letters* 113.14 (Oct. 2014). arXiv: 1404.3565 Publisher: American Physical Society. ISSN: 10797114. DOI: 10.1103/PhysRevLett.113.141602.

[19] E. Kh Akhmedov, V. A. Rubakov, and A. Yu Smirnov. "Baryogenesis via neutrino oscillations". In: *Physical Review Letters* 81.7 (Mar. 1998). arXiv: hep-ph/9803255, pp. 1359–1362. ISSN: 10797114. DOI: 10.1103/PhysRevLett.81.1359.

[20] Takehiko Asaka, Steve Blanchet, and Mikhail Shaposhnikov. "The vmSM, dark matter and neutrino masses". In: *Physics Letters, Section B: Nuclear, Elementary Particle and High-Energy Physics* 631.4 (Mar. 2005). arXiv: hep-ph/0503065, pp. 151–156. ISSN: 03702693. DOI: 10.1016/j.physletb.2005.09.070.

[21] Pasquale Di Bari. "Neutrino masses, leptogenesis and dark matter". In: *Prospects in Neutrino Physics Cavendish Centre* (Apr. 2019). arXiv: 1904.11971.

[22] Pasquale Di Bari, Danny Marfatia, and Ye-Ling Zhou. "Gravitational waves from first-order phase transitions in Majoron models of neutrino mass". In: *Journal of High Energy Physics* 2021.10 (Oct. 2021). arXiv:2106.00025 [astro-ph, physics:hep-ex, physics:hep-ph], p. 193. ISSN: 1029-8479. DOI: 10.1007/JHEP10(2021)193.

[23] Sacha Davidson and Alejandro Ibarra. "A lower bound on the right-handed neutrino mass from leptogenesis". In: *Physics Letters, Section B: Nuclear, Elementary Particle and High-Energy Physics* 535.1-4 (Feb. 2002). arXiv: hep-ph/0202239, pp. 25–32. ISSN: 03702693. DOI: 10.1016/S0370-2693(02)01735-5.

[24] Apostolos Pilaftsis. "CP Violation and Baryogenesis due to Heavy Majorana Neutrinos". In: *Physical Review D* 56.9 (Nov. 1997). arXiv:hep-ph/9707235, pp. 5431–5451. ISSN: 0556-2821, 1089-4918. DOI: 10.1103/PhysRevD.56.5431.

[25] Apostolos Pilaftsis and Thomas E. J. Underwood. "Resonant Leptogenesis". In: *Nuclear Physics B* 692.3 (Aug. 2004). arXiv:hep-ph/0309342, pp. 303–345. ISSN: 05503213. DOI: 10.1016/j.nuclphysb.2004.05.029.

[26] Steve Blanchet and Pasquale Di Bari. "New aspects of leptogenesis bounds". In: *Nuclear Physics B* 807.1-2 (July 2009). arXiv: 0807.0743, pp. 155–187. ISSN: 05503213. DOI: 10.1016/j.nuclphysb.2008.08.026.

[27] Stefan Antusch et al. "Non-unitary Leptonic Mixing and Leptogenesis". In: *Journal of High Energy Physics* 2010.1 (Jan. 2010). arXiv:0910.5957 [hep-ph], p. 17. ISSN: 1029-8479. DOI: 10.1007/JHEP01(2010)017.

[28] K. Moffat et al. "Leptogenesis from Low Energy CP Violation". In: *Journal of High Energy Physics* 2019.3 (Mar. 2019). arXiv:1809.08251 [hep-ph], p. 34. ISSN: 1029-8479. DOI: 10.1007/JHEP03(2019)034.

[29] William Thomson Kelvin. *Baltimore lectures on molecular dynamics and the wave theory of light,* London, 1904.

[30] D. H. Rogstad et al. "Gross Properties of Five Scd Galaxies as Determined from 21-CENTIMETER Observations". In: *ApJ* 176 (Sept. 1972). Publisher: American Astronomical Society, p. 315. ISSN: 0004-637X. DOI: 10.1086/151636.

[31] Horace W. Babcock. "The rotation of the Andromeda Nebula". In: *Lick Observatory Bulletins* 19 (1939). Publisher: Smithsonian Institution, pp. 41–51. ISSN: 0075-9317. DOI: 10.5479/ads/bib/1939licob.19.41b.

[32] D. H. Rogstad, G. S. Shostak, and A. H. Rots. "Aperture synthesis study of neutral hydrogen in the galaxies NGC 6946 and IC 342." In: *Astronomy and Astrophysics* 22 (Jan. 1973). ADS Bibcode: 1973A&A....22..111R, pp. 111–119. ISSN: 0004-6361.

[33] Vera C. Rubin et al. "Rotation of the Andromeda Nebula from a Spectroscopic Survey of Emission Regions". In: *ApJ* 159 (Feb. 1970). Publisher: American Astronomical Society, p. 379. ISSN: 0004-637X. DOI: 10.1086/150317.

[34] V. C. Rubin et al. "Rotational properties of 21 SC galaxies with a large range of luminosities and radii, from NGC 4605 (R=4kpc) to UGC 2885 (R=122kpc)." In: *ApJ* 238 (June 1980). Publisher: American Astronomical Society, pp. 471–487. ISSN: 0004-637X. DOI: 10.1086/158003.

[35] Morton S Roberts et al. “The rotation curve and geometry of M31 at large galactocentric distances.” In: *ApJ* 201 (Oct. 1975). Publisher: American Astronomical Society, pp. 327–346. ISSN: 0004-637X. DOI: 10.1086/153889.

[36] Matthias Bartelmann. “Gravitational Lensing”. In: *Classical and Quantum Gravity* 27.23 (Dec. 2010). arXiv:1010.3829 [astro-ph, physics:gr-qc], p. 233001. ISSN: 0264-9381, 1361-6382. DOI: 10.1088/0264-9381/27/23/233001.

[37] Ramesh Narayan and Matthias Bartelmann. *Lectures on Gravitational Lensing*. en. June 1996.

[38] A. N. Taylor et al. “Gravitational Lens Magnification and the Mass of Abell 1689”. In: *The Astrophysical Journal* 501.2 (July 1998). arXiv: astro-ph/9801158 Publisher: American Astronomical Society, pp. 539–553. ISSN: 0004-637X. DOI: 10.1086/305827/FULLTEXT/.

[39] Priyamvada Natarajan et al. “Mapping substructure in the HST Frontier Fields cluster lenses and in cosmological simulations”. In: *MNRAS* 000 (2016). arXiv: 1702.04348v2.

[40] Alexandre Refregier. “Weak Gravitational Lensing by Large-Scale Structure”. In: *https://doi.org/10.1146/annurev.astro.41.111302.102207* 41 (Nov. 2003). arXiv: astro-ph/0307212 Publisher: Annual Reviews 4139 El Camino Way, P.O. Box 10139, Palo Alto, CA 94303-0139, USA, pp. 645–668. ISSN: 00664146. DOI: 10.1146/ANNUREV.ASTRO.41.111302.102207.

[41] C. L. Bennett et al. “Nine-Year Wilkinson Microwave Anisotropy Probe (WMAP) Observations: Final Maps and Results”. In: *The Astrophysical Journal Supplement Series* 208.2 (Sept. 2013). arXiv:1212.5225 [astro-ph], p. 20. ISSN: 0067-0049, 1538-4365. DOI: 10.1088/0067-0049/208/2/20.

[42] G. Hinshaw et al. “Three-Year Wilkinson Microwave Anisotropy Probe (WMAP) Observations: Temperature Analysis”. In: *The Astrophysical Journal Supplement Series* 170.2 (June 2007). arXiv:astro-ph/0603451, pp. 288–334. ISSN: 0067-0049, 1538-4365. DOI: 10.1086/513698.

[43] G. Hinshaw et al. “FIVE-YEAR WILKINSON MICROWAVE ANISOTROPY PROBE* OBSERVATIONS: DATA PROCESSING, SKY MAPS, AND BASIC RESULTS”. In: *The Astrophysical Journal Supplement Series* 180.2 (Feb. 2009). arXiv: 0803.0732 Publisher: IOP Publishing, p. 225. ISSN: 0067-0049. DOI: 10.1088/0067-0049/180/2/225.

[44] James Alvey et al. “Cosmic Neutrino Background Detection in Large-Neutrino-Mass Cosmologies”. In: *Physical Review D* 105.6 (Mar. 2022). arXiv:2111.14870 [astro-ph, physics:hep-ex, physics:hep-ph], p. 063501. ISSN: 2470-0010, 2470-0029. DOI: 10.1103/PhysRevD.105.063501.

[45] Sungwook E. Hong et al. “Revealing the Local Cosmic Web from Galaxies by Deep Learning”. In: *The Astrophysical Journal* 913.1 (May 2021). arXiv: 2008.01738 Publisher: IOP Publishing, p. 76. ISSN: 0004-637X. DOI: 10.3847/1538-4357/ABF040.

[46] Lerh Feng Low. “Constraints on the composite photon theory”. In: 31.36 (Nov. 2016). Publisher: World Scientific Publishing Company. ISSN: 02177323. DOI: 10.1142/S021773231675002X.

[47] Douglas Clowe et al. “A Direct Empirical Proof of the Existence of Dark Matter”. In: *The Astrophysical Journal* 648.2 (Sept. 2006). arXiv: astro-ph/0608407 Publisher: American Astronomical Society, pp. L109–L113. ISSN: 0004-637X. DOI: 10.1086/508162/FULLTEXT/.

[48] JC Maxwell. “A Treatise on Electricity and Magnetism”. In: *Nature 1873 7:182* 7.182 (Apr. 1873). Publisher: Nature Publishing Group, pp. 478–480. ISSN: 1476-4687. DOI: 10.1038/007478a0.

[49] A Einstein. “ON THE ELECTRODYNAMICS OF MOVING BODIES”. In: (1905).

[50] Luis J Boya. “The Thermal Radiation Formula of Planck (1900)”. In: (2004).

[51] Paul Dirac and ’ Z F Physik. “The quantum theory of the electron”. In: *Proceedings of the Royal Society of London. Series A, Containing Papers of a Mathematical and Physical Character* 117.778 (Feb. 1928). Publisher: The Royal Society, pp. 610–624. ISSN: 0950-1207. DOI: 10.1098/rspa.1928.0023.

[52] F. J. Dyson. “The radiation theories of Tomonaga, Schwinger, and Feynman”. In: *Physical Review* 75.3 (Feb. 1949). Publisher: American Physical Society, pp. 486–502. ISSN: 0031899X. DOI: 10.1103/PhysRev.75.486.

[53] F. J. Dyson. “The S matrix in quantum electrodynamics”. In: *Physical Review* 75.11 (June 1949). Publisher: American Physical Society, pp. 1736–1755. ISSN: 0031899X. DOI: 10.1103/PhysRev.75.1736.

[54] Julian Schwinger. “On quantum-electrodynamics and the magnetic moment of the electron [9]”. In: *Physical Review* 73.4 (Feb. 1948). Publisher: Marshall and Ward, pp. 416–417. ISSN: 0031899X. DOI: 10.1103/PhysRev.73.416.

[55] Julian Schwinger. “Quantum electrodynamics. I. A covariant formulation”. In: *Physical Review* 74.10 (Nov. 1948). Publisher: American Physical Society, pp. 1439–1461. ISSN: 0031899X. DOI: 10.1103/PhysRev.74.1439.

[56] R. P. Feynman. “The Theory of Positrons”. In: *Physical Review* 76.6 (Sept. 1949), pp. 749–759. ISSN: 0031-899X. DOI: 10.1103/PhysRev.76.749.

[57] R. P. Feynman. “Space-time approach to quantum electrodynamics”. In: *Physical Review* 76.6 (Sept. 1949). Publisher: American Physical Society, pp. 769–789. ISSN: 0031899X. DOI: 10.1103/PhysRev.76.769.

[58] R. P. Feynman. “Mathematical formulation of the quantum theory of electromagnetic interaction”. In: *Physical Review* 80.3 (Nov. 1950). Publisher: American Physical Society, pp. 440–457. ISSN: 0031899X. DOI: 10.1103/PhysRev.80.440.

[59] Sheldon L. Glashow. “Partial-symmetries of weak interactions”. In: *Nuclear Physics* 22.4 (Feb. 1961). Publisher: North-Holland, pp. 579–588. ISSN: 00295582. DOI: 10.1016/0029-5582(61)90469-2.

[60] H. Fritzsch, M. Gell-Mann, and H. Leutwyler. “Advantages of the color octet gluon picture”. In: *Physics Letters B* 47.4 (Nov. 1973), pp. 365–368. ISSN: 03702693. DOI: 10.1016/0370-2693(73)90625-4.

[61] C. N. Yang and R. L. Mills. "Conservation of isotopic spin and isotopic gauge invariance". In: *Physical Review* 96.1 (Oct. 1954). Publisher: American Physical Society, pp. 191–195. ISSN: 0031899X. DOI: 10.1103/PhysRev.96.191.

[62] W. J. Marciano. "Standard Model Parameters and the Search for New Physics". In: (Apr. 1988).

[63] Bernard Carr and Florian Kuhnel. "Primordial Black Holes as Dark Matter Candidates". In: *SciPost Physics Lecture Notes* (May 2022). arXiv:2110.02821 [astro-ph, physics:gr-qc, physics:hep-ph], p. 48. ISSN: 2590-1990. DOI: 10.21468/SciPostPhysLectNotes.48.

[64] Bernard Carr, Florian Kuhnel, and Marit Sandstad. "Primordial Black Holes as Dark Matter". In: *Physical Review D* 94.8 (Oct. 2016). arXiv:1607.06077 [astro-ph, physics:gr-qc], p. 083504. ISSN: 2470-0010, 2470-0029. DOI: 10.1103/PhysRevD.94.083504.

[65] D. P. Bennett et al. *The MACHO Project Dark Matter Search*. arXiv:astro-ph/9510104. Oct. 1995.

[66] Timothy D. Brandt. "Constraints on MACHO Dark Matter from Compact Stellar Systems in Ultra-Faint Dwarf Galaxies". In: *The Astrophysical Journal* 824.2 (June 2016). arXiv:1605.03665 [astro-ph], p. L31. ISSN: 2041-8213. DOI: 10.3847/2041-8205/824/2/L31.

[67] Jose A. R. Cembranos. "Modified gravity and dark matter". In: *Journal of Physics: Conference Series* 718 (May 2016). arXiv:1512.08752 [astro-ph, physics:gr-qc, physics:hep-ph], p. 032004. ISSN: 1742-6588, 1742-6596. DOI: 10.1088/1742-6596/718/3/032004.

[68] Riccardo Scarpa. "Modified Newtonian Dynamics, an Introductory Review". en. In: *AIP Conference Proceedings*. Vol. 822. ISSN: 0094243X. Moncao (Portugal): AIP, 2006, pp. 253–265. DOI: 10.1063/1.2189141.

[69] J. W. Moffat. "Scalar-Tensor-Vector Gravity Theory". In: *Journal of Cosmology and Astroparticle Physics* 2006.03 (Mar. 2006). arXiv:gr-qc/0506021, pp. 004–004. ISSN: 1475-7516. DOI: 10.1088/1475-7516/2006/03/004.

[70] Sean M. Carroll and Grant N. Remmen. "What is the Entropy in Entropic Gravity?" In: *Physical Review D* 93.12 (June 2016). arXiv:1601.07558 [gr-qc, physics:hep-th], p. 124052. ISSN: 2470-0010, 2470-0029. DOI: 10.1103/PhysRevD.93.124052.

[71] Howard Baer et al. “Dark matter production in the early Universe: beyond the thermal WIMP paradigm”. In: *Physics Reports* 555 (Feb. 2015). arXiv:1407.0017 [astro-ph, physics:hep-ph], pp. 1–60. ISSN: 03701573. DOI: 10.1016/j.physrep.2014.10.002.

[72] Leanne D Duffy and Karl Van Bibber. “Axions as dark matter particles”. In: *New Journal of Physics* 11.10 (Oct. 2009). Publisher: IOP Publishing, p. 105008. ISSN: 13672630. DOI: 10.1088/1367-2630/11/10/105008.

[73] Stephen J. Asztalos et al. “Searches for astrophysical and cosmological axions”. In: *Annual Review of Nuclear and Particle Science* 56 (2006), pp. 293–326. ISSN: 01638998. DOI: 10.1146/annurev.nucl.56.080805.140513.

[74] Paola Arias et al. “WISPy Cold Dark Matter”. In: *Journal of Cosmology and Astroparticle Physics* 2012.06 (June 2012). arXiv:1201.5902 [astro-ph, physics:hep-ph, physics:hep-th], pp. 013–013. ISSN: 1475-7516. DOI: 10.1088/1475-7516/2012/06/013.

[75] Joerg Jaeckel. “A Family of WISPy Dark Matter Candidates”. In: *Physics Letters B* 732 (May 2014). arXiv:1311.0880 [astro-ph, physics:hep-ph], pp. 1–7. ISSN: 03702693. DOI: 10.1016/j.physletb.2014.03.005.

[76] Lam Hui et al. “Ultralight scalars as cosmological dark matter”. In: *Physical Review D* 95.4 (Feb. 2017). arXiv:1610.08297 [astro-ph, physics:hep-ph, physics:hep-th], p. 043541. ISSN: 2470-0010, 2470-0029. DOI: 10.1103/PhysRevD.95.043541.

[77] Wayne Hu, Rennan Barkana, and Andrei Gruzinov. “Cold and Fuzzy Dark Matter”. In: *Physical Review Letters* 85.6 (Aug. 2000). arXiv:astro-ph/0003365, pp. 1158–1161. ISSN: 0031-9007, 1079-7114. DOI: 10.1103/PhysRevLett.85.1158.

[78] A. Boyarsky et al. “Sterile neutrino Dark Matter”. In: *Progress in Particle and Nuclear Physics* 104 (July 2019). arXiv: 1807.07938, pp. 1–45. ISSN: 01466410. DOI: 10.1016/j.ppnp.2018.07.004.

[79] Manuel Drees. “Dark Matter Theory”. In: *Nuclear and Particle Physics Proceedings* 267-269 (Nov. 2018). arXiv: 1811.06406 Publisher: Elsevier B.V., pp. 323–331.

[80] Gary Steigman, Basudeb Dasgupta, and John F Beacom. "Precise relic WIMP abundance and its impact on searches for dark matter annihilation". In: *Physical Review D - Particles, Fields, Gravitation and Cosmology* 86.2 (2012). arXiv: 1204.3622v3. ISSN: 15507998. DOI: 10.1103/PhysRevD.86.023506.

[81] Debasish Borah et al. "Self-interacting Dark Matter via Right Handed Neutrino Portal". In: *Physical Review D* 105.1 (Jan. 2022). arXiv:2110.00021 [astro-ph, physics:hep-ex, physics:hep-ph], p. 015004. ISSN: 2470-0010, 2470-0029. DOI: 10.1103/PhysRevD.105.015004.

[82] Rafael Yunis et al. "Self-Interacting Dark Matter in Cosmology: accurate numerical implementation and observational constraints". In: *Journal of Cosmology and Astroparticle Physics* 2022.02 (Feb. 2022). arXiv:2108.02657 [astro-ph], p. 024. ISSN: 1475-7516. DOI: 10.1088/1475-7516/2022/02/024.

[83] Adel Bilal. *Introduction to Supersymmetry*. arXiv:hep-th/0101055. Jan. 2001. DOI: 10.48550/arXiv.hep-th/0101055.

[84] Y. Shadmi. "Introduction to Supersymmetry". In: *CERN Yellow Reports* (July 2016). arXiv:1708.00772 [hep-ph], 95 Pages. DOI: 10.5170/CERN-2016-003.95.

[85] S. Girmohanta and R. Shrock. "An Extra-Dimensional Model of Dark Matter". In: *Physical Review D* 104.11 (Dec. 2021). arXiv:2109.02670 [gr-qc, physics:hep-ph, physics:hep-th], p. 115021. ISSN: 2470-0010, 2470-0029. DOI: 10.1103/PhysRevD.104.115021.

[86] Andreas Birkedal et al. "Little Higgs Dark Matter". In: *Physical Review D* 74.3 (Aug. 2006). arXiv:hep-ph/0603077, p. 035002. ISSN: 1550-7998, 1550-2368. DOI: 10.1103/PhysRevD.74.035002.

[87] Ingolf Bischer, Tilman Plehn, and Werner Rodejohann. "Dark Matter EFT, the Third – Neutrino WIMPs". In: *SciPost Physics* 10.2 (Feb. 2021). arXiv:2008.04718 [hep-ph], p. 039. ISSN: 2542-4653. DOI: 10.21468/SciPostPhys.10.2.039.

[88] Tommi Alanne and Florian Goertz. *Extended Dark Matter EFT*. arXiv:1712.07626 [hep-ex, physics:hep-ph]. Mar. 2018. DOI: 10.48550/arXiv.1712.07626.

[89] Lotfi Boubekeur and Stefano Profumo. "On the Tremaine-Gunn Limit with Mass-Varying Particles". In: *Physical Review D* 107.10 (May 2023). arXiv:2302.10246 [astro-ph, physics:hep-ph, physics:hep-th], p. 103535. ISSN: 2470-0010, 2470-0029. DOI: 10.1103/PhysRevD.107.103535.

[90] Takeshi Fukuyama et al. "SO(10) Group Theory for the Unified Model Building". In: *Journal of Mathematical Physics* 46.3 (Mar. 2005). arXiv:hep-ph/0405300, p. 033505. ISSN: 0022-2488, 1089-7658. DOI: 10.1063/1.1847709.

[91] Mikhail Shaposhnikov. "The nuMSM, leptonic asymmetries, and properties of singlet fermions". In: *Journal of High Energy Physics* 2008.08 (Aug. 2008). arXiv:0804.4542 [astro-ph, physics:hep-ph], pp. 008–008. ISSN: 1029-8479. DOI: 10.1088/1126-6708/2008/08/008.

[92] Takehiko Asaka and Mikhail Shaposhnikov. "The νMSM, Dark Matter and Baryon Asymmetry of the Universe". In: *Physics Letters B* 620.1-2 (July 2005). arXiv:hep-ph/0505013, pp. 17–26. ISSN: 03702693. DOI: 10.1016/j.physletb.2005.06.020.

[93] Laurent Canetti, Marco Drewes, and Mikhail Shaposhnikov. "Sterile Neutrinos as the Origin of Dark and Baryonic Matter". In: *Physical Review Letters* 110.6 (Feb. 2013). arXiv:1204.3902 [astro-ph, physics:hep-ph], p. 061801. ISSN: 0031-9007, 1079-7114. DOI: 10.1103/PhysRevLett.110.061801.

[94] Xiangdong Shi and George M. Fuller. "A New Dark Matter Candidate: Non-thermal Sterile Neutrinos". In: *Physical Review Letters* 82.14 (Apr. 1999). arXiv:astro-ph/9810076, pp. 2832–2835. ISSN: 0031-9007, 1079-7114. DOI: 10.1103/PhysRevLett.82.2832.

[95] Palash B. Pal and Lincoln Wolfenstein. "Radiative decays of massive neutrinos". In: *Physical Review D* 25.3 (Feb. 1982). Publisher: American Physical Society, pp. 766–773. DOI: 10.1103/PhysRevD.25.766.

[96] Kevork N. Abazajian. "Resonantly-Produced 7 keV Sterile Neutrino Dark Matter Models and the Properties of Milky Way Satellites". In: *Physical Review Letters* 112.16 (Apr. 2014). arXiv:1403.0954 [astro-ph, physics:hep-ph], p. 161303. ISSN: 0031-9007, 1079-7114. DOI: 10.1103/PhysRevLett.112.161303.

[97] J. Ghiglieri and M. Laine. "Sterile neutrino dark matter via coinciding resonances". In: *Journal of Cosmology and Astroparticle Physics* 2020.07 (July 2020). arXiv:2004.10766 [hep-ph], pp. 012–012. ISSN: 1475-7516. DOI: 10.1088/1475-7516/2020/07/012.

[98] XRISM Science Team. *Science with the X-ray Imaging and Spectroscopy Mission (XRISM)*. arXiv:2003.04962 [astro-ph]. Mar. 2020. DOI: 10.48550/arXiv.2003.04962.

[99] P. Di Bari et al. "Density matrix calculation of the dark matter abundance in the Higgs induced right-handed neutrino mixing model". In: (Aug. 2019).

[100] Luca Nanni. "Fermi's theory of beta decay: a first attempt at electroweak unification". en. In: *Advanced Studies in Theoretical Physics* 13.6 (2019), pp. 281–293. ISSN: 13147609, 13131311. DOI: 10.12988/astp.2019.8939.

[101] K. V. L. Sarma. *Nobel Leptons*. arXiv:hep-ph/9512420. Dec. 1995.

[102] Palash B Pal. "Dirac, Majorana and Weyl fermions". In: (2010). arXiv: 1006.1718v2.

[103] R D Peccei. "Discrete and Global Symmetries in Particle Physics". In: (1998).

[104] Susan Gardner and Xinshuai Yan. "CPT, CP, and C transformations of fermions, and their consequences, in theories with B-L violation". In: *Physical Review D* 93.9 (May 2016). arXiv:1602.00693 [hep-ph, physics:nucl-th], p. 096008. ISSN: 2470-0010, 2470-0029. DOI: 10.1103/PhysRevD.93.096008.

[105] Antonio Pich. "Electroweak Symmetry Breaking and the Higgs Boson". In: *Acta Physica Polonica B* 47.1 (2016). arXiv:1512.08749 [hep-ex, physics:hep-ph], p. 151. ISSN: 0587-4254, 1509-5770. DOI: 10.5506/APhysPolB.47.151.

[106] Michael E. Peskin. *Lectures on the Theory of the Weak Interaction*. arXiv:1708.09043 [hep-ph]. Aug. 2017.

[107] The ALEPH Collaboration et al. "Precision Electroweak Measurements on the Z Resonance". In: *Physics Reports* 427.5-6 (May 2006). arXiv:hep-ex/0509008, pp. 257–454. ISSN: 03701573. DOI: 10.1016/j.physrep.2005.12.006.

[108] Raymond Davis. "A review of the homestake solar neutrino experiment". en. In: *Progress in Particle and Nuclear Physics* 32 (Jan. 1994), pp. 13–32. ISSN: 0146-6410. DOI: 10.1016/0146-6410(94)90004-3.

[109] A. Bellerive et al. "The Sudbury Neutrino Observatory". In: *Nuclear Physics B* 908 (July 2016). arXiv:1602.02469 [hep-ex, physics:nucl-ex, physics:physics], pp. 30–51. ISSN: 05503213. DOI: 10.1016/j.nuclphysb.2016.04.035.

[110] Tim Gershon. "Overview of the CKM Matrix". In: *Pramana* 79.5 (Nov. 2012). arXiv:1112.1984 [hep-ex, physics:hep-ph], pp. 1091–1108. ISSN: 0304-4289, 0973-7111. DOI: 10.1007/s12043-012-0418-y.

[111] Aditya Ankur Patel and Tejinder P. Singh. *CKM matrix parameters from an algebra*. arXiv:2305.00668 [hep-ph]. May 2023.

[112] Carlo Giunti and Marco Laveder. *Neutrino Mixing*. Tech. rep. 2004.

[113] Ivan Esteban et al. "The fate of hints: updated global analysis of three-flavor neutrino oscillations". In: *Journal of High Energy Physics* 2020.9 (Sept. 2020). arXiv:2007.14792 [hep-ex, physics:hep-ph], p. 178. ISSN: 1029-8479. DOI: 10.1007/JHEP09(2020)178.

[114] Claudio Giganti, Stéphane Lavignac, and Marco Zito. "Neutrino oscillations: the rise of the PMNS paradigm". In: *Progress in Particle and Nuclear Physics* 98 (Jan. 2018). arXiv:1710.00715 [hep-ex, physics:hep-ph], pp. 1–54. ISSN: 01466410. DOI: 10.1016/j.ppnp.2017.10.001.

[115] Pasquale Di Bari. "On the origin of matter in the Universe". In: *Progress in Particle and Nuclear Physics* 122 (Jan. 2022). arXiv:2107.13750 [astro-ph, physics:hep-ex, physics:hep-ph], p. 103913. ISSN: 01466410. DOI: 10.1016/j.ppnp.2021.103913.

[116] Ubaldo Dore and Lucia Zanello. *Bruno Pontecorvo and neutrino physics*. arXiv:0910.1657 [hep-ex, physics:hep-ph, physics:physics]. Oct. 2010.

[117] M. C. Gonalez-Garcia. *Neutrino Masses, Mixing, and Oscillations*.

[118] A. Yu Smirnov. *The MSW effect and Solar Neutrinos*. arXiv:hep-ph/0305106. May 2003. DOI: 10.48550/arXiv.hep-ph/0305106.

[119] Isabelle Tanseri et al. “Updated neutrino mass constraints from galaxy clustering and CMB lensing-galaxy cross-correlation measurements”. In: *Journal of High Energy Astrophysics* 36 (Nov. 2022). arXiv:2207.01913 [astro-ph, physics:hep-ph], pp. 1–26. ISSN: 22144048. DOI: 10.1016/j.jheap.2022.07.002.

[120] A. Yu Smirnov. “The MSW effect and Matter Effects in Neutrino Oscillations”. In: *Physica Scripta* T121 (Jan. 2005). arXiv:hep-ph/0412391, pp. 57–64. ISSN: 0031-8949, 1402-4896. DOI: 10.1088/0031-8949/2005/T121/008.

[121] G. Sigl and G. Raffelt. “General kinetic description of relativistic mixed neutrinos”. In: *Nuclear Physics B* 406.1 (Sept. 1993), pp. 423–451. ISSN: 0550-3213. DOI: 10.1016/0550-3213(93)90175-O.

[122] R. Barbieri and A. Dolgov. “Neutrino oscillations in the early universe”. In: *Nuclear Physics B* 349.3 (Feb. 1991), pp. 743–753. ISSN: 0550-3213. DOI: 10.1016/0550-3213(91)90396-F.

[123] Xiangdong Shi. “Chaotic Amplification of Neutrino Chemical Potentials by Neutrino Oscillations in Big Bang Nucleosynthesis”. In: *Physical Review D* 54.4 (Aug. 1996). arXiv:astro-ph/9602135, pp. 2753–2760. ISSN: 0556-2821, 1089-4918. DOI: 10.1103/PhysRevD.54.2753.

[124] Paul Langacker. “Neutrino Masses from the Top Down”. In: *Annual Review of Nuclear and Particle Science* 62.1 (Nov. 2012). arXiv:1112.5992 [hep-ph, physics:hep-th], pp. 215–235. ISSN: 0163-8998, 1545-4134. DOI: 10.1146/annurev-nucl-102711-094925.

[125] Ettore Majorana. “Teoria simmetrica dell’elettrone e del positrone”. it. In: *Il Nuovo Cimento (1924-1942)* 14.4 (Apr. 1937), pp. 171–184. ISSN: 1827-6121. DOI: 10.1007/BF02961314.

[126] Kazuo Fujikawa. “Parity and CP operations for Majorana neutrinos”. In: *Physical Review D* 102.10 (Nov. 2020). arXiv:2008.11390 [hep-ph, physics:hep-th], p. 105001. ISSN: 2470-0010, 2470-0029. DOI: 10.1103/PhysRevD.102.105001.

[127] S. M. Bilenky. *On the Origin of Majorana Neutrino Masses*. arXiv:2010.05336 [hep-ph]. Oct. 2020.

[128] Herbi K. Dreiner, Howard E. Haber, and Stephen P. Martin. "Two-component spinor techniques and Feynman rules for quantum field theory and supersymmetry". In: *Physics Reports* 494.1-2 (Sept. 2010). arXiv:0812.1594 [hep-ph, physics:hep-th], pp. 1–196. ISSN: 03701573. DOI: 10.1016/j.physrep.2010.05.002.

[129] Tsutomu Yanagida. "Horizontal Symmetry and Masses of Neutrinos". In: *Prog. Theor. Phys.* 64 (1980), p. 1103. DOI: 10.1143/PTP.64.1103.

[130] Vedran Brdar et al. "Type-I Seesaw as the Common Origin of Neutrino Mass, Baryon Asymmetry, and the Electroweak Scale". In: *Physical Review D* 100.7 (Oct. 2019). arXiv:1905.12634 [astro-ph, physics:hep-ph], p. 075029. ISSN: 2470-0010, 2470-0029. DOI: 10.1103/PhysRevD.100.075029.

[131] Howard E. Haber. "A tale of three diagonalizations". In: *International Journal of Modern Physics A* 36.04 (Feb. 2021). arXiv:2009.03990 [hep-ph, physics:quant-ph], p. 2130003. ISSN: 0217-751X, 1793-656X. DOI: 10.1142/S0217751X21300027.

[132] J. A. Casas and A. Ibarra. "Oscillating neutrinos and mu –> e, gamma". In: *Nuclear Physics B* 618.1-2 (Dec. 2001). arXiv:hep-ph/0103065, pp. 171–204. ISSN: 05503213. DOI: 10.1016/S0550-3213(01)00475-8.

[133] Stefano Profumo, Leonardo Giani, and Oliver F. Piattella. "An Introduction to Particle Dark Matter". In: (Oct. 2019). arXiv: 1910.05610.

[134] Carlo Cercignani and Gilberto Kremer. *The Relativistic Boltzmann Equation: Theory and Application*.

[135] Scott Dodelson. *Modern Cosmology*.

[136] Leszek Roszkowski, Enrico Maria Sessolo, and Sebastian Trojanowski. "WIMP dark matter candidates and searches - Current status and future prospects". In: *Reports on Progress in Physics* 81.6 (July 2018). ISSN: 00344885. DOI: 10.1088/1361-6633/aab913.

[137] Nathaniel Craig. *Naturalness: A Snowmass White Paper*. arXiv:2205.05708 [hep-ph, physics:hep-th]. May 2022.

[138] Lawrence J. Hall et al. "Freeze-in production of FIMP dark matter". In: *Journal of High Energy Physics* 2010.3 (2010). arXiv: 0911.1120v2. ISSN: 11266708. DOI: 10.1007/JHEP03(2010)080.

[139] Nicolás Bernal et al. "The dawn of FIMP Dark Matter: A review of models and constraints". In: *International Journal of Modern Physics A* 32.27 (June 2017). arXiv: 1706.07442. ISSN: 0217751X. DOI: 10.1142/S0217751X1730023X.

[140] Nicolás Bernal et al. "The Dawn of FIMP Dark Matter: A Review of Models and Constraints". In: *International Journal of Modern Physics A* 32.27 (Sept. 2017). arXiv:1706.07442 [astro-ph, physics:hep-ph], p. 1730023. ISSN: 0217-751X, 1793-656X. DOI: 10.1142/S0217751X1730023X.

[141] M. Fukugita and T. Yanagida. "Barygenesis without grand unification". In: *Physics Letters B* 174.1 (June 1986). Publisher: North-Holland, pp. 45–47. ISSN: 03702693. DOI: 10.1016/0370-2693(86)91126-3.

[142] G. 'T Hooft. "Symmetry Breaking through Bell-Jackiw Anomalies". en. In: *Physical Review Letters* 37.1 (July 1976), pp. 8–11. ISSN: 0031-9007. DOI: 10.1103/PhysRevLett.37.8.

[143] V. A. Rubakov and M. E. Shaposhnikov. "Electroweak Baryon Number Non-Conservation in the Early Universe and in High Energy Collisions". In: *Physics-Uspekhi* 39.5 (May 1996). arXiv:hep-ph/9603208, pp. 461–502. ISSN: 1063-7869, 1468-4780. DOI: 10.1070/PU1996v039n05ABEH000145.

[144] A. D. Sakharov. "Violation of CP Invariance, C asymmetry, and baryon asymmetry of the universe". In: *Pisma Zh. Eksp. Teor. Fiz.* 5 (1967), pp. 32–35. DOI: 10.1070/PU1991v034n05ABEH002497.

[145] W. Buchmüller, P. Di Bari, and M. Plümacher. "Leptogenesis for pedestrians". In: *Annals of Physics* 315.2 (Jan. 2005). arXiv: hep-ph/0401240, pp. 305–351. ISSN: 00034916. DOI: 10.1016/j.aop.2004.02.003.

[146] L. Covi, E. Roulet, and F. Vissani. "CP violating decays in leptogenesis scenarios". In: *Physics Letters B* 384.1-4 (Sept. 1996). arXiv:hep-ph/9605319, pp. 169–174. ISSN: 03702693. DOI: 10.1016/0370-2693(96)00817-9.

[147] Alexey Anisimov, Steve Blanchet, and Pasquale Di Bari. "Viability of Dirac phase leptogenesis". In: *Journal of Cosmology and Astroparticle Physics* 2008.04 (Apr. 2008). arXiv:0707.3024 [hep-ph], p. 033. ISSN: 1475-7516. DOI: 10.1088/1475-7516/2008/04/033.

[148] W. Buchmüller, P. Di Bari, and M. Plümacher. "Cosmic microwave background, matter - Antimatter asymmetry and neutrino masses". In: *Nuclear Physics B* 643.1-3 (Nov. 2002). arXiv: hep-ph/0205349 Publisher: Elsevier, pp. 367–390. ISSN: 05503213. DOI: 10.1016/S0550-3213(02)00737-X.

[149] Steve Blanchet and Pasquale Di Bari. "The minimal scenario of leptogenesis". In: *New Journal of Physics* 14 (Nov. 2012). arXiv: 1211.0512. DOI: 10.1088/1367-2630/14/12/125012.

[150] Aneesh V. Manohar. "Effective Field Theories". In: vol. 479. arXiv:hep-ph/9606222. 1997, pp. 311–362. DOI: 10.1007/BFb0104294.

[151] Riccardo Penco. *An Introduction to Effective Field Theories*. arXiv:2006.16285 [hep-th]. June 2020. DOI: 10.48550/arXiv.2006.16285.

[152] Brian Patt and Frank Wilczek. *Higgs-field Portal into Hidden Sectors*. arXiv:hep-ph/0605188. May 2006.

[153] Ayres Freitas, Susanne Westhoff, and Jure Zupan. *Integrating in the Higgs Portal to Fermion Dark Matter*. arXiv:1506.04149 [hep-ph]. June 2015.

[154] Christoph Englert et al. "Emergence of the Electroweak Scale through the Higgs Portal". In: *Journal of High Energy Physics* 2013.4 (Apr. 2013). arXiv:1301.4224 [hep-ph], p. 60. ISSN: 1029-8479. DOI: 10.1007/JHEP04(2013)060.

[155] Oleg Lebedev. "The Higgs Portal to Cosmology". In: *Progress in Particle and Nuclear Physics* 120 (Sept. 2021). arXiv:2104.03342 [astro-ph, physics:hep-ph], p. 103881. ISSN: 01466410. DOI: 10.1016/j.ppnp.2021.103881.

[156] Rupert Coy and Michael A. Schmidt. "Freeze-in and freeze-out of sterile neutrino dark matter". In: *Journal of Cosmology and Astroparticle Physics* 2022.08 (Aug. 2022). arXiv:2204.08795 [hep-ph], p. 070. ISSN: 1475-7516. DOI: 10.1088/1475-7516/2022/08/070.

[157] Junpei Ikemoto et al. "Higgs Portal Majorana Fermionic Dark Matter with the Freeze-in Mechanism". In: *Progress of Theoretical and Experimental Physics* 2023.8 (Aug. 2023). arXiv:2212.14660 [hep-ph, physics:hep-th], 083B04. ISSN: 2050-3911. DOI: 10.1093/ptep/ptad081.

[158] Edward W. Kolb, Daniel J. H. Chung, and Antonio Riotto. "WIMPZILLAS!" In: arXiv: hep-ph/9810361 ISSN: 0094-243X. AIP, Mar. 2013, pp. 91–105. DOI: 10.1063/1.59655.

[159] Rocky W. Kolb and Andrew J. Long. "Superheavy dark matter through Higgs portal operators". In: *Physical Review D* 96.10 (Aug. 2017). arXiv: 1708.04293 Publisher: American Physical Society. DOI: 10.1103/PhysRevD.96.103540.

[160] Richard Beals and Jacek Szmigielski. "Meijer G-Functions: A Gentle Introduction". en. In: *Notices of the American Mathematical Society* 60.06 (Aug. 2013), p. 866. ISSN: 0002-9920, 1088-9477. DOI: 10.1090/noti1016.

[161] Salvador Centelles Chuliá, Rahul Srivastava, and José W. F. Valle. "Seesaw roadmap to neutrino mass and dark matter". In: *Physics Letters B* 781 (June 2018). arXiv:1802.05722 [hep-ph], pp. 122–128. ISSN: 03702693. DOI: 10.1016/j.physletb.2018.03.046.

[162] Steven Weinberg. "Baryon and Lepton Nonconserving Processes". In: *Phys. Rev. Lett.* 43 (1979), pp. 1566–1570. DOI: 10.1103/PhysRevLett.43.1566.

[163] F. R. Klinkhamer. "Neutrino mass and the Standard Model". In: *Modern Physics Letters A* 28.05 (Feb. 2013). arXiv:1112.2669 [hep-ex, physics:hep-ph], p. 1350010. ISSN: 0217-7323, 1793-6632. DOI: 10.1142/S0217732313500107.

[164] A. Broncano, M. B. Gavela, and E. Jenkins. "The Effective Lagrangian for the Seesaw Model of Neutrino Mass and Leptogenesis". In: *Physics Letters B* 636.6 (May 2006). arXiv:hep-ph/0210271, p. 332. ISSN: 03702693. DOI: 10.1016/j.physletb.2006.04.003.

[165] Oliver Buchmueller, Caterina Doglioni, and Lian-Tao Wang. "Search for dark matter at colliders". In: (2020). arXiv: 1912.12739v1.

[166] Björn Penning. "The Pursuit of Dark Matter at Colliders-An Overview". In: (2018). arXiv: 1712.01391v2 ISBN: 1712.01391v2.

[167] Giorgio Arcadi, Yann Mambrini, and Francois Richard. "Z-portal dark matter". In: *Journal of Cosmology and Astroparticle Physics* 2015.03 (Mar. 2015). arXiv:1411.2985 [hep-ph], pp. 018–018. ISSN: 1475-7516. DOI: 10.1088/1475-7516/2015/03/018.

[168] Antonio Boveia and Caterina Doglioni. "Dark Matter Searches at Colliders". In: (2018). arXiv: 1810.12238v1. DOI: 10.1146/annurev-nucl.

[169] ATLAS Collaboration. "Search for invisible Higgs-boson decays in events with vector-boson fusion signatures using 139 fb^{-1} of proton-proton data recorded by the ATLAS experiment". In: *Journal of High Energy Physics* 2022.8 (Aug. 2022). arXiv:2202.07953 [hep-ex], p. 104. ISSN: 1029-8479. DOI: 10.1007/JHEP08(2022)104.

[170] Anadi Canepa. "Searches for supersymmetry at the Large Hadron Collider". In: *Reviews in Physics* 4 (Nov. 2019), p. 100033. ISSN: 2405-4283. DOI: 10.1016/j.revip.2019.100033.

[171] Oliver Buchmueller, Caterina Doglioni, and Lian-Tao Wang. "Search for dark matter at colliders". In: *Nature Physics* 13.3 (Mar. 2017). arXiv:1912.12739 [hep-ex, physics:hep-ph], pp. 217–223. ISSN: 1745-2473, 1745-2481. DOI: 10.1038/nphys4054.

[172] Marc Schumann. "Direct Detection of WIMP Dark Matter: Concepts and Status". In: *Journal of Physics G: Nuclear and Particle Physics* (Mar. 2019). ISSN: 0954-3899. DOI: 10.1088/1361-6471/ab2ea5.

[173] M Klasen, M Pohl, and G Sigl. "Indirect and direct search for dark matter". In: (2015). arXiv: 1507.03800v1.

[174] Julien Billard et al. "Direct Detection of Dark Matter-APPEC Committee Report * Committee Members". In: (). arXiv: 2104.07634v1.

[175] Gintaras Duda, Ann Kemper, and Paolo Gondolo. "Model Independent Form Factors for Spin Independent Neutralino-Nucleon Scattering from Elastic Electron Scattering Data". In: *Journal of Cosmology and Astroparticle Physics* 2007.04 (Apr. 2007). arXiv:hep-ph/0608035, pp. 012–012. ISSN: 1475-7516. DOI: 10.1088/1475-7516/2007/04/012.

[176] R. Bernabei et al. *The dark matter: DAMA/LIBRA and its perspectives*. arXiv:2110.04734 [astro-ph, physics:hep-ex, physics:hep-ph, physics:physics]. Oct. 2021. DOI: 10.48550/arXiv.2110.04734.

[177] J. Amare et al. "Annual modulation results from three-year exposure of ANAIS-112". In: *Physical Review D* 103.10 (May 2021). arXiv:2103.01175 [astro-ph, physics:hep-ex], p. 102005. ISSN: 2470-0010, 2470-0029. DOI: 10.1103/PhysRevD.103.102005.

[178] H. S. Lee et al. "Search for Low-Mass Dark Matter with CsI(Tl) Crystal Detectors". In: *Physical Review D* 90.5 (Sept. 2014). arXiv:1404.3443 [astro-ph, physics:hep-ex, physics:physics], p. 052006. ISSN: 1550-7998, 1550-2368. DOI: 10.1103/PhysRevD.90.052006.

[179] DM-Ice Collaboration et al. "First search for a dark matter annual modulation signal with NaI(Tl) in the Southern Hemisphere by DM-Ice17". In: *Physical Review D* 95.3 (Feb. 2017). arXiv:1602.05939 [astro-ph, physics:hep-ex, physics:physics], p. 032006. ISSN: 2470-0010, 2470-0029. DOI: 10.1103/PhysRevD.95.032006.

[180] Kaixuan Ni and Laura Baudis. "Direct Dark Matter Searches with CDMS and XENON". In: *Advances in Space Research* 41.12 (Jan. 2008). arXiv:astro-ph/0611124, pp. 2019–2023. ISSN: 02731177. DOI: 10.1016/j.asr.2007.02.071.

[181] CRESST Collaboration et al. "First results from the CRESST-III low-mass dark matter program". In: *Physical Review D* 100.10 (Nov. 2019). arXiv:1904.00498 [astro-ph], p. 102002. ISSN: 2470-0010, 2470-0029. DOI: 10.1103/PhysRevD.100.102002.

[182] C. E. Aalseth et al. *Search for An Annual Modulation in Three Years of CoGeNT Dark Matter Detector Data*. arXiv:1401.3295 [astro-ph, physics:hep-ex, physics:hep-ph]. Jan. 2014. DOI: 10.48550/arXiv.1401.3295.

[183] Michela Lai. "Recent results from DEAP-3600". In: *Journal of Instrumentation* 18.02 (Feb. 2023). arXiv:2302.14484 [hep-ex], p. C02046. ISSN: 1748-0221. DOI: 10.1088/1748-0221/18/02/C02046.

[184] D. Franco. *Light dark matter search with DarkSide-50*. arXiv:2306.12151 [astro-ph, physics:hep-ex]. June 2023. DOI: 10.48550/arXiv.2306.12151.

[185] J. Aalbers et al. "First Dark Matter Search Results from the LUX-ZEPLIN (LZ) Experiment". In: *Physical Review Letters* 131.4 (July 2023). arXiv:2207.03764 [astro-ph, physics:hep-ex], p. 041002. ISSN: 0031-9007, 1079-7114. DOI: 10.1103/PhysRevLett.131.041002.

[186] XENON Collaboration et al. "The XENON1T Dark Matter Experiment". In: *The European Physical Journal C* 77.12 (Dec. 2017). arXiv:1708.07051 [astro-ph, physics:hep-ex, physics:physics], p. 881. ISSN: 1434-6044, 1434-6052. DOI: 10.1140/epjc/s10052-017-5326-3.

[187] C. Amole et al. “Dark Matter Search Results from the Complete Exposure of the PICO-60 C$_3$F$_8$ Bubble Chamber”. In: *Physical Review D* 100.2 (July 2019). arXiv:1902.04031 [astro-ph, physics:hep-ex, physics:physics], p. 022001. ISSN: 2470-0010, 2470-0029. DOI: 10.1103/PhysRevD.100.022001.

[188] Carlos Blanco et al. “Dark Matter Direct Detection with Quantum Dots”. In: (). arXiv: 2208.05967v1.

[189] Rebecca K. Leane. *Indirect Detection of Dark Matter in the Galaxy*. arXiv:2006.00513 [astro-ph, physics:hep-ph]. May 2020.

[190] Tracy R. Slatyer. *TASI Lectures on Indirect Detection of Dark Matter*. arXiv:1710.05137 [astro-ph, physics:hep-ph]. Oct. 2017.

[191] Christopher Dessert, Nicholas L. Rodd, and Benjamin R. Safdi. “The dark matter interpretation of the 3.5-keV line is inconsistent with blank-sky observations”. In: *Science* 367.6485 (Mar. 2020). arXiv:1812.06976 [astro-ph, physics:hep-ph], pp. 1465–1467. ISSN: 0036-8075, 1095-9203. DOI: 10.1126/science.aaw3772.

[192] Christopher Dessert et al. *Was There a 3.5 keV Line?* arXiv:2309.03254 [astro-ph, physics:hep-ph]. Sept. 2023. DOI: 10.48550/arXiv.2309.03254.

[193] Marco Chianese et al. “Constraints on heavy decaying dark matter with current gamma-ray measurements”. In: *Journal of Cosmology and Astroparticle Physics* 2021.11 (Nov. 2021). arXiv:2108.01678 [astro-ph, physics:hep-ph], p. 035. ISSN: 1475-7516. DOI: 10.1088/1475-7516/2021/11/035.

[194] Marco Chianese et al. “Decaying dark matter at IceCube and its signature on High Energy gamma experiments”. In: *Journal of Cosmology and Astroparticle Physics* 2019.11 (Nov. 2019). arXiv:1907.11222 [astro-ph, physics:hep-ex, physics:hep-ph], pp. 046–046. ISSN: 1475-7516. DOI: 10.1088/1475-7516/2019/11/046.

[195] Masahiro Kawasaki et al. “Revisiting CMB constraints on dark matter annihilation”. en. In: *Journal of Cosmology and Astroparticle Physics* 2021.12 (Dec. 2021). Publisher: IOP Publishing, p. 015. ISSN: 1475-7516. DOI: 10.1088/1475-7516/2021/12/015.

[196] Anja Butter et al. “Searching for dark matter subhalos in the Fermi-LAT catalog with Bayesian neural networks”. In: *Journal of Cosmology and Astroparticle Physics* 2023.07 (July 2023). arXiv:2304.00032 [astro-ph, physics:hep-ph], p. 033. ISSN: 1475-7516. DOI: 10.1088/1475-7516/2023/07/033.

[197] LHAASO Collaboration et al. “Constraints on heavy decaying dark matter from 570 days of LHAASO observations”. In: *Physical Review Letters* 129.26 (Dec. 2022). arXiv:2210.15989 [astro-ph, physics:hep-ph], p. 261103. ISSN: 0031-9007, 1079-7114. DOI: 10.1103/PhysRevLett.129.261103.

[198] IceCube Collaboration et al. “The IceCube Neutrino Observatory: Instrumentation and Online Systems”. In: *Journal of Instrumentation* 12.03 (Mar. 2017). arXiv:1612.05093 [astro-ph, physics:physics], P03012–P03012. ISSN: 1748-0221. DOI: 10.1088/1748-0221/12/03/P03012.

[199] SNO Collaboration et al. “Combined analysis of all three phases of solar neutrino data from the Sudbury Neutrino Observatory”. In: *Physical Review C* 88.2 (Aug. 2013). Publisher: American Physical Society, p. 025501. DOI: 10.1103/PhysRevC.88.025501.

[200] Borexino Collaboration et al. “Precision Measurement of the $^{7}\mathrm{Be}$ Solar Neutrino Interaction Rate in Borexino”. In: *Physical Review Letters* 107.14 (Sept. 2011). Publisher: American Physical Society, p. 141302. DOI: 10.1103/PhysRevLett.107.141302.

[201] The KamLAND Collaboration. *Reactor On-Off Antineutrino Measurement with KamLAND*. arXiv:1303.4667 [hep-ex, physics:nucl-ex, physics:physics]. Mar. 2013. DOI: 10.48550/arXiv.1303.4667.

[202] Super-Kamiokande Collaboration et al. “Atmospheric neutrino oscillation analysis with external constraints in Super-Kamiokande I-IV”. In: *Physical Review D* 97.7 (Apr. 2018). arXiv:1710.09126 [hep-ex], p. 072001. ISSN: 2470-0010, 2470-0029. DOI: 10.1103/PhysRevD.97.072001.

[203] IceCube Collaboration et al. “Determining neutrino oscillation parameters from atmospheric muon neutrino disappearance with three years of IceCube DeepCore data”. In: *Physical Review D* 91.7 (Apr. 2015). arXiv:1410.7227 [hep-ex, physics:physics], p. 072004. ISSN: 1550-7998, 1550-2368. DOI: 10.1103/PhysRevD.91.072004.

[204] L. Haegel. "The latest T2K neutrino oscillation results". In: *Proceedings of The European Physical Society Conference on High Energy Physics — PoS(EPS-HEP2017)*. arXiv:1709.04180 [hep-ex]. Oct. 2017, p. 112. DOI: 10.22323/1.314.0112.

[205] Daya Bay Collaboration et al. "Measurement of electron antineutrino oscillation with 1958 days of operation at Daya Bay". In: *Physical Review Letters* 121.24 (Dec. 2018). arXiv:1809.02261 [hep-ex, physics:physics], p. 241805. ISSN: 0031-9007, 1079-7114. DOI: 10.1103/PhysRevLett.121.241805.

[206] The Double Chooz Collaboration. "First Double Chooz $\mathbf{\theta_{13}}$ Measurement via Total Neutron Capture Detection". In: *Nature Physics* 16.5 (May 2020). arXiv:1901.09445 [hep-ex, physics:physics], pp. 558–564. ISSN: 1745-2473, 1745-2481. DOI: 10.1038/s41567-020-0831-y.

[207] G. Bak et al. "Measurement of Reactor Antineutrino Oscillation Amplitude and Frequency at RENO". In: *Physical Review Letters* 121.20 (Nov. 2018). arXiv:1806.00248 [hep-ex], p. 201801. ISSN: 0031-9007, 1079-7114. DOI: 10.1103/PhysRevLett.121.201801.

[208] K. Abe et al. "Constraint on the Matter-Antimatter Symmetry-Violating Phase in Neutrino Oscillations". In: *Nature* 580.7803 (Apr. 2020). arXiv:1910.03887 [hep-ex], pp. 339–344. ISSN: 0028-0836, 1476-4687. DOI: 10.1038/s41586-020-2177-0.

[209] B. J. P. Jones. *The Physics of Neutrinoless Double Beta Decay: A Primer*. arXiv:2108.09364 [hep-ph, physics:nucl-ex, physics:nucl-th]. Feb. 2022.

[210] Thomas J Bowles. "Tritium Beta Decay and the Search for Neutrino Mass". en. In: 25 (1997).

[211] R. G. Hamish Robertson. "Direct determination of neutrino mass". en. In: *Journal of Physics: Conference Series* 173.1 (June 2009), p. 012016. ISSN: 1742-6596. DOI: 10.1088/1742-6596/173/1/012016.

[212] M. Daum, R. Frosch, and P.-R. Kettle. "The charged and neutral pion masses revisited". en. In: *Physics Letters B* 796 (Sept. 2019), pp. 11–14. ISSN: 03702693. DOI: 10.1016/j.physletb.2019.07.027.

[213] T. Fukuyama, K. Matsuda, and H. Nishiura. "CP Violation in Neutrinoless Double Beta Decay and Neutrino Oscillation". In: *Physical Review D* 57.9 (May 1998). arXiv:hep-ph/9711415, pp. 5844–5850. ISSN: 0556-2821, 1089-4918. DOI: 10.1103/PhysRevD.57.5844.

[214] Heinrich Päs and Werner Rodejohann. "Neutrinoless double beta decay". en. In: *New Journal of Physics* 17.11 (Nov. 2015). Publisher: IOP Publishing, p. 115010. ISSN: 1367-2630. DOI: 10.1088/1367-2630/17/11/115010.

[215] S. Dell'Oro et al. "Neutrinoless double beta decay: 2015 review". In: *Advances in High Energy Physics* 2016 (2016). arXiv:1601.07512 [astro-ph, physics:hep-ph], pp. 1–37. ISSN: 1687-7357, 1687-7365. DOI: 10.1155/2016/2162659.

[216] S M Bilenky and C Giunti. "Neutrinoless Double-Beta Decay: a Probe of Physics Beyond the Standard Model". In: (2015). arXiv: 1411.4791v2.

[217] GERDA Collaboration et al. "Final Results of GERDA on the Search for Neutrinoless Double-$\ensuremath{\beta}$ Decay". In: *Physical Review Letters* 125.25 (Dec. 2020). Publisher: American Physical Society, p. 252502. DOI: 10.1103/PhysRevLett.125.252502.

[218] EXO-200 Collaboration et al. "Search for Majorana neutrinos with the first two years of EXO-200 data". In: *Nature* 510.7504 (June 2014). arXiv:1402.6956 [hep-ex, physics:nucl-ex, physics:physics], pp. 229–234. ISSN: 0028-0836, 1476-4687. DOI: 10.1038/nature13432.

[219] KamLAND-Zen Collaboration et al. "Search for the Majorana Nature of Neutrinos in the Inverted Mass Ordering Region with KamLAND-Zen". In: *Physical Review Letters* 130.5 (Jan. 2023). arXiv:2203.02139 [hep-ex, physics:physics], p. 051801. ISSN: 0031-9007, 1079-7114. DOI: 10.1103/PhysRevLett.130.051801.

[220] D. Q. Adams et al. "Search for Majorana neutrinos exploiting millikelvin cryogenics with CUORE". In: *Nature* 604.7904 (Apr. 2022). arXiv:2104.06906 [nucl-ex], pp. 53–58. ISSN: 0028-0836, 1476-4687. DOI: 10.1038/s41586-022-04497-4.

[221] IceCube Collaboration et al. "IceCube Sensitivity for Low-Energy Neutrinos from Nearby Supernovae". In: *Astronomy & Astrophysics* 535 (Nov. 2011). arXiv:1108.0171 [astro-ph], A109. ISSN: 0004-6361, 1432-0746. DOI: 10.1051/0004-6361/201117810.

[222] S. Ansoldi et al. “The Blazar TXS 0506+056 Associated with a High-energy Neutrino: Insights into Extragalactic Jets and Cosmic-Ray Acceleration”. en. In: *The Astrophysical Journal Letters* 863.1 (Aug. 2018). Publisher: The American Astronomical Society, p. L10. ISSN: 2041-8205. DOI: 10.3847/2041-8213/aad083.

[223] R Abbasi et al. “Searches for Connections between Dark Matter and High-Energy Neutrinos with IceCube IceCube Collaboration”. In: (2022). arXiv: 2205.12950v1.

[224] IceCube Collaboration et al. “Search for neutrinos from decaying dark matter with IceCube”. In: *The European Physical Journal C* 78.10 (Oct. 2018). arXiv:1804.03848 [astro-ph], p. 831. ISSN: 1434-6044, 1434-6052. DOI: 10.1140/epjc/s10052-018-6273-3.

[225] Francis Halzen and Ali Kheirandish. *IceCube and High-Energy Cosmic Neutrinos*. arXiv:2202.00694 [astro-ph, physics:hep-ex, physics:hep-ph]. Feb. 2022.

[226] P. S.Bhupal Dev et al. “Heavy right-handed neutrino dark matter and PeV neutrinos at IceCube”. In: *Journal of Cosmology and Astroparticle Physics* 2016.8 (June 2016). arXiv: 1606.04517 Publisher: Institute of Physics Publishing. ISSN: 14757516. DOI: 10.1088/1475-7516/2016/08/034.

[227] Chien Yi Chen, P. S.Bhupal Dev, and Amarjit Soni. “Two-component flux explanation for the high energy neutrino events at IceCube”. In: *Physical Review D - Particles, Fields, Gravitation and Cosmology* 92.7 (Nov. 2015). arXiv: 1411.5658 Publisher: American Physical Society. ISSN: 15502368. DOI: 10.1103/PhysRevD.92.073001.

[228] Arman Esmaili and Pasquale Dario Serpico. “Are IceCube neutrinos unveiling PeV-scale decaying dark matter?” In: *Journal of Cosmology and Astroparticle Physics* 2013.11 (Aug. 2013). arXiv: 1308.1105. ISSN: 14757516. DOI: 10.1088/1475-7516/2013/11/054.

[229] ANTARES Collaboration. *ANTARES: the first undersea neutrino telescope*. arXiv:1104.1607. June 2011. DOI: 10.48550/arXiv.1104.1607.

[230] A. Albert et al. *Review of the online analyses of multi-messenger alerts and electromagnetic transient events with the ANTARES neutrino telescope*. arXiv:2211.07551. Feb. 2024. DOI: 10.48550/arXiv.2211.07551.

[231] ANTARES collaboration et al. *Limits on Dark Matter Annihilation in the Sun using the ANTARES Neutrino Telescope*. arXiv:1603.02228. May 2016. DOI: 10.48550/arXiv.1603.02228.

[232] A. Margiotta. *The KM3NeT infrastructure: status and first results*. arXiv:2208.07370. Nov. 2022. DOI: 10.48550/arXiv.2208.07370.

[233] S. Aiello et al. *Astronomy potential of KM3NeT/ARCA*. arXiv:2402.08363. Oct. 2024. DOI: 10.48550/arXiv.2402.08363.

[234] Steve Blanchet and Pasquale Di Bari. "Flavour effects on leptogenesis predictions". In: *Journal of Cosmology and Astroparticle Physics* 3 (July 2007). arXiv: hep-ph/0607330. ISSN: 14757516. DOI: 10.1088/1475-7516/2007/03/018.

[235] Anupama Atre et al. "The search for heavy Majorana neutrinos". In: *Journal of High Energy Physics* 2009.5 (Jan. 2009). arXiv: 0901.3589. ISSN: 11266708. DOI: 10.1088/1126-6708/2009/05/030.

[236] M. G. Aartsen et al. "Search for neutrinos from decaying dark matter with IceCube: IceCube Collaboration". In: *European Physical Journal C* 78.10 (Apr. 2018). arXiv: 1804.03848 Publisher: Springer New York LLC. ISSN: 14346052. DOI: 10.1140/epjc/s10052-018-6273-3.

[237] H. Arthur Weldon. "Covariant calculations at finite temperature: The relativistic plasma". In: *Physical Review D* 26.6 (1982), pp. 1394–1407. ISSN: 05562821. DOI: 10.1103/PhysRevD.26.1394.

[238] Edward W Kolb and Stephen Wolfram. "Baryon Number Generation in the Early Universe". en. In: (1980).

[239] Björn Garbrecht, Frank Glowna, and Pedro Schwaller. "Scattering rates for leptogenesis: Damping of lepton flavour coherence and production of singlet neutrinos". In: *Nuclear Physics B* 877.1 (Mar. 2013). arXiv: 1303.5498, pp. 1–35. ISSN: 05503213. DOI: 10.1016/j.nuclphysb.2013.08.020.

[240] R. Barbieri and A. Dolgov. "Neutrino oscillations in the early universe". In: *Nuclear Physics, Section B* 349.3 (Feb. 1991). Publisher: North-Holland, pp. 743–753. ISSN: 05503213. DOI: 10.1016/0550-3213(91)90396-F.

[241] P. Di Bari and R. Foot. "Active-sterile neutrino oscillations in the early Universe: Asymmetry generation at low [Formula Presented] and the Landau-Zener approximation". In: *Physical Review D - Particles, Fields, Gravitation and Cosmology* 65.4 (Mar. 2002). arXiv: hep-ph/0103192, p. 12. ISSN: 15502368. DOI: 10.1103/PhysRevD.65.045003.

[242] Riccardo Barbieri et al. "Baryogenesis through leptogenesis". In: *Nuclear Physics B* 575.1-2 (Nov. 2000). arXiv: hep-ph/9911315 Publisher: Elsevier, pp. 61–77. ISSN: 05503213. DOI: 10.1016/S0550-3213(00)00011-0.

[243] Nicole F. Bell, Raymond R. Volkas, and Yvonne Y.Y. Wong. "Relic neutrino asymmetry evolution from first principles". In: *Physical Review D - Particles, Fields, Gravitation and Cosmology* 59.11 (Sept. 1999). arXiv: hep-ph/9809363. ISSN: 15502368. DOI: 10.1103/PhysRevD.59.113001.

[244] Atri Bhattacharya et al. "Update on decaying and annihilating heavy dark matter with the 6-year IceCube HESE data". In: *Journal of Cosmology and Astroparticle Physics* 2019.5 (Mar. 2019). arXiv: 1903.12623 Publisher: Institute of Physics Publishing. ISSN: 14757516. DOI: 10.1088/1475-7516/2019/05/051.

[245] Graham D. Kribs, Takemichi Okui, and Tuhin S. Roy. "Viable Gravity-Mediated Supersymmetry Breaking". In: *Physical Review D* 82.11 (Dec. 2010). arXiv:1008.1798 [hep-ph, physics:hep-th], p. 115010. ISSN: 1550-7998, 1550-2368. DOI: 10.1103/PhysRevD.82.115010.

[246] Robert Brandenberger and Jerome Martin. "Trans-Planckian Issues for Inflationary Cosmology". In: *Classical and Quantum Gravity* 30.11 (June 2013). arXiv:1211.6753 [astro-ph, physics:gr-qc, physics:hep-ph, physics:hep-th], p. 113001. ISSN: 0264-9381, 1361-6382. DOI: 10.1088/0264-9381/30/11/113001.

[247] Elena Graverini. “Flavour anomalies: a review”. In: *Journal of Physics: Conference Series* 1137 (Jan. 2019). arXiv:1807.11373 [hep-ex, physics:hep-ph], p. 012025. ISSN: 1742-6588, 1742-6596. DOI: 10.1088/1742-6596/1137/1/012025.